Computational modelling of mycobacterium infection and innate immune response in zebrafish

Viana de Carvalho, R.

Computational Modeling of *Mycobacterium* Infection and Innate Immune Response in Zebrafish

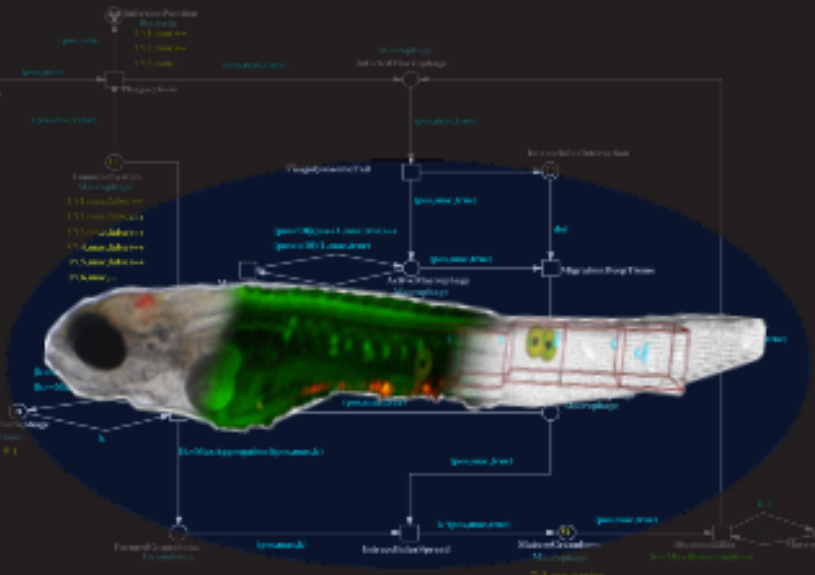

Rafael Viana de Carvalho

Computational Modeling of *Mycobacterium* Infection and Innate Immune Response in Zebrafish

Rafael Viana de Carvalho

ISBN: 978-94-6259-881-2

Computational Modeling of *Mycobacterium* Infection and Innate Immune Response in Zebrafish

Proefschrift

ter verkrijging van
de graad van Doctor aan de Universiteit Leiden,
op gezag van Rector Magnificus Prof. Mr. C.J.J.M. Stolker,
volgens besluit van het College voor Promoties
te verdedigen op 15 oktober 2015
klokke 13.45 uur

door

Rafael Viana de Carvalho
Geboren te Rio Branco-AC, Brazil, in 1981

Promotiecommissie

Promotor

Prof. Dr. J. N. Kok

Co-promotor

Dr. Ir. F. J. Verbeek

Overige Leden

Prof. Dr. H. P. Spaink

Prof. Dr. M. Koutny, Newcastle University

Dr. H. C. M. Kleijn

The studies described in this thesis were performed at Leiden Institute of Advanced Computer Science and supported by the Monesia Programme of the Erasmus Mundus External Cooperation Window and by the Science Without Borders Programme of Conselho Nacional de Pesquisa (CNPq).

Table of Contents

Preface

Modeling biological systems is an important process in the endeavor of investigations in the life-sciences. Many studies rely on construction, simulation and analysis of models applying methods, which vary from schematic drawings to complex systems of equations, in order to understand function and behavior of biological phenomena. It is a challenger to model the complex interplay of the cause-and-effect among components that represents a specific biological behavior, e.g. regulatory pathways. It requires an analysis of *in vivo* and *in vitro* experiments, gathering information and data by category, such as concentration over time in response to a certain stimulus. Therefore it is possible to create reductive methods to represent the biological system.

Computational biology has provided tools and methods to investigate how these interactions give rise to the function and behavior of that system. In this thesis we consider computational methods to model biological behavior, in particular the *mycobacterium* infection process. The scope of this thesis is to model and simulate the dynamics of the infection and the interactions between its components from a macro level (i.e. cell) to a micro level (i.e. molecular, protein). In addition, we analyze qualitative and quantitative the model, providing simulation of different scenarios of specific testable hypotheses about a biological system. The aim of this thesis is to provide and validate a computational method for modeling and simulate biological process, considering its functionalism, scalability and portability. Throughout the thesis one particular application domain is used, *Mycobacterium marinum* infection in zebrafish and the innate immune response.

This dissertation presents the modeling aspects of the mycobacterial infection process and innate immune response. From the choice of the modeling formalism, addressing the qualitative and quantitative aspects of the model as well as simulation results from different scenarios. The goal is to create an accurate model that represents the early stage of the infection process. In the first chapter an overview is given of modeling methods used to represent a biological behavior. Their relevance and characteristics are presented followed by a description on the technique used in the models presented on the followed chapters. The first chapter establishes a context for the subsequent chapters, 2 to 5, in which a series of models are presented, describing characteristics and scenarios of the infection process.

1. Introduction

Based on:

Carvalho, Rafael V., Davids, Willem, Meijer, Annemarie H., Verbeek, Fons J.: Spatio-temporal Modelling and Simulation of Mycobacterium Pathogenesis Using Petri nets. In: BIONETICS2011. Lecture Notes of the Institute for Computer Sciences, Social Informatics and Telecommunications Engineering, vol. 103, pp 236-241, Springer (2012).

And

Carvalho, Rafael V., Kleijn, Jetty, Meijer, Annemarie H., Verbeek, Fons J.: Modeling Innate Immune Response to Early Mycobacterium Infection. In: Computational and Mathematical Methods in Medicine, vol. 2012, 12 pages (2012).

Papel	Paper
E tudo que eu pensei e tudo que eu falei e tudo que me contaram era papel.	And everything I've though and everything I've said and everything they've told me was paper.
E tudo que descobri amei detestei: papel.	And everything I've discovered loved hated: paper.
Papel quanto havia em mim e nos outros, papel de jornal de parede de embrulho papel de papel papelão	Paper everything that was in me and in the others, paper news-paper wallpaper wrapping paper paper-paper papier-mâché
Carlos Drummond de Andrade, Brasil (1902 – 1987)	Carlos Drummond de Andrade, Brazil (1902 – 1987)

Abstract

Modeling of biological systems is evolving into the description, simulation and analysis of the behavior and interdependent relationships of biological phenomena. The process of formulating a model relies on the synergistic combination of experimentation, theory and formalization of the processes that happen in such systems. In this chapter we describe the characteristics of the modeling process and a broad view of the formal models used to model biological systems. We choose the Petri net formalism as modeling technique, describing its structure and characteristics applied in the models described in the following chapters. This thesis is about an application of Petri nets in biology; the examples will directly refer to or rely on biological context.

1.1 Modeling systems biology

Modeling is the art of representing, manipulating and communicating an object, process or concept. In the dictionary[1], the verb to 'model' is defined as "to plan or form after a pattern" or "to produce a representation or simulation of". As one can easily realize, for the modeling is necessary to observe, to gather information and generate hypotheses that are consistent with the data collected. Systems biology is an empirical science. It represents facts of life with a complex structure. Modeling biological systems is an endeavor to better understand the inner workings and emergent properties of such system.

The core of systems biology relies on the construction of models describing biological behavior. The aim is to study biological components, i.e. molecules, cells, organs or entire species, and their complex interactions, in order to understand the processes and emergent properties that happen within such systems. There is ample scientific use for models that represent biological behavior: education, using the biological information to describe system characteristics; analysis and prediction, testing which assumptions about the system best fit the data and eventually, to predict response to different stimuli; instrumentation or device, designing an "alternative system" to circumvent experiments that are too costly, time consuming or ethically undesirable.

In order to build a model that will represent biological behavior, it is necessary to collect the information, select the most relevant components and construct first a simplified version of the entity we want to model. This process is referred to as the modeling decisions; and basically it takes into account the properties of the information, the purpose of the model and the aspects of the structure and the process on which the model focuses. Therefore, model formalism is required to define, implement and simulate the model and it is part of the modeling decision process to choose the formalism that will be used to describe a biological problem. In this chapter, we focus on the modeling decisions and the formalisms that are commonly used in modeling biological behavior. First, we discuss about the model properties that are considered to make the modeling decision. Subsequently, we describe the formal methods used to model biological behavior. We emphasize the formalism chosen to model the case study presented in the following chapters. In this chapter we also briefly introduce how the formalism that we will use in this thesis, the Petri net, is successfully used in the domain of biology. We will explain that the current status of the PN formalism allows us to gradually build a model of increasing complexity. Modern biology research is capable of producing lots of data that together represent a biological system; the systems biology approach is to integrate all these different components and data in order to understand the system and its interacting components. We think that the concurrent aspects and different layers can be well

[1] Merriam-Webster online dictionary: www.merrian-webster.com/dictionary, access on March 2015

represented in a Petri net and therefore in this thesis, using a case study, we further investigate mapping of complex systems studied in the context of systems biology. The different modeling aspects are explored and probed with the different Petri net methods. A problem typical to systems biology is one in which multiple organisms are involved and interact on different levels – and in order to integrate these levels procedures need to be developed. Therefore, a system with an invader-host interaction common to disease models was chosen to further develop these procedures. More specifically, the invader host system of tuberculosis (*Mycobacterium*) is studied using the zebrafish model. It addresses infection and response mechanisms on various levels of detail. The *Mycobacterium* infection and the response is a very interesting system to study we aim to also use it to push the limits of modeling forward.

1.2 Modeling process and properties

Every modeling process starts by an analysis of the problem; this is essential for a clear definition of the questions one asks the model. What do we want to model? What is the aim? What should the model achieve? This step includes the definition of the **model objective** and it implies a certain level of understanding of the problem. In the attempt to understand the problem, it is necessary to state what the model will represent, and how to analyze its output. Once the objective of the modeling is defined, the next step is to **collect the information and data** about the problem consulting scientific literature and/or empirical data together with discussions with field experts. After stating the objective and gathering the data, the next step in the modeling process is to **define a hypothesis**. The hypothesis is the basis for the model and the results will depend on it. On basis of the hypothesis that we can formulate the **model structure**, correlating the acquired information and the model objective, considering only the data that are relevant for the specific purpose of the model. Therefore, in this step we define the level of detail that will be modeled and based on the model properties start to construct the model.

It is crucial to analyze the model properties to define the model structure. Therefore, interpretation of the requirements of the model and the aspects of the information/data are acquired to define the properties of the structure and process on which the model focuses.

A model is considered **descriptive** when it represents the observed data without considering directly the processes that produce these data. An example is a graphical representation of the steps of the cell cycle: G2 phase (cells with duplicated chromosome); Mitosis (chromosome separation and cell division); G1 phase (cells with one chromosome); Synthesis (chromosome duplication). It gives the information about the cell process but there is no data about the variables that trigger the process (molecules interaction, rates, time).

A **mechanistic model** assumes that a complex system can be understood by examining the working of its individual parts and the manner in which they are coupled. For instance, for modeling the genetic pathways underlying the cell division, one should consider the data about molecular interactions, rates and time consuming.

Other model properties are related to the dynamics of the process, which is studied. A model can be static or dynamic**.** A **static model** represents structures that do not provide time dependency. The model refers more to the structure than to the behavior of the system. These models are considered descriptive and not mechanistic.

A **dynamic model** describes relevant information that can be put in a chronological, time dependent order. It models systems that represent a process flow, what an object does essentially with many possibilities that may arise. Such models can be both descriptive and mechanistic. The models presented in Chapter 2 and 3 are examples of a dynamic descriptive model and a dynamic mechanistic model respectively.

Another two important model properties to be considered are directly related to the information and data acquired. A **qualitative model** describes processes without using exact experimental data. The model relies on the examination, analysis and interpretation of observations. The purpose is to describe underlying meanings and patterns of relationships, including classifications of types of phenomena and entities in the biological system. A qualitative model helps to obtain an in-depth understanding of biological behavior and the reasons that govern such behavior (why and how, not just what, where, when).

The **quantitative model** is based on systematic empirical investigation of biological phenomena from experimental data that are available. The model allows via statistical, mathematical and/or computational analysis, to make predictions about future states in its behavior. A quantitative model can contribute, for example, in the prediction of results from experiments and generation of further hypothesis about the biological behavior.

The construction of a model to describe a biological system does not always require exact quantitative data. A qualitative model is a starting point for modeling processes for which experimental data are still incomplete. When experimental data are available, a migration to a quantitative model can be realized by including variable and extending the model complexity. This thesis shows this process in its Chapters 2 to 5 where we start to model qualitatively and then migrate to a quantitative model. Each model represents an extension of the previous model adding a layer of complexity and more data information. The convenience in the process of transformation from qualitative to quantitative model is directly related to the formal method used to implement the model and will be discussed in the next sections.

1.3 Formal models

Further to the definition given in section 1.1, a model can be seen as description of a system designed to help an observer to understand how the system works and to be able to predict on the behavior of such system. Models are typically conceptual, existing as an idea, a computer program or a set of mathematical conceptualizations. Next, formal models are methods to represent the knowledge of a system using computational and/or mathematical structures. For systems biology, the theory of concurrency is at the basis of most approaches that have been applied. Many different formal methods, languages and modeling paradigms exist, that depend on the information, data and the model properties that guide the modeling process.

In systems biology, **Mathematical models** are, most often, equation based models that express mathematical relationships between quantities and how they change over time. The language in which they are specified is denoted by a set of equations that describes different parts, components or processes of a system and their behavior.

Next, **Computational models** are based on algorithmic process models that are executable and progress from state to state, not necessary time dependent. They use an algorithm/programing language to specify an abstract execution engine to mimic a design or natural phenomenon.

In an extended review, Fisher and Henzinger [35] distinguished between computational and mathematical models and how they are used to model biological phenomena. They survey the applicability and benefits of both approaches and how they can be interconnected. Essentially the distinctions are related to important information that drives the modeling decision, such as:

I. **Discrete or continuous:**

   A discrete model represents the behavior of the system in distinct spatial and/or temporal steps. The state variables change only at a countable number of points in time. In the time points an event or a change in state occurs. In a continuous model the behavior of the system is represented continuously. The state variables change in a continuous way, and not abruptly from one state to another. In fact, the number of states is infinite.

II. **Deterministic or nondeterministic:**

In deterministic models, series of events are determined at the onset and are precise. It is possible to predict what will happen in the system. In nondeterministic (stochastic) models, multiple outcomes of the processes can occur and the behavior of the system cannot be entirely predicted. In stochastic models, the rates and/or probabilities of events that can occur are included.

III. **Sequential or concurrent:**

As the name suggest, in a sequential model the events occur sequentially and a process cannot start before its predecessor has ended. It will always depend on information of the pre-process. In a concurrent model, different events can occur at the same time. Most process in biological system can be characterized by concurrency, and therefore should be modeled in such a manner

Although the description of mathematical models is based on equations, in systems biology computer power is used to describe and analyze such models. Therefore, algorithms and programs are used to implement such models. In the research presented in this thesis, we designate mathematical models as those models that are using process algebras, term rewriting systems or different mathematical structures; i.e. Stochastic Differential Equations, Ordinary Differential Equations, Partial Differential Equations and Delay Differential Equations. These mathematical models also include methods that are inspired by biological phenomena such as Brane Calculi [15], P-Systems [96], Biocham [14] and Calculus of Looping Sequence (CLS) [6]. Next, there are computational methods based on concurrent systems; i.e. Calculus of Communicating Systems (CCS) [27], π-Calculus[99], Bio-PEPA [2, 23], agent-based model (ABM) [46, 108], Petri nets [86, 98] as well as variants of this method [49, 61]. The modeling technique of Petri nets (PNs) is widely used to model biological behavior due its flexibility and strong emphasis on concurrency and local dependency. It comprises an abstract model of information flow, providing a graphical representation and a formal mathematical definition. The Petri Net model is the formalism that is used to model the biological behavior presented in this thesis. In the following section, we will provide an overview about Petri nets, its classes and definitions.

1.4 Petri nets

Based on a graphical representation and an underlying mathematical structure, the Petri net formalism is applicable to model the behavior of a concurrent distributed system that can be described in terms of system states and changes in these system states. Among the advantages to use Petri nets to model biological systems we can state that the model

- Has an intuitive graphical representation and a directly executable model

- Has a strong mathematical foundation providing a variety of analysis techniques
- Addresses structural and behavioral properties and also their relationship
- Integrates qualitative and quantitative methods as well as analysis techniques and simulation/animation
- Covers discrete and continuous, deterministic and stochastic, sequential and concurrent methods including hybrid techniques for quantitative and qualitative analysis
- Has a range of tools to support the implementation, simulation and analysis of the models

In the formal sense, a Petri net is a directed, finite, bipartite graph. Typically without isolated nodes, a PN is basically composed of three main elements [33]:

Places: are passive nodes that refer to conditions or local states of a system; they can be used, e.g. to represent resources; *Transitions*: are active nodes that describe local state changes in the system;

Directed arcs: specify relationships between local states and local actions by depicting the relations between places and transitions.

Tokens: are elements used to represent information in local states;

Places, transitions and arcs describe the static structure of the Petri net and how they are connected. A transition has *input places* to which it is connected by a number of places with a direct arc leading to the transition. Next, it has *output places* connected by a direct arc from the transition. Direct connections between two places or two transitions are not allowed. The tokens can be distributed in the places in order to define a state of the Petri net, referred to as a *marking*. The *state space* of a Petri net is the set of all possible markings.

The dynamic properties of the system are governed by a firing rule. It relates the transitions that can occur when enabled and then move tokens around the places in a Petri net. A transition can fire (occur) depending on the presence of tokens in its input places. The transitions fire by consuming the tokens from each of its input places and then producing (deposing) tokens on each of its output places. One of the elegant elements of the Petri Net formalism is the graphical notation; the notation helps to understand the flow of information through the net. A place is represented by a circle and a transition by a rectangle. Arcs connect a place to a transition. Tokens are represented by dots that pass through the net (cf. Figure 1.1).

The basic standard class of the formalism consists of place/transition Petri nets (PTNs). These nets are discrete and have no association with time or probability. Possible behaviors of the system are analyzed in terms of causalities and dependencies, without any quantification. A Petri net model can be enhanced with special read and inhibitor arcs as a means of modeling activation or inhibition of activities respectively. In addition, features can be added allow one to connect sub-models in a

hierarchical structure. In Chapter 3 we present a model that represents the bacterial-macrophage interaction in such a multi-scale structure.

There are several ways to add time to a net for quantitative modeling. In Continuous Petri nets (CPN) the discrete values of the net are replaced by continuous (real) values to represent concentrations over time [48]. In Stochastic Petri nets (SPN) an exponentially distributed firing rate (waiting time) - typically state dependent and specified by a rate function – is associated with each transition [85]. Hybrid Petri nets (HPN) [28] allow one to combine continuous and stochastic features of the process to be modeled.

Initially studied in [83, 88, 115, 116] and summarized by Marsan [78], Stochastic Petri nets can be considered as a timed Petri net in which the timings have stochastic values, where a firing delay (rate functions) is associated with each transition. It specifies the amount of time that must elapse before the transition can fire. This firing delay is a random variable following an exponential probability distribution. The semantics of a SPN with exponentially distributed firing delays for all transitions are described by a continuous time Markov chain (CTMC). Their firing transition follows the standard firings rule of QPNs, and do not consume time. The Stochastic Petri nets can also be enhanced with modifier arcs, which allow pre-places to modify the firing rate of a transition without influence on its enable state. There are also the special transitions: 1) deterministic which its firing delay is specified by an integer constant; 2) immediate which have zero delay and always high priority; and 3) scheduled which is a special case of deterministic transition which is specified at an absolute point in the simulation time at which it might occur (it will always depend if it is enable).

The Colored Petri nets, proposed by Jensen [60, 62], is an extension to the PN formalism in which information is added in the form of ‘colors’ (data types) assigned to tokens, allowing further operation and structure abstraction. The functional programming language Standard ML is used to manipulate and test data, providing a flexible way to create compact and parameterizable models. In a Colored Petri nets, to regulate the occurrence of transitions there are arc expressions that specify which tokens can flow over the arcs; and guards that are in fact Boolean expressions used to decide which transitions instances exist.

In the Colored Petri net, a transition is enabled (allowed to fire) if it has no input place, or if each of its input places is sufficiently marked by tokens: i.e. the arc expressions evaluate to a multi-set of token colors that should be available in the corresponding preceding place. In addition, the guard of the transition – if present – should evaluate to true for the given binding. When a transition fires a multi-set of colored tokens are consumed (taken) from each of the preceding places, according to the evaluation of the expression on the arc. A multi-set of colored tokens is produced (added), in correspondence with the arc expression, to each successor place. The overall state space of the Petri net is determined by the firing sequences consisting of iterated occurrences of transitions [33].

A typical example of a Colored Petri net and its components is depicted in **Figure 1.1**. Here both the graphical representation and the values that make of the QPN^C are given.. **Figure 1.1 (a)** shows the declaration of the data values assigned to the net defining two color-sets: *count* with integer values, and *individual* with a string *mm*; a constant *Max* with an integer value; the two variables: *k* and *x* used in arc expressions and the guard of the transition. The color-sets are assigned to places and the tokens on each place will have a color from a color-set assigned to the place. In **Figure 1.1 (b)** the net is defined with place *P1* (with color-set *individual*) containing 1 token with the color *mm*, place *P2* (with color-set *count*) containing one token with the integer value "1", and place *P3* (with color-set *individual*) without token. The transition *T1* is connected with the place *P1* by a read-arc that works as a test arc: if there is a token in *P1*, as described by the binding of *x* and that satisfies the firing rule, then the transition can occur, producing a token on the output places, but not consuming the token read in *P1*. Transition *T1* is connected to place *P2* by two arcs indicating that it will consume and produce tokens according to the arc expressions. **Figure 1.1 (c)** shows the new marking obtained when *T1* has read *P1* and consumed the token in *P2*, adding a new token in *P2* and P3 according to the firing rule. Repeating this process, the firing sequence will stop in the end state as shown in **Figure 1.1 (d)**. In this case, the guard condition turns false since the value of the token in *P2* does not fulfill the condition.

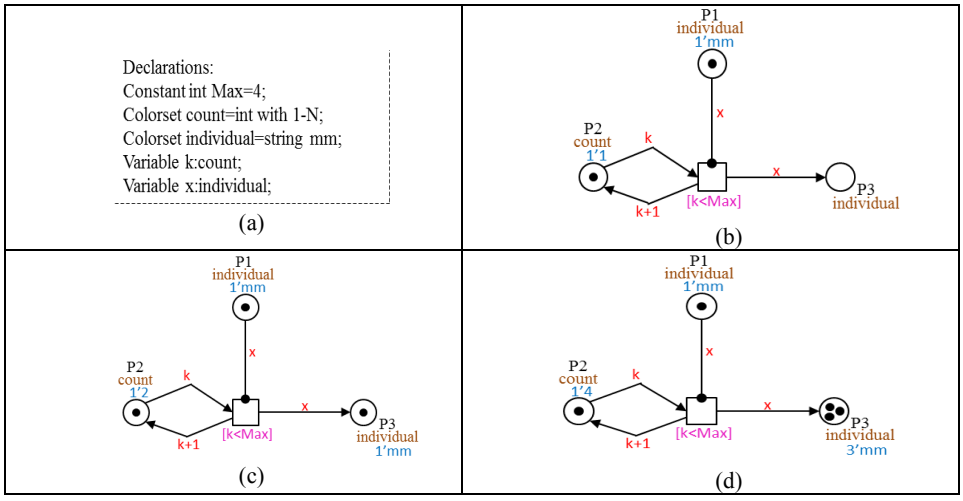

Figure 1.1. Colored Petri net example. **(a)** Declarations of the data types and variables. **(b)** Colored Petri net components. **(c)** State of the net after firing the transition. **(d)** End state of the net; the transition is not able to fire since the condition of the guard is not satisfied.

The Petri net and its colored extension permit to organize the formalism in a set of modules as a family of related Petri net classes, sharing structure, but being specialized by their kinetic information, dividing it in colored and uncolored: QPN – QPN^C (colored), SPN – SPN^C (colored),

CPN – CPN^C (colored), HPN – HPN^C (colored). The conversion of these classes can be realized by a folding process. This process groups similar model components in one colored model by defining color-set and the set of arc expression. The unfolding process dismembers a colored Petri net in one or more similar nets without colors. Moving between the colored and uncolored level changes the style of representation, but not necessary the net structure, though there may be loss of information in some direction. Heiner et al. [50] produced a classification of the different nets and **Figure 1.2** depicts their structure paradigm of the Petri nets formalism. . For practical reasons we adapt this classification as, in our case, this closely aligns with the tools that we use to compose the net. In Chapter 2 we present a qualitative colored Petri nets representing the dynamics of the infection process. In Chapter 4 and 5 we demonstrate the portability of the Petri nets formalism throughout its classes by presenting a QPN^C and a SPN^C respectively. A formal definition of the underlying Petri net classes used in this thesis can be found in **Appendix A, Appendix B and Appendix C.**

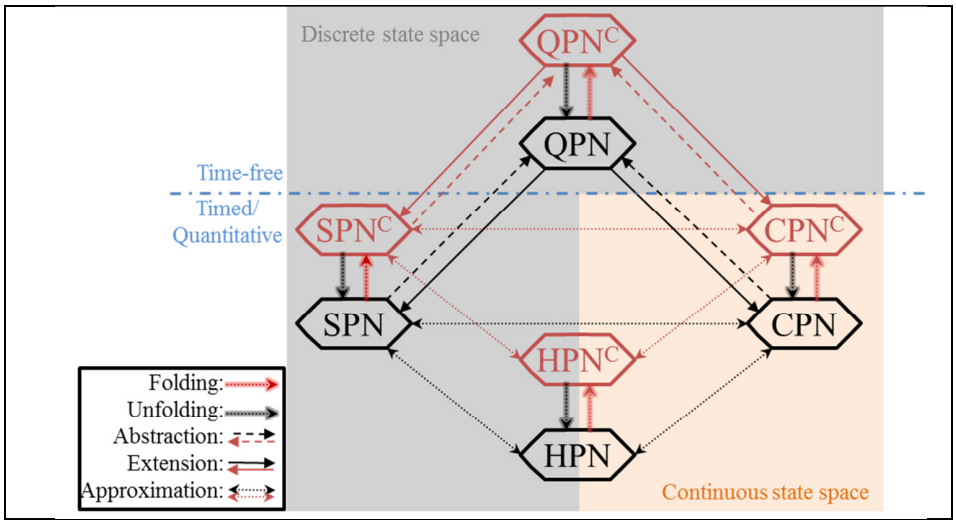

Figure 1.2. Paradigm structure of the Petri nets formalism. According to [50].

1.5 Model analysis

We have seen that for a model to represent the behavior of a biological system, it has to concisely summarize and replicate the information about the biological process as present in the system. Once a model has been constructed, it should serve as a clear description of the system, and can be unequivocally communicated. Therefore, an analysis of the model is required in order to verify and validate its structure and behavior. A reliable model is responsible to reproduce a biological process bringing evidences in reproduce a specific behavior and confidence on its predictive capability.

For the analysis of a model it is necessary to refer to the model objective and the information and data used in the modeling process. In the process of analysis we can test the model: does the model represent the hypothesis at hand?. Is the data concisely represented?. Does the model reproduce the problem? Moreover, the analysis of the model must consider the characteristics of the biological system that have been used to define the model properties (cf. Section 1.2). A **verification analysis** evaluates if the model meets its specification by checking the structure and behavior of the model. A **validation analysis** intends to ensure meeting the operational requirements by executing a model checking on the result.

One important (experimental) strategy to verify and validate the model is using simulation. The analysis of the results of a simulation can demonstrated the proper behavior of the model and also it can contribute to possibly further refine the model so the results approximate reality as close as possible. Although model simulations will never replace laboratory experiments, a model allows one to probe system behavior in ways that would not be possible in the lab. Simulations can be carried out quickly (often in seconds) and incur no real cost. Model behavior can be explored in conditions that are otherwise difficult to achieve in a laboratory settings. Every aspect of model behavior can be observed at all time-points. Furthermore, model analysis yields insights into why a system behaves the way it does, thus providing links between network structure modeled and observed in real experiments.

1.6 Petri nets in biology

In our descriptions until now it has been implicitly assumed that the Petri net formalism is applied on a case from the domain on biology, especially due to the concurrent nature that is overwhelmingly present in biological systems. The Petri net formalism has been successfully applied in systems biology in the representation of networks [67]; in particular, applications of Petri nets in regulatory and metabolic pathways [3, 45, 52, 59, 98, 128]. In addition to conventional graphical representations, the flow of information can be demonstrated and visualized. Different networks can be connected and what-if scenarios can be tried to understand the effect of presence and/or absence of a component. The common denominator of these domains is the concurrent behavior that needs to be captured in a model.

Systems biology requires integration and a next step in the application of Petri nets is to use it in the integration of the components in a systems biology analysis. Such components are described at different levels, the process level, the organismal level, the organ/tissue level, the molecular level and the gene level. A collection of PN's typically can integrate all these levels. We need to investigate how this can be done in the best possible manner and rather than constructing a theoretical framework, we investigate how the existing PN variants can be invoked in a multi-scale problem. The infection of *Mycobacterium* to a host is such a typical problem. It already includes two players each with the own agenda and still their strategies interfere. The *Mycobacterium tuberculosis* is the evil-doer for tuberculosis in human. In order to study the infection of mycobacterium a model system is used, the zebrafish. In zebrafish the *Mycobacterium marinum* is used to infect the host. The infection in the zebrafish model is used a case study to understand the process itself, how it can be represented in a Petri net and how it can be elevated in a Petri net representing a systems biology approach. In the next chapters the zebrafish infection is further explained in order to map it to a Petri net model. These models then gradually integrate more layers are able to represent this complex invader-host process.

1.7 Structure of this Thesis

This thesis is structured as follows: In Chapter 2, the steps related to the dynamics of the mycobacterial infection process and early immune response are used as basis for the first model. In this chapter, a qualitative model is presented in which one can visualize the process involved in the infection from the moment the bacteria enter in the host: Immune system detection, phagocytosis, migration, proliferation, granuloma formation and infection dissemination are the steps that drive the dynamics of the infection process. Chapter 3 presents a model that represents how the bacteria explore regulatory pathways, to evade host immune responses and enhance the infection inside the immune cell. In this chapter the introduction of hierarchical modeling process is introduced. The hierarchical model provides an overview of the important host-cell signaling pathways that occur at multiple (molecular, intracellular and intercellular) scales. Chapter 4 demonstrates the power of the computational method by coupling the two models from the previous chapters in one hierarchical structure. It presents a qualitative model that represents the infection process from the molecular interaction to granuloma dissemination. It is possible to correlate the information of the model, its structure and its results to behavior observed *in vivo*. Moreover, a 3D visualization is added to support the interpretation of the biological process. In Chapter 5, the qualitative model presented previously is extended to a quantitative model that, through support of empirical data, enables to do quantitative analysis as well as perform simulations and predictions. Data from zebrafish infection

studies were used as a basis for such quantitative model and different simulation scenarios were performed in order to verify and validate the model.

Following the content of Chapters 1 to 5, it gradually optimizes the knowledge and functionality of the modeling decisions by increasing the complexity of the model so as to better reproduce the biological behavior. As a result, new methodologies of modeling a biological system using computational methods were developed. An overview and discussion of this thesis is presented in Chapter 6 with the insights obtained from the research explored in previous chapters as well as pointing to new directions in the research of modeling biological systems.

2 Modeling innate immune response to early *Mycobacterium* infection

Based on:

Carvalho, Rafael V., Kleijn, Jetty, Meijer, Annemarie H., Verbeek, Fons J.: Modeling Innate Immune Response to Early Mycobacterium Infection. In: Computational and Mathematical Methods in Medicine, vol. 2012, 12 pages (2012).

Ленинград	Leningrad
Я вернулся в мой город, знакомый до слез, До прожилок, до детских припухлых желез.	I am back in my city, dear to me like my tears Like small veins, swollen glands of my infancy years.
Ты вернулся сюда, - так глотай же скорей Рыбий жир ленинградских речных фонарей.	You have come here, now go ahead in one gulp Down the fish-oil of Leningrad's river lights lamps.
Узнавай же скорее декабрьский денек, Где к зловещему дегтю подмешан желток.	Can you make out this day of December that's marred By the egg-yolk stirred into the menacing tar.
Петербург, я еще не хочу умирать: У тебя телефонов моих номера.	Petersburg! I don't want to die yet! You've still got my phone numbers I'm here to get.
Петербург, у меня еще есть адреса, По которым найду мертвецов голоса.	Petersburg! There're the addresses that I have had Where I still can find voices of those who are dead.
Я на лестнице черной живу, и в висок Ударяет мне вырванный с мясом звонок.	I dwell on the backstairs, and my temple is hit By the doorbell ripped out by the flesh of its meat.
И всю ночь напролет жду гостей дорогих, Шевеля кандалами цепочек дверных.	All night long I am waiting for my dear guests, As I stir the door chain shackles, having no rest.
Осип Мандельштам, Россия (1891 – 1938)	Osip Mandelstam, Russia (1891 – 1938)

Abstract

In the previous chapter we presented a survey of the importance of modeling biological system and the aspects involved in the process of designing a model. In this chapter we start the modeling process by defining the biological problem, the model objective and formulate the first model based on the information collected so far. In this chapter we present a simplified model that represents only part of the biological problem. The result points out the direction of the next steps in the modeling process, and how to extend the model in order to create a more accurate model of the biological problem here defined.

2.1 Introduction

Tuberculosis (TB) is an infectious disease responsible for million deaths annually. About one third of the world's population is infected with the pathogen that causes this disease, *Mycobacterium tuberculosis* (Mtb) [129]. Most infections are controlled by the host's immune system and remain asymptomatic. However, the *M*tb is capable to persist in the host inside granulomas, highly organized structures characterized by the presence of differentiated macrophages, lymphocytes and other immune cells that contain, but fail to eradicate, the pathogen [36, 81]. The key to success of *M*tb infection lies, at least in part, with the ability of the bacteria to proliferate inside host macrophages despite the antimicrobial properties of these cells. Some of the infecting bacteria can survive for extended periods within macrophages and in a granuloma. They establish long-term infections that may resurface later, for example when the host's immune system is compromised due to malnutrition, HIV co-infection, or immunosuppressive treatment. Insight in the mechanisms that contribute to this long and complex relationship between pathogen and host is essential to the understanding of the fundamental aspects of TB [26].

Various animal models are used to mimic *Mtb* pathogenesis in humans, each having their specific strengths as well as limitations. In recent years, the zebrafish has emerged as a valuable addition to mammalian models. They are genetically tractable and have an immune system with innate and adaptive branches, very similar to the human immune system. A particularly useful property is the transparency of the embryos, which allows for real-time imaging of the interaction between pathogens and host immune cells [30, 32, 80, 117]. *Mycobacterium marinum (Mm)*, one of the closest relatives of *Mtb*, is used to study mycobacterial pathogenesis in zebrafish. It causes a systemic tuberculosis-like infection in zebrafish, with the formation of structured granulomas that closely resemble those in human TB. The use of this model has recently contributed important insights into the function of the granuloma in expansion and dissemination of mycobacteria during the early stages of infection [82].

Mathematical and computational modeling provides an important additional avenue for the further exploration of disease dynamics. It offers powerful and complementary tools for the study of the host pathogen interaction. Gathering and analyzing the information from the animal model in a computational modeling process, makes it possible to describe, simulate, analyze and predict the mechanism and interactions behind the infection process in intuitive and easily analyzable terms. Agent Based Model (ABM) are a computational formalism based on rules that govern autonomous agents [7]. It can be used to model discrete as well as stochastic events in biology. Pappalardo et al. have implemented and simulated models using ABM and Cellular Automata to study the vaccine administration and immune response to cancer in mice [4, 92, 93]. Kirschner et al. have utilized ABM to model and simulate the *Mtb* disease and the host-pathogen interaction [65, 66, 72]. They

suggest ABM as an appropriate method for exploring complex spatiotemporal systems such as granuloma formation [108]. The PN formalism has already been successfully applied on case studies in biology to create, verify and validate models. Stochastic Active Networks (SAN) forms an extended Petri net model that uses probabilistic time, and is in particular useful for performance evaluation. Tsavachiou et al. [118] have used SAN in modeling and quantitative evaluation of the biological pathways involved in menopause. They use biological pathways and experimental data in an accurate quantitative model to simulate and compare to *in vivo/in vitro* experiments. Peleg et al. [94] have used Colored Hierarchical Petri nets to study effects of mutations in tRNA on the protein translation. They define qualitative models of molecular function at different levels of granularity. The application domain of tRNA was chosen due the abundant literature on tRNA molecular structure as well as the diseases that relate to abnormal structure.

Regarding the mycobacterial infection process, the interaction with host-pathogen is complex and much remains unknown. Significant specific immune factors present on the mycobacterial infection process still poorly understood. To date, mathematical and computational models applied to mycobacterial infection have been used to explore specific aspects at various biological scales (e.g. intracellular, cell-cell interactions, and cell population dynamics) [65, 72, 108]. The mycobacterial infection process thus is composed of numerous sub-processes, some of which are mutually dependent; giving rises to a very complex set of interactions. A model describing the process at a dynamic level that can connect such sub-processes is missing. Therefore we take the construction of a model of the infection mechanism at a higher level of granularity as a starting point for our modeling efforts and explorations. The availability of such a model enables to connect and visualize the whole infection process. This top-down approach allows identifying, modeling and testing of the lower level processes in both qualitative and quantitative manner. The input for these lower level processes can be obtained from both empirical research and literature data.

The *zebrafish* model of mycobacterium infection, based on *Mm* infection, has been identified as very useful in the understanding of host-mycobacteria interactions during early stages of infection. This model system is used to generate experimental data that elucidate the pathogenesis as well as to transfer the findings to the human case. The perspective of analysis from *in vivo/in vitro* studies requires an integration layer. Therefore, experimental data can be understood in the range of complex interactions that are underlying the infection process. We intend to construct such integration layer from an *in silico* perspective using the Petri net formalism as a modeling method to simulate bacteria-host interactions in early stages of tuberculous granuloma formation. As indicated, our starting point is to construct such a model from a higher level of abstraction. We, therefore, have designed a PN by first identifying the dynamics of the infection process; i.e., phagocytosis of mycobacteria by macrophages, the migration of infected macrophages to deeper tissue, the growth of mycobacteria within individual macrophages, and the granuloma formation and maturation [82].

These processes were represented in a colored qualitative Petri net (QPN^C) using the Snoopy software [54], a tool for modeling and animating/simulating hierarchical graph-based formalisms.

In our approach, we design the elements involved in the dynamics of the infection process by describing their causal relations. We have identified entities such as the zebrafish, the macrophage, the granuloma and the bacteria, in this manner the phases of the infection process are addressed. For the moment, time and probability are not considered. In this manner, our model explores the disease on a high level of abstraction, modeling the factors that are crucial to visualize the mycobacterial infection process and the early immune response. Complex processes involving cell-cell or cell-bacteria communication can be modeled in small scale process and incorporated into the model as a hierarchical layer. The model shows the cause-effect relations that trigger the infection process through a graphical representation in a manner biologists can grasp immediately. Now, as the model incorporates the process of infection, the toolbox of the biologist is extended with an approach that allows to perform "what-if" as part of the experimentation whereas, at the same time new experimental findings can be added to the model in a close collaboration between empirical and modeling scientists.

The remainder of this paper is structured as follows. In Section 2.2 we discuss the pathogenesis of the mycobacterium infection in Zebrafish in more detail and next we introduce the building blocks of the QPN^C and the software that we have used to build the model. In Section 2.3 as a result, we provide a series of design considerations to come to an implementation of the model. Finally in Section 2.4 we present the conclusion and discussion.

2.2 Materials and methods

2.2.1 The zebrafish model of mycobacterial pathogenesis

The zebrafish is naturally susceptible to infections caused by *Mycobacterium marinum* (*Mm*), genetically closely related to *Mycobacterium tuberculosis* (*Mtb*). The *Mm* infection shares pathological hallmarks with *Mtb* infection. Like other pathogenic mycobacteria, *Mm* causes chronic infection of macrophages resulting in tuberculous granulomas, making it a useful model to study mycobacterial pathogenesis [8]. Zebrafish embryos have functional innate immune cells (macrophages and neutrophils), while their adaptive immune system is not yet functional. Injected bacteria into the blood circulation or into tissue initiate the experimental infection of zebrafish embryos. Macrophages that are attracted to the site of infection take up the mycobacteria by a process called phagocytosis. Real-time imaging of infected zebrafish embryos has allowed the direct observation of the arrival of phagocytes at the infection site and their uptake of bacteria. The

macrophages are the primary cell type infected with *Mm,* however also infected neutrophils have been observed [6, 8] and were recently shown to play an important role in Mm infection control [130]. In **Figure 2.1** an Mm infection in a zebrafish is depicted.

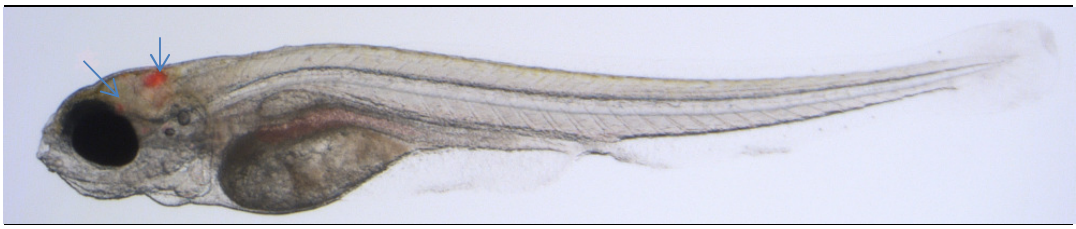

Figure 2.1: Microscope image of a zebrafish larva infected with *Mycobacterium marinum* by injection used for the study on infection progression and immune system response. Image is obtained with a Leica Stereo Fluorescence Microscope commonly used in zebrafish research. Here the microscope image is depicted with an overlay of a fluorescent channel (red) in which the bacteria are visualized. The arrows indicate granulomas that have developed after an induced infection with *Mycobacterium marinum.*

Inside the macrophage, bacteria can be exposed to bactericidal mechanisms and degraded in lysosomes. However, intracellular mycobacteria are predominantly distributed between the early and late phagosomal compartments, with some also escaping into the cytoplasm [22, 23]. Similar to *Mtb*, *Mm* escapes from lysosome degradation and its survival inside macrophages is facilitated through the dynamic modulation of a range of cellular processes. These include inhibition of pathways involved in the fusion of the phagosome with lysosomes, antigen presentation, apoptosis, and the activation of bactericidal responses [104, 113, 114]. Mycobacterial interference with the host signaling machinery severely compromises the immune defenses. Therefore, mycobacteria multiply inside the macrophage over time causes its death, thereby enabling further spreading of the infection.

Once it has become infected with mycobacteria, the macrophage starts to induce recruitment of uninfected macrophages. Studies have established an important role for a mycobacterial virulence factor, the ESX-1 secretion system, in the recruitment of new macrophages to granulomas and the expansion of infected macrophages [5, 25, 26]. These macrophages efficiently find and phagocytosis infected macrophages and bacteria that are released from dead cells. In this process these macrophages are getting infected too and the aggregated macrophages become activated. A transformation reflected by an increase in their size and subcellular organelles, ruffled cell membranes and enhanced phagocytic and microbicidal capabilities. A common feature of all *mycobacterium* granulomas is the further differentiation of the macrophages into epithelioid cells. They have tightly interdigitated cell membranes in zipper-like arrays linking adjacent cells. Those aggregates grow into organized structures that are referred to as granulomas, lumps of immune cells that surround the infection [114].

Primary granulomas are capable of disseminating infection throughout the body by egression of infected macrophages. This process suggests that granuloma macrophages constitute the major mechanism for dissemination of the infection [32]. These granulomas are the hallmark of the tuberculosis disease in both human and animal models. In **Figure 2.2** a schematic representation is depicted of the early stages of the mycobacterial of the pathogenesis infection process.

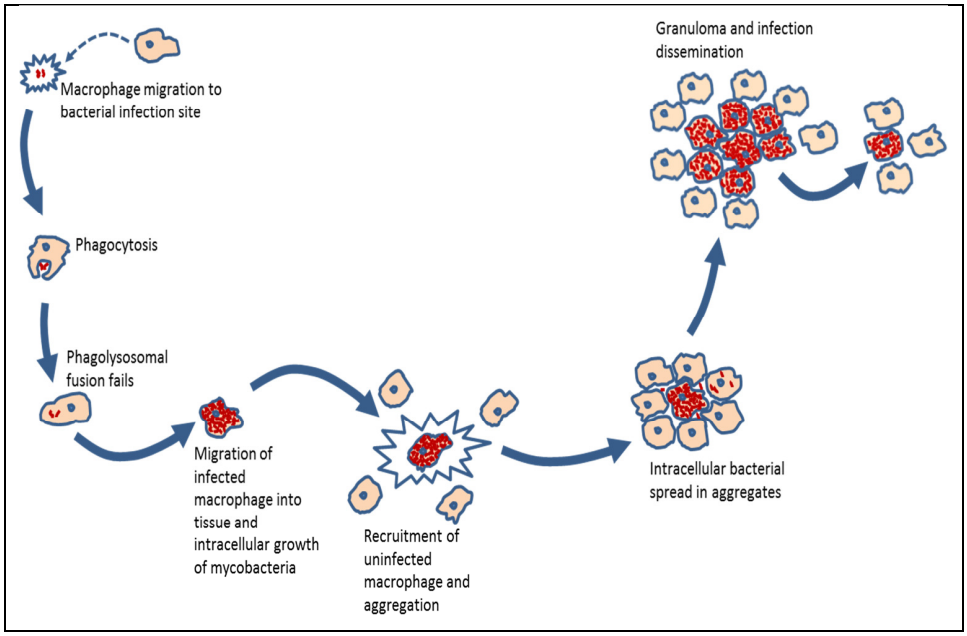

Figure 2.2: Schematic representation of the early stages of the immune response to the early stages of the mycobacterial infection process. Figure is an authors' rendition adapted from [71]

2.2.2 Computational model

Experimental research has generated a tremendous amount of insights into host-pathogen interactions that occur during mycobacterial infections. Mathematical and computational models can offer powerful and complementary methods in support for better understanding the mechanisms behind the infection process in intuitive and easily analyzable terms. Amongst these methods we can refer to modeling approaches such as Brane Calculi [15], π-Calculus [99], Agent Based Modeling (ABM) [108] and Petri nets (PN) [98]. These modeling methods can be used to describe, simulate, analyze and predict the behavior of biological system by turning what is known about the biology into equations and/or rules to describe and ultimately understand the system. Previously, we proposed a system for modeling, simulating and visualizing the *Mycobacterium* infection and granuloma formation. We discussed the basic layout and the modeling challenges for this approach.

Moreover, evaluated between computational methods the Petri net as an appropriate method for the modeling of the infection process [18].

In order to create a flexible, compact and parameterizable model, we decided to use a QPN^C to model the early stages of the infection process and granuloma formation. Although standard Petri nets can be used to model parts of our problem, such as reaction processes and biochemical components, it becomes impractical to represent different levels of abstraction, when in addition, other aspects have to be taken into account such as the physical and spatial organization of the organism, from the intracellular to the intercellular level and beyond (molecular, cellular, tissues). Colored Petri nets allow the description of several similar network structures in a concise and well-defined way, providing a flexible template mechanism for network designers. In Colored Petri nets, tokens can be distinguished by their colors. This allows one to discriminate levels (molecules, metabolites, proteins, secondary substances, genes, etc.). In addition, the tokens colors can be used to distinguish between sub-populations of a species in different locations (cytosol, nucleus and so on). A formal definition of the Colored Petri nets can be found in **Appendix C.**

2.2.3 Software and hardware platform

Several tools are available to model biological systems using Petri nets, simulate their dynamic behavior and analyze their structure. The Snoopy software provides an extensible, adaptive and multiplatform framework to design, animate and simulate Petri nets [54]. Its design facilitates the modular implementation of our QPN^C model allowing future extensions to be added through hierarchical organization of Petri nets. We have used the Snoopy software to implement and animate our net with two different operating systems (OS): Windows 7 (HP Intel core i7, 4 Gb RAM) and Mac OS 10.6 (MacBook Pro Intel core i7, 4 Gb RAM). The main difference between the two platforms is the additional features in the user-interface for the Windows implementation. The QPN^C model runs with the same accuracy on both OS-versions. This illustrates the platform independency of the Snoopy software framework.

2.3 Results

We have modeled the role of the innate immune system in the early stages of a *mycobacterial* infection. Our approach is to provide a large-scale model that drives the infection behavior using Colored Petri net. We have defined the color sets $\mathbf{\Sigma}$, places $\mathbf{P}$, transitions $\mathbf{T}$, and the initial marking $\mathbf{I}$ present in our $\mathbf{QPN^C} = (\mathbf{\Sigma}, \mathbf{P}, \mathbf{T}, \mathbf{A}, \mathbf{C}, \mathbf{G}, \mathbf{E}, \mathbf{I})$.

2.3.1 Set of color sets $\boldsymbol{\Sigma}$

We have defined five simple color sets: ***Position, Individual, Status and Count***; and four compound color sets: ***Macrophage, Bacteria, Proliferation, Granuloma*** composed of the basic colors sets. They represent empirical information from the infection process:

- ***position:*** is an integer value representing the location of a macrophage, bacteria and/or granuloma;
- ***individual:*** is a string value (mm, mac) used to identify bacteria and macrophages*;*
- ***status:*** is a Boolean value, it can represent the infection status (healthy/infected) of a macrophage or the saturation of a proliferation;
- ***count:*** is an integer value representing a threshold for the simulation;
- ***Macrophage:*** is composed of ***Position***, ***Individual*** and ***Status*** colors and represents host macrophage immune cells;
- ***Bacteria:*** is composed of ***Position*** and ***Individual*** colors and represents *M. Marinum* bacteria that will be injected;
- ***Proliferation:*** is composed of ***Count***, ***Individual*** and ***Status*** colors and represents the amount of infected aggregated macrophages;
- ***Granuloma:*** is composed of ***Position***, ***Individual*** and ***Count*** colors and represents granulomas with the amount of macrophages.

2.3.2 Set of places $\boldsymbol{P}$

The set of places of our QPN^C is defined as:

$\boldsymbol{P = \{Infection, ImmuneSystem, Phagocytosis, Migration, BactGrowth, Checkpoint, Condition, DeadMacrophage, RecruitmentCount, AgregationAmount, StopSignaling, Maturation, Dissemination\}}$

They represent population of cells and multicellular complexes that are part of our model:

- ***C(Infection)={Bacteria}:*** a place with the mycobacteria that intrude the host;
- ***C(ImmuneSystem)={Macrophage}:*** a place containing the immune cells (healthy macrophages) that will react to an infection signaling;
- ***C(Phagocytosis)={Macrophage}:*** a place containing the infected macrophages;
- ***C(Migration)={Macrophage}; C(BactGrowth)={Proliferation}:*** places containing information about the bacterial replication within one macrophage and its movement;
- ***C(DeadMacrophage)={Macrophage}***; ***C(AgregationAmount)={Granuloma}:*** places containing dead macrophages and the aggregation of recruited healthy macrophages (granuloma);

- ***C(Maturation)={Macrophage}; C(Dissemination)={count}:*** places containing information about the infected aggregated macrophages (intracellular bacterial spread) and the control of the infection dissemination;
- ***C(Checkpoint)={status}*;*C(Condition)={status}*;*C(RecruitmentCount)={coun}; C(StopSignaling) = {count}:*** places controlling the flow of the simulation.

2.3.3 Set of transitions ***T***

The set of transitions of our model is defined as:

$$\boldsymbol{T} = \{\boldsymbol{BacSignalling}, \boldsymbol{MacSignalling}, \boldsymbol{IntracelullarSpread}, \boldsymbol{Spread}, \boldsymbol{t1}, \boldsymbol{t2}, \boldsymbol{t3}, \boldsymbol{t4}\}$$

They describe important events that govern the infection process, refer to the molecular interaction, signaling reaction and intracellular changes; they also regulate some thresholds that control the simulation:

- ***BacSignalling:*** represents the signaling process when bacteria reach the host;
- ***MacSignalling:*** represents the signaling process of an infected macrophage after its death (recruitment of healthy macrophages);
- ***IntracelullarSpread:*** represents the bacterial replication among the aggregated macrophage in the granuloma;
- ***Spread:*** represents the dissemination of granuloma infection;
- ***t1, t2, t3 and t4:*** represent the control-thresholds of the simulation.

2.3.4 Initial marking ***I***

The initial marking in our model determines for each place the number and type of colored tokens initially present in the places. We have the condition markings that are fixed and used to control the process, and the example markings, which are used in our example and can be modified without changing the workflow. They are defined as:

Condition markings:

- ***I(Checkpoint)=1`(true):*** initialized for checking if the bacterial replication inside the macrophage reaches its limits;
- ***I(RecruitmentCount)=1`(0):*** initialized for counting the number of macrophages recruited to aggregate into the dead macrophage;
- ***I(BactGrowth)=1`(1,mm,true):*** initialized to trigger replicating the bacteria inside the macrophage;
- ***I(Dissemination)=1`(0):*** initialized to keep count of the dissemination of the granuloma.

- ***I(Condition)=1`(true):*** initialized to enable one infected macrophage become dead and start the signaling process.

Example markings:

- ***I(Infection)=1`(1,mm) + 1`(2,mm) + 1`(3,mm):*** defines the initial concentration of the mycobacteria that will intrude the host. We have defined three different positions to represent different injection sites;
- ***I(ImmuneSystem)=1`(1,mac,false) + 1`(2,mac,false) + 1`(3.mac,false) + … + 1`(10,mac,false):*** defines the initial concentration of healthy macrophages in the host. The positions and amount of healthy macrophages are empirical and used just to represent their presence in the host;

All other places are initially empty, i.e. there are no tokens at the onset.

2.3.5 Implementation and execution of the model

Our model is motivated by the biological problem discussed in Section 2.2 and it specifically focuses on the process of granuloma formation and infection dissemination. The environment of the model represents the innate immune response based on the *Mycobacterium marinum* infection process in the zebrafish embryo. Although at this level, the QPN^C model can be used to describe the early immune response to any kind of mycobacterial infection process. The elements of the Colored Petri net described in the previous sections represent key factors involved in the processes of infection, innate immune response, and granuloma formation. The rules of the model represent the biological interactions as described in Section 2.2.1, i.e.:

- Signaling of intruding bacteria detected by healthy macrophages followed by phagocytosis;
- Migration and intracellular bacterial replication within infected macrophages and their death;
- Recruitment and migration of healthy macrophages in response to the dead macrophage signals;
- The aggregation process and granuloma formation;
- The bacterial spread in the aggregate macrophage and the infection dissemination.

Figure 2.3 shows the prototype model in a Colored Petri net implemented using the Snoopy. Arrows labeled with a black dot as an arrow head are so called testing arcs: they represent two arcs in opposite directions between the place and transition with an identical arc expression, however, the tokens are not consumed, just tested for their presence.

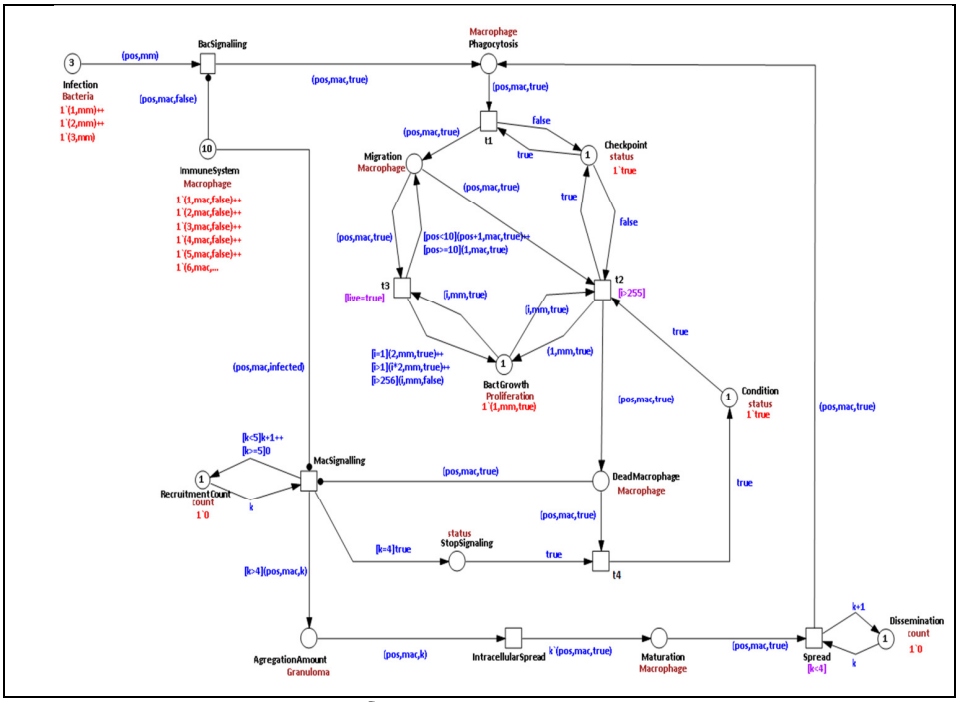

Figure 2.3: Screenshot of the QPN^{C} modeling the early stages of the immune response to the mycobacterial infection process implemented in snoopy software.

As initial conditions to our model, we have defined some numbers as boundaries to check the behavior of the net using the simulation mode in the Snoopy software. The intracellular bacterial spread is limited to a concentration of 255 bacteria. In the literature no specific information was found about the capacity of a macrophage or about its absolute position. In early stages of the zebrafish embryos it is known where the macrophages are not present [30]. For this reason we have defined 10 relative positions to represent the presence of macrophages and their movement during the infection process and granuloma formation. In order to keep the model straightforward, we also limit the concentration of aggregated macrophages (cf. Fig. 2.5). Next, we have defined a threshold concerning the infection dissemination; i.e. we limit the concentration of dissident macrophages that are released from the granuloma. Although from *in vivo/in vitro* experiments it seems that the dissemination is regulated by the adaptive immune system [5, 15], we have not considered this to be in the scope of our model.

The infection starts when the mycobacteria intrude the host. In our model we concentrate on three different positions of the mycobacteria **(1,*mm*)**, **(2,*mm*)**, **(3,*mm*)**. Each position represents different injection sites used in the experiments with the zebrafish animal model (yolk, caudal vein or hindbrain ventricle). In our example, the bacteria are detected by the innate immune system by signals to immune cells. The model describes healthy macrophage **(1, mac, false)**, **(2, mac, false)**,

(3, mac, false) … **(10, mac, false)**, to take up the bacteria (phagocytosis). **Figure 2.4** shows this process.

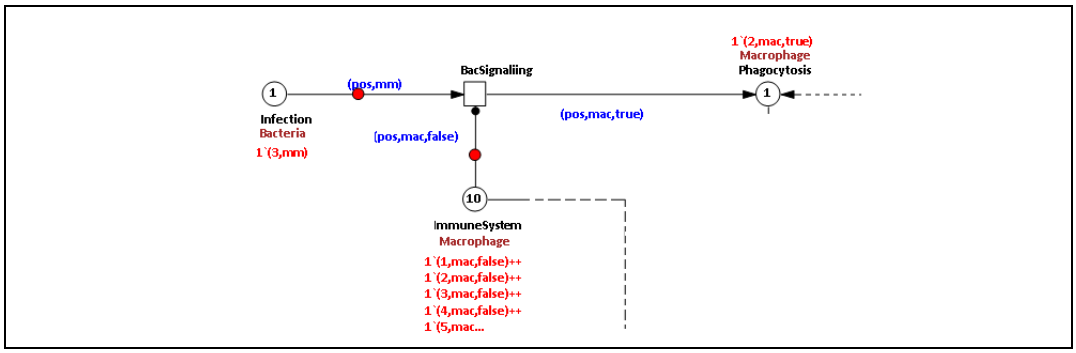

Figure 2.4: Screenshot of the infection detection and phagocytosis process.

After phagocytosis, the bacteria start to proliferate and move within the macrophage; the macrophage changes its position, moving to deep tissue while the bacteria replicate inside the macrophage. The intracellular growth of mycobacteria is modeled as bacterial multiplication until a concentration of 255; causing the death of the macrophage. **Figure 2.5** depicts this process.

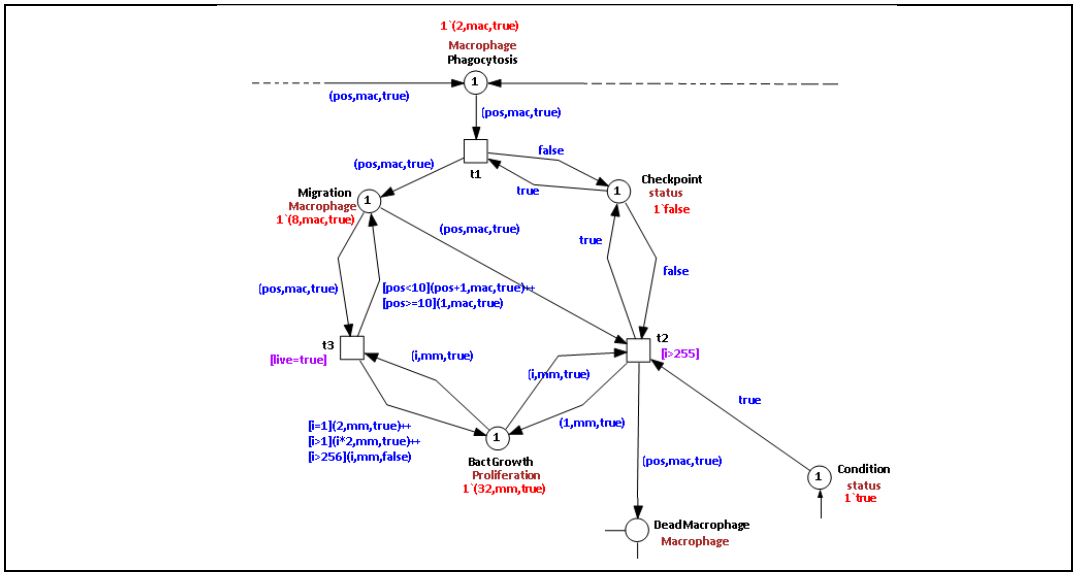

Figure 2.5: Screenshot of the migration and bacterial replication within macrophage causing its death.

A dead macrophage starts to signal, recruiting new healthy macrophages to take up the infected macrophage and the bacteria. In this way aggregates of immune cells are formed. The aggregates contain the bacteria but are unable to get rid of them. This process is visualized in **Figure 2.6** where

a dead macrophage **1`(10, mac, true)** is recruiting new macrophages to aggregate. The recruitment of macrophages is controlled by the **MacSignalling** transition that stops when four healthy macrophages are recruited. The numbers of macrophages that are recruited are set such that a minimal number will give rise to the formation of a granuloma. The latter is important in the development of the infection and the disease in general. The number can be increase if a particular scenario for an *in silico* experiments so requires. It will not alter the general layout of the net rather create different balances. The place **RecruitmentCount** controls that.

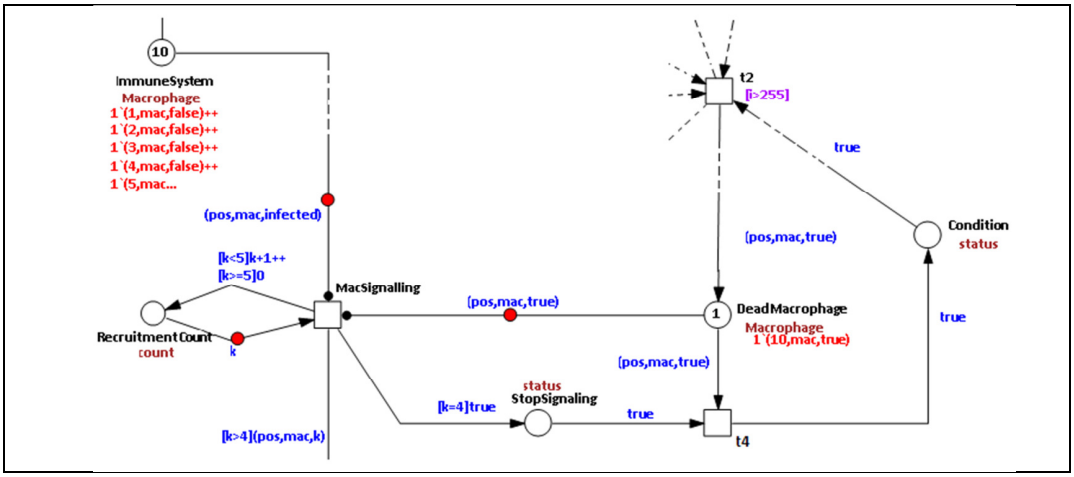

Figure 2.6: Screenshot of the dead macrophage signaling and aggregation process.

As these aggregates grow, structures develop that are referred to as tuberculous granulomas, lumps of immune cells that surround the infection. **Figure 2.7** shows the representation of this process in our model, where one granuloma is formed at the position 10 with a concentration of five macrophages10 **1`(10, mac, 5)**.

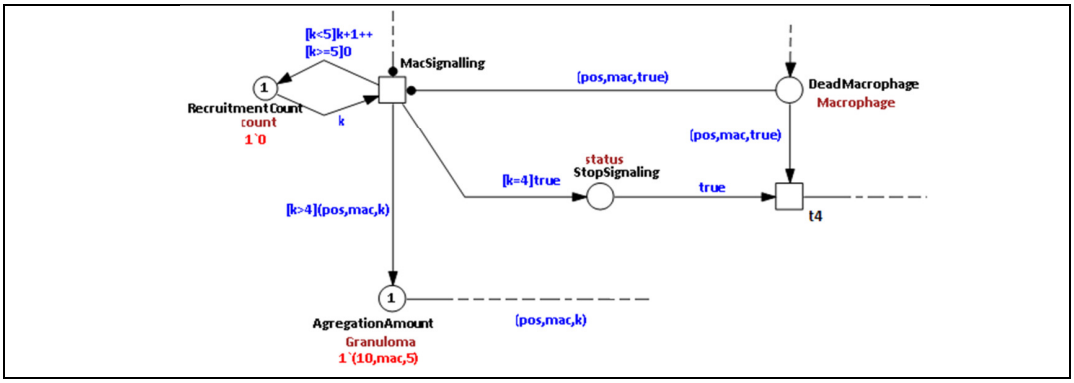

Figure 2.7: Screenshot of the granuloma formation process.

The intracellular mycobacterial spread in the granuloma is visualized in our model by the process depicted in **Figure 2.8**. There, all five immune cells that form the granuloma on the position 10 {**5`(10, mac, true)**} get infected and start the process of dissemination.

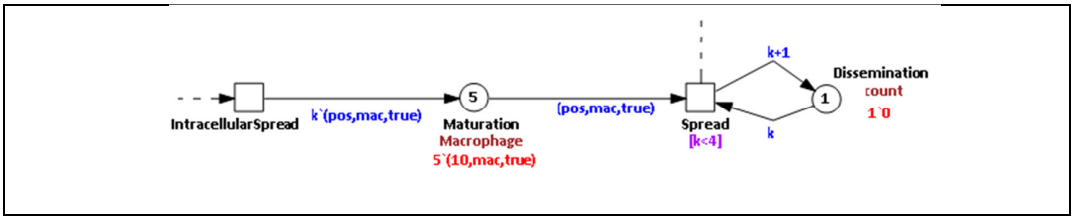

Figure 2.8: Screenshot of the intracellular mycobacterial spread and infection dissemination process.

In the dissemination process, an infected macrophage leaves the granuloma structure {**3`(10, mac, true)**} and starts another infection. The process repeat: moving, hosting an intracellular mycobacterial replication, dying and repeating the granuloma formation process on another position. This process is visualized in **Figure 2.9**.

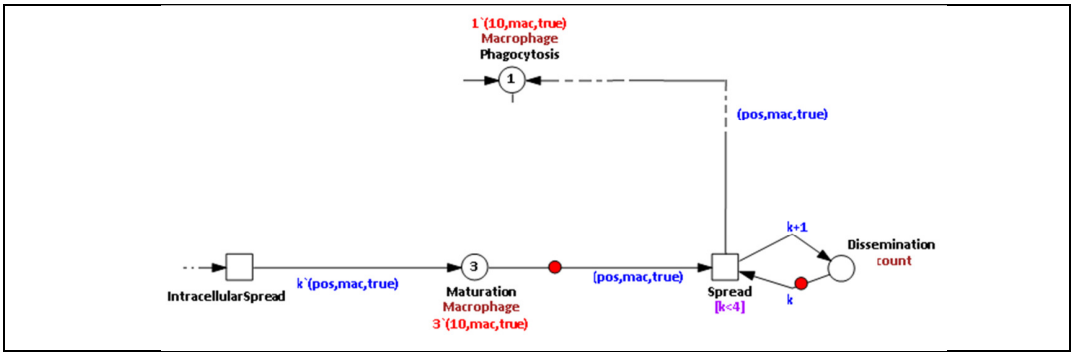

Figure 2.9: Screenshot of the granuloma formation process on the dissident infected macrophages on different positions.

The outcome of our model reproduces the early stages of the mycobacterial process and the innate immune response. We used the animation mode available in the Snoopy software to verify the dynamic behavior of our model. This property allows to animate the token-flow of the net as well as to observe the causality of the model and its behavior. For inspection and perusal, the animation sequence can be found at http://bio-imaging.liacs.nl/galleries/cpn-mmarinum.

2.4 Conclusion and discussion

The aim of this work is to introduce a modeling approach new to the modeling of the innate immune response in a model; this model represents the dynamic behavior of the mycobacterial infection

process. We consider our model to represent a high level of abstraction in which the infection process can be visualized in a large-scale model. We use the Petri net formalism as a formal modeling method because of its extensible, modular, easy and intuitive construction properties different from other and more broadly used modeling frameworks [49]. We have developed a high level abstraction of the infection process by designing a PN by acknowledging the major processes of the *mycobacterium* infection together with the basic actors that are involved in these processes.

As a result we have delivered a QPN^C model that expresses, at a high level of abstraction, the details that are involved in the early stage of mycobacterial infection. Information about the mycobacterial infection process, the innate immune response and the infection dissemination can be observed in our model. Through a parameterizable net, the model assembles information about the host-pathogenesis interaction phases. It provides a visualization of the structure and dynamics of the infection process. The scalability of our model allows extension on different levels of abstraction providing the aggregation of independent and related model hierarchically i.e., gene expression pathways, molecular process, cell-to-cell interaction events, etc. In this manner allowing experiments that simultaneously track molecular, cellular, tissue, organism and population scale events. Biologists have greatly appreciated the visualization of the processes through the animation of the PN.

Several reliable tools have been developed to create and investigate qualitative and quantitative properties of Petri nets by structural analysis, simulation of time-dependent dynamic behavior and model checking. In the research presented here we have chosen the Snoopy software [54] to implement and animate our model. This software is extensible, and adaptive through support of simultaneous use of several models. Moreover, it is platform-independent. Further extensions are to investigate the quantitative properties of the process. Such can be accomplished using the Charlie tool [38] so as to verify and validate the net and further analyze our model.

A systems biology approach, integrating both modeling and experimental aspects, has much to contribute to the study of host-pathogen interactions. Biological processes that are relevant to the immune response occur at different scales or levels of resolution: i.e., molecular, cellular and tissue level [39, 40]. Development of multi-scale, multi-compartment models based on *in vivo/in vitro* experimental data is essential to create a computational system that reflects this biological behavior [77]. Starting from the abstract model of the global infection process as presented in this work, future extensions can be modeled. Therefore, sub-models representing processes on tissue, cellular and molecular scale will hierarchically connect as a single model. In close collaboration with the empirical scientist and using the model, we intend to perform *in silico* experiments that are otherwise impractical or not feasible *in vivo* or *in vitro*. Thereby, predicting results of new experiments and generate further hypotheses about the immune system response to mycobacterial infection. The QPN^C model presented in this paper is the cornerstone of that process.

In summary, we have developed a straightforward model to explore the early mycobacterial infection and the immune response. Modeling the steps that regulate the infection process require further testing on both theoretical and experimental level. The results of these *in silico* experiments/findings can become the input for further analysis. It will support, for example, identification of key parameters or mechanisms, interpretation of data, or comparison of the capability of different mechanisms to (re)generate the observed data. Finally, a model that successfully describes existing experimental data may be used in the prediction of results from new experiments. It can generate further hypotheses about the immune system response to mycobacterial infection, helping to unravel the mechanisms of TB infection [91]. As indicated from the design of our QPN^C, the next steps in the development of the net are to add lower level processes representing the tissue, cellular and molecular interactions relevant to the infection process. The QPN^C accommodates this as hierarchical layers. Along with these layers numerical data will become available that will allow to elaborate on the quantitative aspects of this process. The interplay of hierarchical levels and quantitative information has the potential to develop to a powerful tool for the research in tuberculosis disease. Hopefully it will further mature in a paradigm for integrated research to infection diseases.

3 Multi-scale Petri net model of the bacterial–macrophage interaction

Based on:

Carvalho, Rafael V., Kleijn, Jetty, & Verbeek, Fons J.: A Multi-Scale Extensive Petri Net Model of the Bacterial-Pathogen Interaction. In: Heiner, M. (ed.) 5th International Workshop on Biological Process & Petri Nets. Pp. 15-29. CEUR Workshop Proceedings 1159, Tunis, Tunisia (2014).

O, Arbeid	Oh, Labor
Niet de partijen Niet de stellingen Niet de woorden Niet het zijn	Not the parties Not the propositions Not the words Not the being
Leven of sterven Winnen of verliezen Het is alles een Recht of waarheid Blijft alles het zelfde Zonder arbeid is er geen	To live or die To win or lose It is all one Law or truth Everything remains the same Without labor, there is none
Arbeid alleen kost al dit leven Leven is dus arbeid alleen.	Just labor costs all this life So life is just labor.
Marinus van der Lubbe, Nederland (1909 – 1934)	Marinus van der Lubbe, Netherlands (1909 – 1934)

Abstract

A primordial step in the modeling process is refinement. This becomes feasible once more information about the phenomenon under study, i.e. bacterial infection, is collected. Therefore, we can extend the model allowing more complexity according to the information acquired. The previous chapter has indicated the direction for the refining process, where increasing the complexity is directed to modeling the interactions that occur at cellular and molecular level. In this chapter we, therefore, gather the information about the complex pathways related to the infection persistence modeling them in a hierarchical structure. The result is a model that can perform qualitative simulations in order to mimic the alternatives that might occur during the infection.

3.1 Introduction

Tuberculosis (TB) is the second greatest killer disease worldwide due to a single infectious agent: *mycobacterium tuberculosis (Mtb)* [129]. Effective vaccination against tuberculosis is a challenge; a better understanding of the host-pathogen relationship provides an important key for new treatments. The host innate immune response is the first line of defense against invading microbes. It recognizes the pathogen in the first stage of infection and initiates an appropriate immune response. Therefore it has been the subject of much scientific research involving mycobacterial infection [24, 30, 69, 71, 110, 111] .

The complex interactions between bacteria and the immune cell involve various structures and processes that control, activate and inhibit proteins and signaling pathways in a dynamical system that determines the outcome of an infection [20]. A systematic approach to modeling these interactions should help to comprehend the events that occur between the host and pathogen [124]. Different methods have been used to model the mycobacterial infection process: Gammack *et al*. [41] provided a mathematical model based on Ordinary Differential Equation (ODE) to investigate the early and initial immune response to Mtb. Such work has inspired Segovia-Juarez *et al*. [108] to implement the ODEs that regulate the interaction between host and pathogen using an agent-based approach, and Warrender *et al*. [124] use the CyCells simulator tool to simulate the interactions in Early *mycobacterium* infection.

Mathematical models, like those based on differential equations, are difficult to obtain and analyze when the number of interdependent variables grows and when the relationship depends on qualitative events. The computational models used for this problem offer an additional avenue for exploring the infection dynamics through the visualization of a specific behavior simulation. However, in both cases the interactions between bacteria and the immune cells and their structures are not intuitively described. The interactions are embedded in programing code and/or described in rules, which are not straightforward to interact with, nor comprehend their relationship.

A graphical representation of the interactions and influences among the various molecular and cellular components that involve the bacteria and host immune cells that also captures the dynamics of the system should be very useful. The framework of Petri nets represents a well-established technique in computer science for modeling distributed systems [105] and they have been successfully used to model biological behavior. Heiner *et al*. [52] propose a methodology of incremental modeling using Petri nets. They develop and analyze a qualitative model of the apoptotic pathway. In our previous work [19] we have developed a qualitative model of the mycobacterial infection process and the innate immune response. We modeled the cell dynamics level, characterized by the steps that are involved in the *Mycobacterium marinum* infection and granuloma formation in zebrafish.

In this paper, we extend our model and focus on interactions between the bacteria and the host immune cells - specifically the macrophages - in a multi-scale model. We identify and connect the important pathways involved in the host-pathogenic interactions that act over different scales (molecular, intracellular, and intercellular) during the innate immune response. The model captures the quintessential functional processes of the macrophage upon exposure to mycobacteria, their interconnections, subsequent signals and activation of the immune response. It provides a visualization of the signaling pathways that the host immune cell utilizes to terminate the infection as well as the way the pathogen exploits the pathways of the macrophages to enhance its intracellular survival persistence. This Petri net model makes it possible to perform "what-if" situations as part of the experimentation, simulating possible pathway disruptions and the consequences to the infection process. In this paper, we demonstrate the power of the Petri net formalism in modeling signaling and metabolic pathways that are involved in the host-pathogen interaction in a multi-scale model. We simulate and animate three different dynamics to mimic the alternatives that might occur once a bacterium is phagocytized by a macrophage and persists in infection. As a next step we plan to consider a qualitative validation of the model so as to confirm consistency and correctness of its biological interpretation.

3.2 Mycobacteria interaction with macrophages

Macrophages play rather contradictory roles in infection and disease as they are likely the first host immune cells to respond to invading mycobacteria, and yet aid in subsequent dissemination of the bacteria [37]. The successful parazitation of macrophages by mycobacteria involves the inhibition of several host-cell processes, which allows the bacteria to survive inside the host cells. The host processes that are inhibited by the pathogenic bacteria include fusion of *Phagosome* with *Lysosomes*, antigen presentation, apoptosis and the stimulation of bactericidal response [68].

Mycobacterial cells release a mixture of lipids and glycolipids that interfere on the macrophage response towards elimination and enabling bacterial survival [104]. Mannosylated Lipoarabinomannam (ManLAM) is one of the major modulators of phagosome maturation [112]. It prevents fusion of mycobacterial phagosome with the late endosome and lysosome by inhibiting the Calmoduling-Ca^{2+} phosphotidol-inositol-3 kinase [40]. Ca^{2+} also has an influence on the apoptotic pathways since it increases the permeability of mitochondrial membranes releasing pro-apoptotic elements to facilitate apoptosis [68]. ManLAM also influences the apoptosis by phosphorylating the apoptotic protein Bad leaving the anti-apoptotic protein Bcl-2 free which inhibits caspase activity and functions as an anti-apoptotic regulator [1].

Macrophages and T cells produce many cytokines that promote or inhibit protective response to the mycobacterial infection. An important family of cytokines is the interleukin-10 (IL-10), which

regulates the pro-inflammatory (PICs) and anti-inflammatory (AICs) cytokines. The bacteria can limit macrophage apoptosis by inducing the production of IL-10 which blocks the synthesis of Tumor-Necrosis Factor (TNF), a stimulator of apoptosis in infected macrophage [84, 107]. It is likely that bacteria prevent apoptosis in the early phase of infection to allow them to replicate efficiently. However, in the later phase, they induce or are unable to prevent cell death, which might facilitate their systemic dissemination through uptake into immune cells [68].

3.3 Cell-cell host pathogen interaction

The modulation of host signaling mechanism is a dynamic process requiring mycobacterial components that trigger or inhibit the host response such as the fusion of Phagosome with Lysosomes, antigen presentation, apoptosis and stimulation of bactericidal responses due to the activation of pathways that leads to the bacterial survival. The immune cells can identify the pathogen through Pattern Recognition Receptors (PRRs), which are found on the cell surface, on the endosomes and on cytoplasm. It triggers a cascade of events that leads to proinflammatory and antimicrobial response through the phagosome maturation pathway. Van der Vaart et al. reviewed the PRRs that identify invading microbes, as well as the innate immune effector mechanisms that they activate in zebrafish embryos [120]. The maturation of the phagosome forms the late-phagosome, which fuses with the lysosome forming the phagolysosome. It can digest the pathogen and leads to the bacterial death [11, 12, 102]. The mycobacteria are using several strategies to avoid the maturation of the phagosome and the key contributor is mannosylated lipoarabinomannan (ManLAM), a glycolipid of the mycobacteria cell wall. ManLAM is involved in the inhibition of phagosome maturation by inhibiting both calcium (Ca2+) concentration of increase in the macrophage as well as the concentration of Calmoduling-Ca2+ phosphotidol-inositol-3 kinase (PI3K) which is responsible for leading the maturation of the phagosome and driving the fusion with the lysosome [40, 76, 122]. To accomplish complete arrest and prevent the phagosome maturation, a second mycobacterial macromolecule, SapM, is released degrading the existing Phosphatidylinositol 3-phosphate (PI3P), a phospholipid found in the cell membrane involved in the phagosomal maturation [97]. A schematic representation of the phagosomal maturation arrest by the pathogenic mycobacteria is given in **Figure 3.1.**

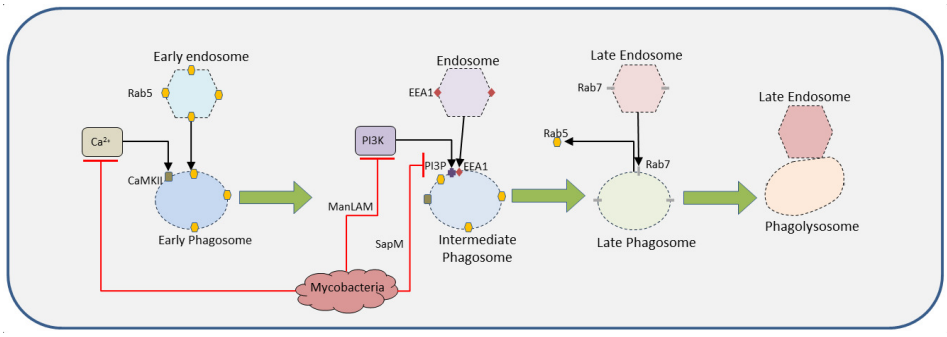

Figure 3.1: Schematic overview of the phagosomal maturation pathway blocked by pathogenic mycobacteria according to Koul et al. [68]. Nascent phagosome acquires Rab5 recruiting PI3K that generate PI3P. Pathogenic mycobacteria block the rise in cellular Ca^{2+}, recruitment of PI3K to the phagosome and degrading PI3P through Sap-M

When the immune cell is not able to kill the bacteria through the phagolysosome, the macrophage activates the apoptosis thereby programming its own death and signaling to other defense mechanisms. Once the maturation fails, the apoptotic programme is mainly activated by the extrinsic apoptosis pathway, which is initiated by the binding of ligands to death receptors. The apoptotic program also activates the intrinsic pathway, which involves translocation of cytochrome-C from mitochondria to the cytosol. The activation of the caspase cascade and degradation of genomic DNA are characteristics of apoptotic cell death [68]. Mycobacteria alter host apoptotic pathways interfering on the intrinsic death pathway preventing the increase in cytosolic Ca2+ concentration. Mycobacteria also inhibit caspase activity and functions by stimulating the phosphorylation of the apoptotic protein Bad [76, 103]. Mycobacteria limit macrophage apoptosis by inducing the production of cytokines such as interleukin-10 (IL-10). These cytokines interfere with one of the apoptosis stimulators of the macrophage in the extrinsic apoptosis pathway, the tumor-necrosis factor-α (TNF- α) [25, 84]. Mycobacteria take advantage of blocking these defense mechanisms of macrophages - phagocytosis and apoptosis - to proliferate inside the cell till a necrosis breakdown. Therefore, bacteria disseminate the infection through the other immune cells that aggregate with that particular infected macrophage to take over the infection. The apoptotic pathway is depicted in **Figure 3.2**.

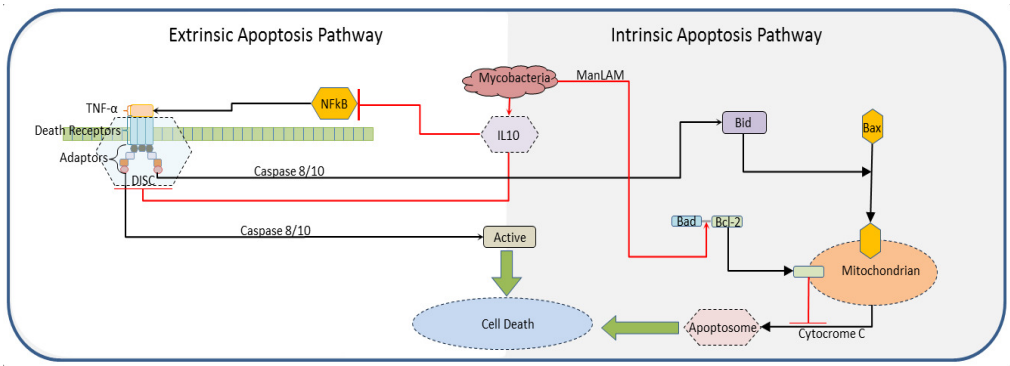

Figure 3.2: Apoptotic pathway inhibition by pathogenic mycobacteria according to Koul et al. [68]. Pathogen mycobacteria interfere in intrinsic apoptotic pathway suppressing Ca^{2+} and releasing Bcl-2. In the extrinsic apoptotic pathway it inhibits binding ligands and DISC formation.

3.4 Molecular host pathogen interaction

At the molecular level the most important interactions occur in both the phagosomal maturation pathway and in the apoptosis pathway. In both cases, the mycobacteria interfere in different ways to guarantee their survival and proliferation. Ca^{2+} is a key messenger that is released from intracellular storage. An increase in cytosolic Ca^{2+} concentration promotes the phagosomal maturation process by regulating calmodulin and the multifunctional serine/threonine protein kinase CaMKII [76]. CaMKII is important to PI3K activation and recruitment of early endosomal antigen 1 (EEA1) to the phagosomal membrane, which is extremely important in the process of phagosomal maturation. PI3K is also essential for the production of the lipid regulator phosphatidylinositol 3-phosphate (PI3P), which forms a ligand together with EEA1 leading to an intermediate phagosome. The intermediate phagosome maturates to the late endosome after EEA1 dissociation and acidic expression due to accumulation of the proton-ATPase [39, 114]. Through releasing ManLAM, the mycobacteria inhibit the rise of the Ca^{2+} concentration in macrophages and also the PI3K activation. It prevents the generation of PI3P degrading the existing PI3P by the action of SapM.

Despite the fact that phagosome fail to fuse with the lysosomes to degrade the bacteria, pathogen-derived material is released in the host cell lysosomes and on cell surface of the infected macrophage, which can induce the apoptosis process [106]. Mycobacteria influence the host apoptosis through several mechanisms, which interfere in the intrinsic and extrinsic apoptosis pathways. The cytosolic Ca^{2+} facilitates apoptosis by increasing the permeability of mitochondrial membranes. This process promotes the release of pro-apoptotic elements such as cytochrome-C. In the cytosol, cytochrome-C associates with procaspase-9 and apoptosis protease forming a signaling complex called the apoptosome, which activates the induction of apoptosis [70]. ManLAM interferes in the intrinsic apoptosis pathway not only by inhibiting the concentration of Ca^{2+} but also

through stimulation of the phosphorylation of the apoptotic protein Bad. The Bad phosphorylation leaves BCL-2 free by which the release of cytochrome c is prevented.

The extrinsic apoptosis pathway is induced by Toll-like receptors (TLRs) that identify the virulence mycobacterial pathogen. Those receptors trigger the synthesis of tumor-necrosis factor-α (TNF-α) - a stimulator of apoptosis – trough the TLR signaling pathway. To do so, an important adaptor factor protein, the Myeloid differentiation factor 88 (MYD88) recruits a family of kinases (IRAK) that will form "Myddosome" signaling complex [119]. This signaling complex activates nuclear factor kB (NF-kB) to transcript target gene to synthesize TNF-α [68]. The tumor necrosis factor binds with death receptors leading to a cascade of events that will release caspase 8 and 10. It also leads the formation of a death-inducing signal complex (DISC) resulting on the apoptotic vesicles [70, 132]. Pathogen mycobacteria interfere in this process by inducing the production of immunosuppressive cytokine interleukin-10 (IL-10). IL10 inhibits the phosphorylation of NF-kB, and thereby the synthesis of TNF-α. It also inhibits the DISC formation and consequently, the extrinsic apoptotic pathway fails.

3.5 Petri net model of the bacterium–macrophage interaction

We have formulated a Petri net model of the processes triggered in the macrophage in response to mycobacterial infection. The model is based on an extensive literature survey (cf. Sections 3.2 to 3.4) and on extending our previous model [19]. The model captures the interactions between the immune cell and the pathogen once a bacterium is phagocytized. The model is hierarchical and has three different levels of representations to mimic the signal processing that activates/inhibits the pathways related to the macrophage response to the bacteria. The first level models the overall actions from the system started after the phagocytosis and it represents the cell-cell interaction between the macrophage and the bacteria. The second level representing the intracellular interaction models two important signaling pathways: the Phagosome Maturation which is responsible for the degradation of the infection through antimicrobial components; and the Apoptotic Pathway which is the macrophage mechanism responsible to resolve the infection in response to virulence factors. It represents an alternative way to the phagolysosome. The third level represents the molecule-molecule interactions that occur on the level of Phagosome Maturation and Apoptotic pathways.

To model the host-pathogen interaction we use a qualitative Petri net as implemented in the Snoopy software [50] using maximal concurrency semantics. All formal definitions can be found in **Appendix A**. The pathways described in Section 3.2 to 3.4 represent a complex process involving various host-bacterial factors in a heavy cross-talk interaction. To get a consistent view of the entire interaction process, we express the most important reactions simplifying the pathways at different levels of abstraction. We define each biochemical compound or receptor as a place. The relations

between biochemical substances are basically represented by transitions with corresponding arcs modeling biochemical reactions, inhibitions/degradations (using inhibitor arcs) or signaling/catalytic atomic events (using read arcs). To hierarchically connect the sub-nets we use coarse transitions and coarse places structuring all the levels as a tree as shown in **Figure 3.3**. The top level (the root) models the overall view of the system, starting by interactions that occur in the cellular boundary and its consequences. It is connected to the sub-nets (mid-level) through coarse transitions which link to the molecular level modeled in coarse places (the leaves of the tree). This structure increases the granularity of the model along the levels. Deeper is the level more detailed is the sub-net. **Table 3.1** describes each sub-model implemented hierarchically and the respectively level of interaction.

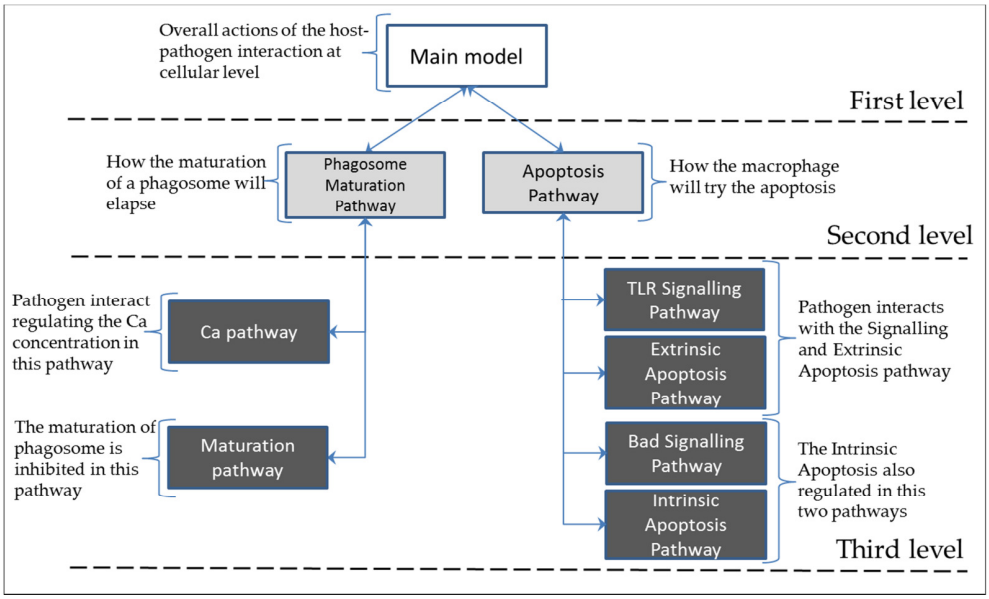

Figure 3.3: Hierarchical structure of the net. The three levels are implemented in independent interconnected sub-nets

Table 3.1: Set of places per hierarchical structure and the scale in which they occur

Level	*Scale*	*Description*
Main model	**Intercellular**	Models the states of the macrophage and the interaction that occur ate the intercellular level.
Phagosome Maturation Pathway	**Intracellular**	Implemented by the coarse transition **Phagosome_Maturation_Pathway**, it models the interactions at the intracellular level that triggers the phagosome maturation process. It connects the molecular scale with the intracellular scale.
Apoptosis Pathway	**Intracellular**	Implemented by the coarse transition **Apoptosis_Pathway**, it models the interactions at the intracellular level that triggers the apoptosis process. It connects the molecular scale with the intercellular scale.
Ca_pathway	**Molecular**	Coarse place that models the molecular interactions that produce/inhibit calcium and CMKII.
Maturation_pathway	**Molecular**	Coarse place that model the molecular interactions that leads/inhibits the maturation of the phagosome process.
TLR_Signaling_Pathway	**Molecular**	Coarse transition that models the molecular interactions that leads to the activation/inhibition of pro-inflammatory cytokines.
Bad_Signaling_Pathway	**Molecular**	Coarse transition that models the molecular interactions that triggers/inhibits the phosphorylation of Bad apoptotic protein.
Extrinsic_Apoptosis_Pathway	**Molecular**	Coarse place that models the molecular interactions related to the extrinsic apoptosis process.
Intrinsic_Apoptosis_Pathway	**Macrophage**	Coarse place that models the molecular interactions related to the intrinsic apoptosis process.

3.6 Model definition

We start the modeling with the interaction between the bacteria inside the macrophage once it is in the host. The first level of our Petri net model is given in **Figure 3.4**. The input place **Infected_macrophage** represents this situation. The sequence of interaction events happens once there are bacteria infecting the macrophage. This process is represented in the net by a token that is present at the input place, detected by three reading arcs that trigger the interactions. The macrophage uses the PRRs to detect the presence of the pathogen and starts the phagosome maturation process. The bacteria start its protein secretion system and counter attack by releasing SapM to degrade existing PI3P in the cytosol and ManLAM to interfere in the maturation of the phagosome. The maturation of phagosome is modeled in a deeper level by the coarse transition **Phagosome_Maturation_Pathway**. ManLAM also interfere in the apoptosis process, which is modeled in a deeper level in the coarse transition **Apoptosis_Pathway**. The presence of ManLAM triggers the macrophage production of the cytokine IL10 and also interferes in both pathways. **Phagosome_Maturation_Pathway** interacts with **Apoptosis_Pathway** releasing calcium and bactericidal material that was not degraded by the maturation.

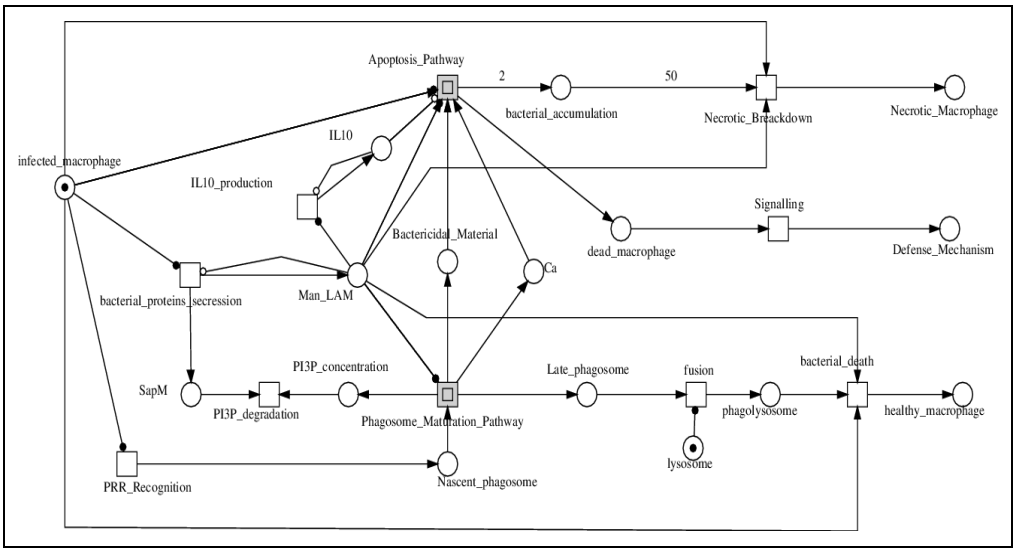

Figure 3.4: Petri net of host-pathogen interaction at the top (root) level. The coarse transitions: **Phagosome_Maturation_Pathway** and the **Apoptosis_Pathway** contain the second level of the model and are represented here by a double square.

In our model there are three different scenarios: The phagosome maturation occurs in the **Phagosome_Maturation_Pathway,** leading to a late phagosome that will fuse with lysosome digesting the bacteria, and turning the macrophage healthy. The second scenario can occur if the maturation fails. The apoptosis process in the **Apoptosis_Pathway** is triggered, leading to a dead macrophage that will signal for another defense mechanism. The third scenario occurs when both pathways (maturation and apoptosis) are failing at the molecular level. In that case the bacteria proliferate and accumulate in the macrophage till a necrosis breakdown, releasing all the pathogenic material to the surrounding cells. To represent the proliferation and accumulation of bacteria, we use weighted arcs that double the amount of bacteria, as accumulated in the place **Bacterial_accumulation**. The breakdown of the macrophage occurs when it reaches a threshold of 50 bacteria, thereupon a weighted arc fires the transition **Necrotic_breackdown**. Here we should note that the weighted arcs, with weights 2 and 50, are examples to express the idea of bacterial proliferation.

Following the hierarchical tree, at the second level we have: **Phagosome_Maturation_Pathway** and **Apoptosis_Pathway**. They are two sub-nets, which basically connect the cellular interaction (top level) with the molecular interactions at the biochemical pathways implemented in the coarse places (the branches of the tree). **Figure 3.5** depicts these sub-nets respectively. At this level we have the signaling started in the cell surface (first level) that will trigger the production/interaction between molecules. For example, the production/releasing of calcium is triggered by the PRRs and this process occurs at **Ca_pathway**; the PIP3 concentration and bactericidal material that are not degraded at the **maturation_pathway** and interact with the top level. We also have the interaction between the cytokine IL10 from the top level with the pro-inflammatory cytokines that will interfere in the TNF-α in the **Extrinsic_Apopthosis_Pathway** and ManLAM interfering in the BCL2 activation, which will act in the **Intrinsic_Apopthosis_Pathway**.

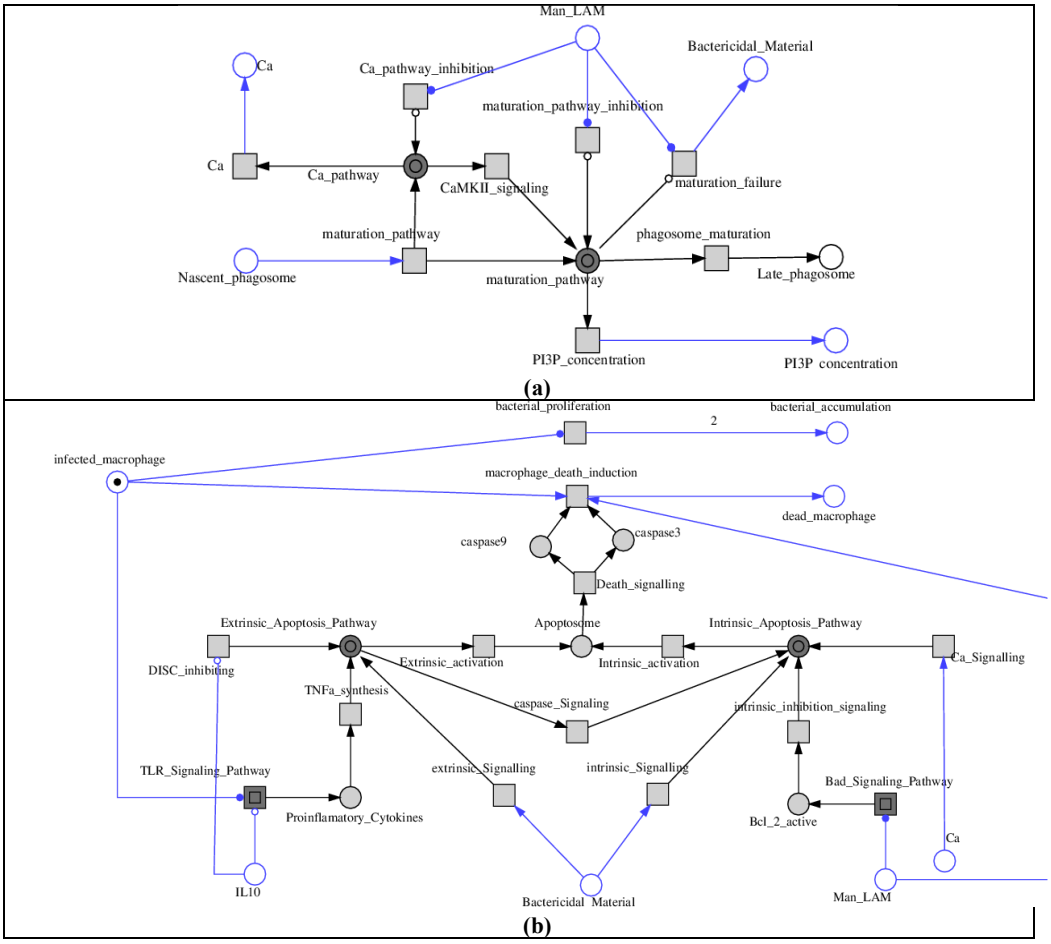

Figure 3.5: Second level. **(a)** The **Maturation_Pathway** Sub-net which connects the cellular level with the molecular interactions in the production of calcium (**Ca_pathway**) and phagosomal maturation (**Maturation_pathway**) implemented in another sub-net level (coarse places). **(b) Apoptosis_Pathway** Sub-net which connects the cellular level with the molecular interactions in the pro inflammatory cytokines, Bcl2 activation and their influences in the extrinsic and intrinsic apoptosis pathway.

At the deeper level of the hierarchical model, we have modeled six related but independent sub-nets. They represent the important molecular pathways responsible for: the production of calcium/CMKII in **ca_pathway** and phagosome maturation and PI3P concentration in **maturation_pathway,** both implemented in coarse places; activation of pro-inflammatory cytokines in **TLR_Signaling_Pathway** and Bcl2 activation in **Bad_Signalling_Pathway**, both implemented in coarse transitions; and also the interactions that occur in the intrinsic and extrinsic apoptosis pathways implemented in the coarse places **Extrinsic_Apopthosis_Pathway** and **Intrinsic_Apopthosis_Pathway** respectively. In **Figure 3.6** all sub-nets in the branches of the proposed hierarchical model are depicted.

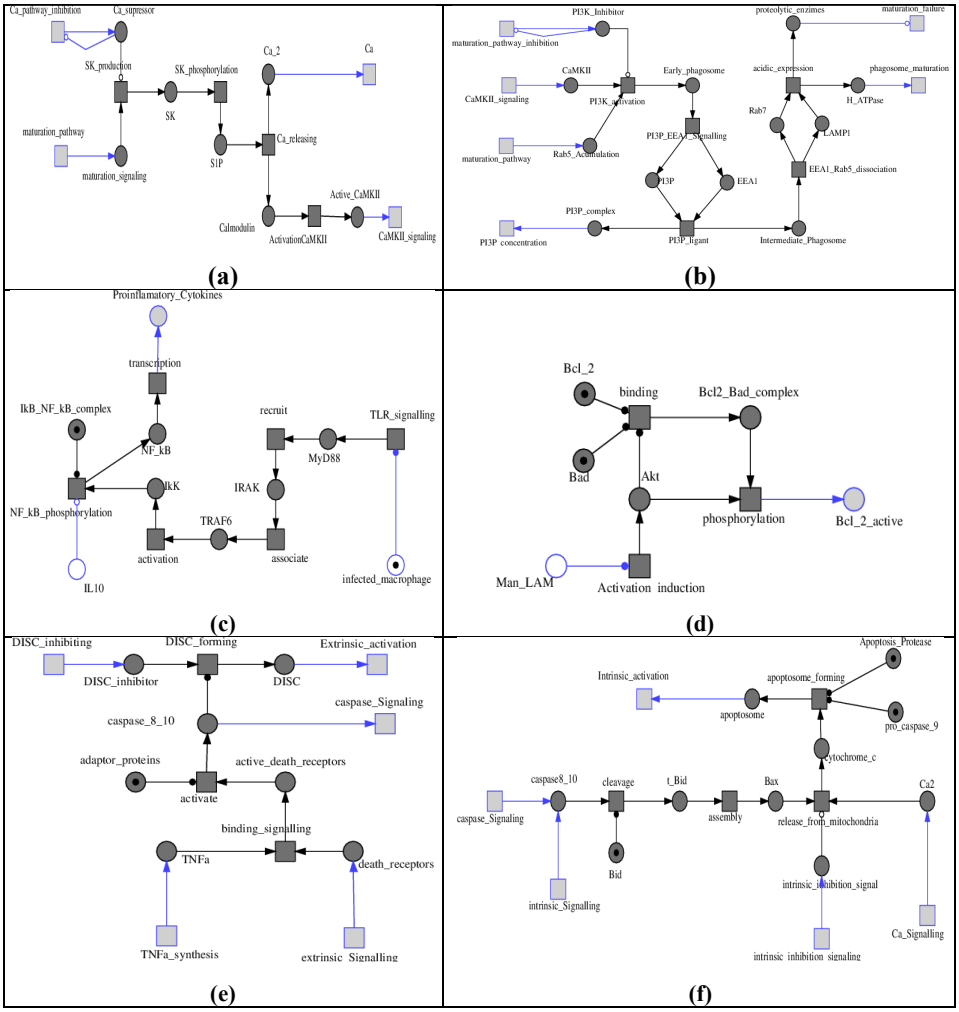

Figure 3.6: Sub-nets that implement the molecular pathway interaction. **(a)** Ca^{2+} and CaMKII. **(b)** Phagosome maturation pathway and PI3P. **(c)** TLR signaling and pro-inflammatory cytokines. **(d)** Bad/BCL2 phosphorylation. **(e)** Extrinsic apoptosis pathway. **(f)** Intrinsic apoptosis pathway.

3.7 Animation and validation

Animation and validation are important tools in order to provide a consistent model for biological behavior. They allow experimenting with different situations and possibilities of the model as well as checking for integrity and correspondence to the real world. Simulation and analysis for qualitative and quantitative behavior prediction are other steps necessary to certify a useful model. For the model presented here, we also performed nonscientific simulation and validation. For this we employed the animation mode available in the Snoopy software. This feature allows animating the token flow of the net through all the sub-nets, visualizing the causality of the model and its behavior. Three different animations for the scenarios, previously discussed, were performed to

experience the events that can occur in the model. For inspection and perusal, the animations can be found at http://bio-imaging.liacs.nl/galleries/epn-infection/.

To validate the model, it is necessary to define validation criteria for a consistency check. To do so, we have to consider that our model is based on a heuristic procedure of collecting information from the literature, perhaps with different interpretations, modeled from the process perspective (top level) down to the molecule perspective (leaves). We built a large model composed of sub-models and to provide a complete analysis, it is necessary to verify each component individually and them the system as a whole, which increases the complexity of the validation even with computational support. Basic qualitative behavior properties can be checked using the Charlie analyzer tool [126]. Heiner *et al.* have used as example, p-invariants and t-invariants to analyze case studies in biochemical pathways in [51]. We started to analyze the structural and behavior properties of our model based on results from the Charlie tool which should then be biological meaningful. As a first result, we found that our model is not structurally bounded and not reversible. This implies that indeed the net allows for the proliferation of the bacteria and the infection process is not reversible.

3.8 Conclusion

In mycobacterial infection, the dynamics of the interactions between the host and bacteria form a complex system involving numerous activations, inhibitory and control structures that determine the outcome of the infection. A systems approach is essential to comprehend the significance of the multiple events that occur simultaneously among the various molecular and cellular components of the host and pathogen.

Here, we seek to model the interaction of the macrophage upon exposure to pathogenic mycobacteria, capturing important functional processes and their interconnections including signaling and activation/inhibition of the immune responses on different levels of abstraction. The Petri net formalism has proved to be a useful modeling approach to describe and interconnect different abstract levels into a large and extensive model [52, 79] In Chapter 2 we have developed a Colored Petri net model to explore the early mycobacterial infection and the immune response, modeling the steps that regulate the infection process. In this chapter we focus on the processes occurring in different scales, from the cell and descend to molecular interactions relevant to the infection process. Therefore, we use a qualitative Petri net modeling different pathways in sub-nets, interconnecting them in a hierarchical structured model. The model provides a visualization of the processes occurring at multiple scales using levels that can be operated independently. It also describes the interconnections and signals that influence the host pathogen interaction.

In the model we express, at different levels of abstraction, the details that are involved in the macrophage-mycobacterium interaction. Information about the proteins released by the bacteria,

their interference in the immune response and the pathways involved in this process are observed in our model. It is possible to visualize the dynamics of the molecular and cellular interaction as well as analyze different scenarios performing "what-if" simulations as part of the experimentation. In this manner, different animation/simulation can be accomplished. The model represents the information about host-pathogen interaction available in the literature but the scalability of our model allows extension to a more complete system.

As part of the modeling process, we used the Charlie analyzer [126] to check basic properties of the model and its consistency. As a next step, an extensive analysis of more structural and behavior properties is necessary to validate the model. We also intend to extend to a quantitative model where, with support of experimental data rather than the examples we used until now. In this manner we would be able to perform quantitative simulations and behavior analysis. This can contribute, for example, in the prediction of results from new experiments and generation of further hypotheses about the innate immune system response to mycobacterial infection. Another challenge is to combine the models implemented in different classes of Petri nets in one system. One solution is to adapt each model in a Hybrid Petri net, or abstract the models in a Nets-within-Nets approach where the communication of the tokens occurs via predefined interfaces which are dynamically bounded [57].

In summary, in this chapter we have presented a model that explores the interaction between mycobacterial pathogen and macrophage, modeling the dynamics in three different level of abstraction while interconnecting them in a hierarchical structure. We have checked the structural behavior of our model through an analysis tool. The interplay of hierarchical levels and qualitative/quantitative information has the potential to develop a powerful tool for the research in tuberculosis disease.

4 Coupling of Petri net models of the mycobacterial infection process

Based on:

Carvalho, Rafael V., Heuvel, Jeroen H., Kleijn, Jetty, Verbeek, Fons J.: Coupling of Petri Net Models of the Mycobacterial Infection Process and Innate Immune Response. In: Computation, vol.3, 150-76 (2015).

Misterio	Mystery
¿Por qué estoy vivo	Why am I living
y el vaso lleno de agua	and the glass full of water
y la puerta cerrada	and the door shut
y el cielo igual que ayer	and the sky just like yesterday
y los pájaros dorados	and the birds golden
y mi lengua mojada	and my mouth wet
y mis libros en orden?	and my books in a row?
¿Por qué estoy muerto	Why am I dead
y el vaso igual que ayer	and the glass just like yesterday
y la puerta dorada	and the door golden
y el cielo lleno de agua	and the sky full of water
y los pájaros en orden	and the birds in a row
y mi lengua cerrada	and my mouth shut
y mis libros mojados?	and my books wet?
Jorge Eduardo Eielson, Peru (1924 –2006)	Jorge Eduardo Eielson, Peru (1924 –2006)

Abstract

Refinement a model may lead to an expansion of the model when more detailed processes are added. A modular and extensible model is important to support the increase of the model structure. Besides, a hierarchical organization to support the model design is necessary in order to be able to conceptualize the model object. The previous chapter has proposed an extension for the model in Chapter 2. Although it was a refinement of the model, it was implemented separately as an independent but correlated sub-model. In this chapter we combine the two models previously described exploring the modular structure of the formalism. The resulting model explicitly reflects the organization of the biological process in hierarchical modular structure. In addition, we provide a 3D simulation tool that is able to animate the model and relating it to an *in vivo* situation. This chapter also addresses the new directions in the refining process, moving from a qualitative to a quantitative approach.

4.1 Introduction

The understanding of the highly complex world of immunology is a major challenge for scientists in the fields of biology, medicine and pharmacology. For the description of biological phenomena related to the immune system, the modeling, simulation, and analysis of the immune system are considered important practices and these can contribute to improved diagnostics and optimized immune treatments. For that purpose, mathematical and computational methodologies have been utilized to create models that represent biological behavior. These models can support explanations of the interaction mechanisms between pathogenic agents and the defense mechanism in intuitive and yet analyzable terms.

In the context of our research, a mathematical model is a formal model describing by means of equations relationships between quantities and how quantities change over time. Computational models such as agent-based models (ABMs) describe dependencies between activities of components of a system. Combinations of the two approaches have been used to describe, simulate, and analyze the networks and interactions in the immune system [16, 21, 44, 75, 77]. Pappalardo *et al*. provided an extensive study on vaccine administration and immune response to cancer in mice by implementing and simulating models using ABMs and cellular automata [4, 92, 93]. Gammack *et al*. [41] provided a mathematical model based on Ordinary Differential Equations (ODEs) to investigate the early and initial immune response to mycobacterial infection (Mtb) in mice. This work has inspired Segovia-Juarez *et al*. [108] to implement the ODEs that regulate the interaction between host and pathogen using an ABM approach. Warrender *et al.* [124] use the CyCell simulator tool to simulate the interactions in early mycobacterial infection.

The different scales of the models can be an obstacle in modeling the infection process and the immune response. For biologists, it is intuitive to establish a process that involves cells, molecules and/or organs. It is, however, not trivial to identify the line of information retrieval that connects/switches from one level to the next [109]. A multi-scale approach has been used to connect interactions at molecular, cellular, and tissue level as well as the modeling of the dynamics from a spatial and temporal perspective. Multi-scale models, including how to connect different individual levels, have been extensively explored, see e.g. [34, 42, 109, 123]. In the study of the mycobacterial infection process and immune response, establishing an adequate method to account for multi-scale processes is still a challenge. In mathematical models, like those based on differential equations, the interactions are described in rules and equations, whereas computational models are embedded in programming code with which one cannot interact in a straightforward manner and neither can one directly understand its structure.

Thus, a graphical representation of the interactions and influences among various components that involve the bacteria and host immune cells, i.e. molecules and proteins, that also captures the

dynamics of the system would be very useful. The Petri net formalism (PN) represents a well-established technique in which a graphical representation is combined with a mathematical basis for modeling distributed concurrent systems [100, 101]. Petri nets are successfully used to model biological behavior [67, 128]. Heiner *et al*. [52] propose a methodology of incremental modeling using Petri nets to develop and analyze a qualitative model of the apoptotic pathway. Albergante *et al*. [3] have developed a Petri net model that simulates the formation of hepatic granuloma for *Leishimania donavani* infection in mice.

In previous work [19], we have developed a qualitative Petri net model of the mycobacterial infection process and the subsequent innate immune response. We organized our model at the level of cell dynamics, and it is characterized by steps involved in the *Mycobacterium marinum* infection and granuloma formation in zebrafish. Subsequently, we used Petri nets to model the interactions between the bacteria and the host immune cell in a multi-scale approach [17], connecting important pathways involved in the host-pathogen interactions that are acting over different scales (molecular, intracellular, and intercellular) during the innate immune response.

In this paper, we extend our two previous models by combining them in a hierarchical fashion, so as to jointly represent the mycobacterial infection process and innate immune response. The qualitative model captures the relationship between the pathogen and the host immune cells, i.e. the bacteria and the macrophages, from the perspective of cell dynamics down to interactions at intercellular, intracellular, and molecular level. The hierarchical model provides a visualization of the infection process from the moment the bacteria enter the host: the migration, proliferation, granuloma formation, and dissemination. Moreover, it models the signaling pathways that a macrophage employs to terminate the infection and the way the bacterium exploits those pathways to enhance its intracellular survival persistence. In this paper we introduce an additional visualization, which renders the infection process as modeled and simulated with the qualitative Petri nets on a 3D mesh model of the zebrafish. It is possible to correlate the information of the net, its structure and its results to behavior observed *in vivo*. In this manner, we demonstrate the power of the Petri net formalism by modeling and animating the mycobacterial infection from the perspective of different but yet interconnected scales. By coupling the resulting Petri net model with the 3D mesh model visualization is added that supports the interpretation of the biological process.

The remainder of this paper is structured as follows. In Section 2 we focus on the material and methods including the description of the colored qualitative Petri net, the history of modeling and our extensions to the visualization of net information. In Section 3 we provide a detailed discussion of our hierarchical Petri net model by defining of all of its constituent components and boundary conditions. In Section 4 we show our results for both the hierarchical Petri net of the *Mycobacterium* infection and the 3D visualization of the infection process as we have modeled it.

Finally, in Section 5 we present our conclusions and discuss the results as well as directions of our future work.

4.2 Material and methods

4.2.1 Biological model

Human tuberculosis is caused by the bacteria *Mycobacterium tuberculosis* (*Mtb*), and causes over a million deaths every year [129]. *Mycobacterium marinum* (*Mm*) is genetically closely related to *Mtb* and, like other pathogenic mycobacteria, causes chronic infection of macrophages resulting in tuberculous granulomas [24]. The Zebrafish (*Danio rerio*) is naturally susceptible to infections caused by *Mm*. The zebrafish embryo has functional innate immune cells (macrophages and neutrophils) while its adaptive immune system is not yet functional. This makes it a useful model to study the mycobacterial pathogenesis [8]. An experimental infection in zebrafish embryos is initiated by an injection of bacteria into the blood circulation or tissue [8, 113]. Upon infection, immune cells, mostly macrophages, are triggered and migrate to the site of injection to take up the bacteria by a process called phagocytosis. Mycobacterial interference with the host signaling machinery severely compromises the immune defenses. This enables the mycobacteria to proliferate inside the macrophage. Over time, this causes the rupture of the macrophage and initiates a further spread of infection [8, 30]. In this paper we report on our further explorations of the bacteria-macrophage interaction and infection process using the *Mm* infection in a zebrafish model.

Mycobacterium prevents the anti-bacterial mechanisms of macrophages by inhibiting several host-cell processes, which include the fusion of phagosome with lysosomes, antigen presentation, apoptosis and stimulation of bactericidal response [68]. Lipids and glycolipids released by the bacteria, such as Mannosylated Lipoarabinomannam (ManLAM), prevent the fusion of the mycobacterial phagosome with the late endosome and lysosome. The prevention of phagolysosome formation can occur by the inhibition of the Calmodulin-Ca^{2+} phosphotidol-ionositol-3kinase (PI3K) at a molecular level [40]. The lower concentration of Ca^{2+} also has influence in the apoptotic pathway since it reduces the permeability of mitochondrial membranes by suppressing the apoptosis process [68]. ManLAM also suppresses apoptosis by phosphorylating the apoptotic protein BAD. This phosphorylation releases Bcl-2, which inhibits the caspase activity and functions as an anti-apoptotic regulator [1]. Another strategy of the mycobacteria to avoid the apoptosis is by inducing the production of interleukin-10 (IL-10) which blocks the synthesis of Tumor-Necrosis Factor (TNF), a stimulator of apoptosis in infected macrophage [84, 107].

By preventing phagolysosome formation and apoptosis, the bacteria survive and are able to efficiently replicate inside the macrophage while the macrophage is moving in the blood circulation. Once the infected immune cell is overloaded with mycobacteria, it gets out of the circulatory system and attaches to a tissue. The infected macrophage dies, triggering an immune response by recruiting uninfected macrophages [31, 32, 113]. New macrophages are attracted to the infection, and absorb the infected macrophages and bacteria cells. The process repeats itself as bacteria also infect these immune cells. A common feature of all *Mycobacterium* infections is the further differentiation of macrophages into epithelioid cells that have their cell membranes tightly clustered in linking adjacent cells. These aggregates grow into organized structures that are referred to as granulomas [114]. Primary granulomas are capable of disseminating infection throughout the body by withdrawal of infected macrophages. This suggests that granuloma macrophages constitute the major mechanism for dissemination of the infection [32]. **Figure 4.1** depicts the infection process from the perspective of cell dynamics. At the phagolysosome fusion process we have represented, at one scale down, the interactions between macrophage and bacteria at intercellular, intracellular and molecular level.

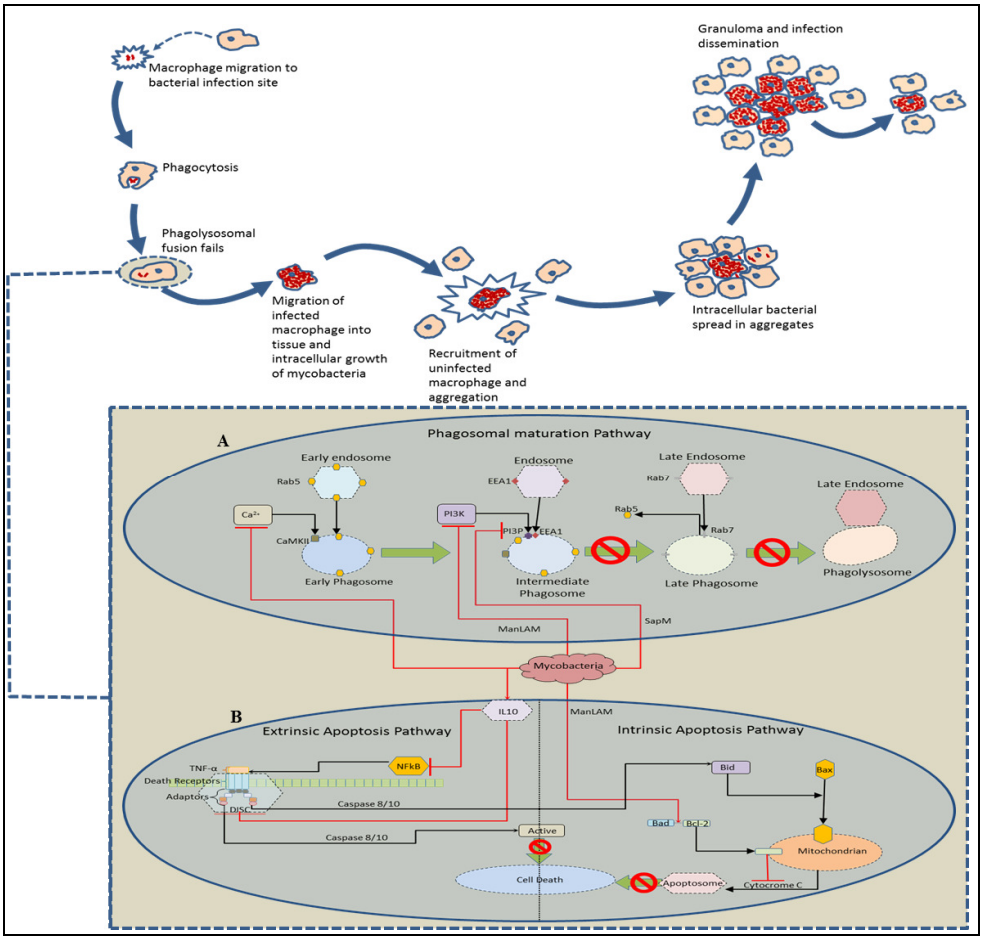

Figure 4.1. Infection at cell dynamic level and interaction between macrophage and bacteria at intercellular, intracellular, and molecular level (partially adapted from [17]). **A** is a graphical representation of the molecular interactions in the phagosome maturation pathway and **B** is a graphical representation of the apoptosis pathway.

4.2.2 Background on previous PN models

At the onset of our modeling work [19] we have used colored qualitative Petri nets (QPN^C) to model the early stages of the mycobacterial infection process and granuloma formation. In all of our modeling work we have used an infection model of *Mycobacterium marinum* in zebrafish embryos as this allows us to connect with empirical work. We defined a qualitative model on the level of cell dynamics in the early stage of the infection and dissemination. The process goes through the following stages: (1) migration of the macrophage to the infection site, i.e. the initial positioning of the bacteria, (2) phagocytosis, (3) migration into tissue, (4) bacterial replication within an individual macrophage, (5) bacterial burst and recruitment of uninfected macrophages, (6) aggregation to a granuloma, and (7) dissemination of the infection.

Our subsequent research focused on defining a qualitative Petri net model representing the interactions between macrophages and bacteria [17], from the moment the pathogen is inside the host immune cell through a process of phagocytosis. We created a hierarchical model based on an extensive literature survey, dividing the Petri net model in three different containers (levels). Each container represents a sub-model of the signaling cascade that activates or inhibits important pathways related to the host immune response to the pathogen. The first level models the cell-cell interaction between bacterium and macrophage. The second level represents the intracellular interaction and models two important signaling pathways: the phagosome maturation, which leads to the phagolysosome process that kills the bacteria; and the apoptotic pathway, which is the macrophage mechanism responsible for acting in response to virulence factors, as an alternative way to the phagolysosome. The third level models the molecule-molecule interactions that occur on the phagosome maturation and apoptotic pathways.

In the research described in this paper, we now combine our former models [17, 19] into one hierarchical structure in order to capture the infection process from the level of molecular interactions to the level of granuloma formation. In order to accomplish this, we have converted the QPN model and its hierarchical sub-models into a colored Petri net. This process assigns a colored token to represent a discrete value for the presence or absence of a protein, therefore modeling the activation or inhibition of a specific pathway. We combine the two colored qualitative Petri nets models in one hierarchical structure.

4.2.3 Software environment for PN modeling

We use the Snoopy software [50] to implement our colored Petri nets and to simulate their dynamic behavior. Snoopy provides a unifying Petri net framework with all the Petri nets classes and extensions. Conversion between classes according is possible to the paradigm structure of the formalism. It is a multiplatform where one can design, animate and simulate Petri nets models. It provides features that facilitate the implementation of our Petri nets in a hierarchical and modular structure. In this structure each module works as a container, allowing future extensions to be added without the need to change the structure of the model.

4.2.4 3D visualization environment for PN modeling

In addition to the “classical” visualization of the Petri net focusing on state transition and token progression, we have extended the visualization with a 3D environment. We project the animation of the interaction between host and pathogen onto a 3D representation of our model system, i.e. the

zebrafish embryo. This computational environment thus illustrates how the infection develops and progresses in a spatial context using the output of Petri net model.

To construct the 3D model and produce the dynamic visualization, we use OpenGL as graphical library, structuring the code in object oriented C++. To represent the zebrafish embryo we have created a 3D mesh object derived from a microscope image. The visualization has the purpose to render and animate the process as modeled in the Petri net providing its representation as well as how the infection process is affected. Therefore, it is necessary to read from Snoopy the markup file of the model in its resulting state space. This requires execution of the Petri net model from its initial markings to the end state.

The Petri net captures the essence and flow of the infection. It, however, cannot provide a complete visualization of the spatio-temporal aspects in relation to our model system. From the state space of the net, the 3D visualization essentially replays the infection process in the zebrafish embryo. The flow of this 3D animation resembles the *in vivo* biological behavior of the infection. As the qualitative colored Petri net is used, time is not relevant and its progress is only represented by the sequence of events that occur during the infection. The quantities that are read and represented by the visualization are the colored tokens (cf. Section 3) defined in the Petri net model. They are used as boundaries to limit and represent the qualitative aspect of the infection.

4.3 Implementation

The biological processes described in Section 4.2.1 occur at different scales, i.e. the molecular, the cellular, and the tissue level. Therefore, in this study, we have designed our qualitative colored Petri net model in a hierarchical structure with four different levels of representation. The model reproduces the dynamics of the steps that are involved in the infection process and innate immune response. It also models the signaling pathways activated by macrophage in response to the bacteria and how the bacteria explore this to proliferate. The implemented levels operate as containers where level 1 represents the large scale model, which contains the entire small-scale model. The information flow is triggered on the top level but eventually flows in both directions (top-down and bottom-up). **Figure 4.2** depicts the hierarchical structure of the net. The level 1 provides a model for the phases of the infection process: infection detection and phagocytosis, phagolysosome failure, bacterial proliferation, migration of infected macrophages to deep tissue, death of macrophages, recruitment of new immune cells and granuloma formation, intracellular spread and granuloma dissemination. At level 2 we have modeled the bacteria and macrophage interaction on the intercellular scale. This is directly connected to level 3 in which we model the interactions at the intracellular scale; here, the important pathways related to the bacterial proliferation are modeled.

At level 4 we have assembled the important interactions from the molecular perspective influencing the infection process.

Snoopy supplies features for the design and systematic construction of larger Petri nets. In hierarchically structured nets, coarse places and coarse transitions hide place-bordered (transition-bordered) sub-nets. Through these, it is possible to zoom in the model to a specific sub-model and check a local behavior.

In the following sections, we present the color-set Σ, places P, transitions T and the initial marking I from the main model i.e. level 1 as well as the coarse places and transitions that compose our hierarchical structured model, a qualitative colored Petri net specified as $(\Sigma, P, T, A, C, G, E, I)$.

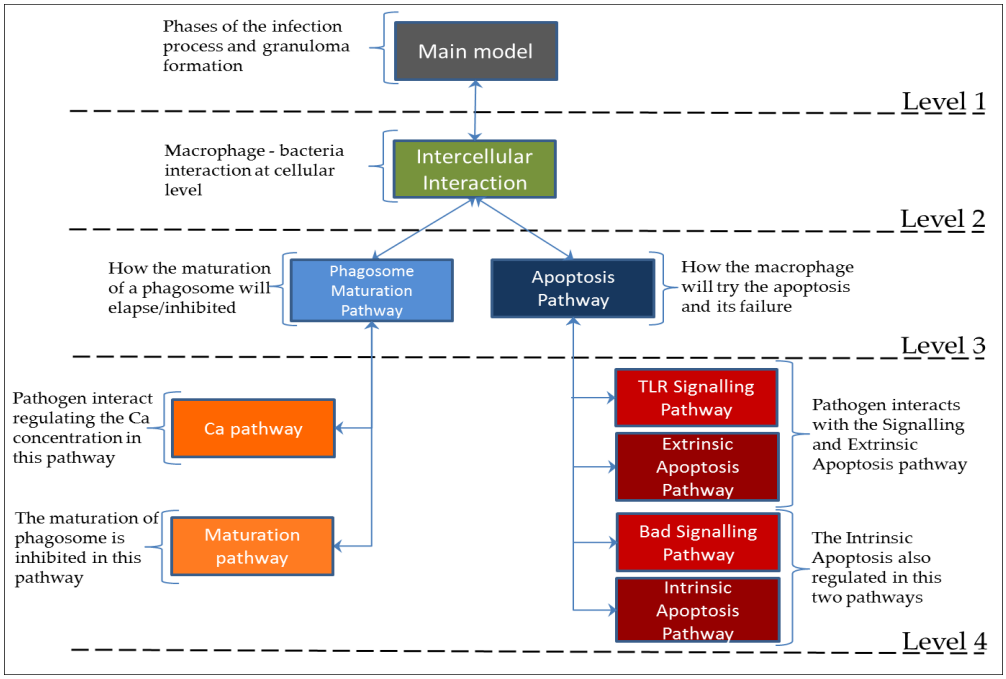

Figure 4.2. Hierarchical structure of the model. The levels are implemented as independent and interconnected sub-nets, following the structure of [17].

4.3.1 Set of color-sets Σ

The set of color-sets from [19] is extended with a new color-set **Dot**. This is a color-set with only one element as a color. It is used to define discrete numbers of markings that represent the presence or absence of a molecule, protein or cell in the sublevels of our model. **Table 4.1** describes the 5 simple color-set defined in our model. We introduce three compound color-set as product of simple color-set predefined. **Table 4.2** describes the compound color-sets of the model**.**

Table 4.1: Simple color-sets defined for the colored Petri net model

Color-set	*Data type*	*Description*
position	Integer	Represents a location (of a macrophage, bacteria and/or granuloma) within the zebrafish embryo
individual	String	Distinguishes bacteria and macrophages (**mm, mac**) respectively
status	Boolean	Represents the infection status of a macrophage, i.e. healthy=true; infected=false
count	Integer	Represents a threshold for the simulation in the recruitment of macrophage and the dissemination of a granuloma
Dot	dot	Default black color, used to evaluate a condition being true or false for a specific molecule or protein, or to count a number of cells

Table 4.2: Compound color-sets defined for the colored Petri net model

Color-set	*Product type*	*Description*
Bacteria	**position, individual**	Represents the *Mycobacterium marinum* bacteria that are modeled
Macrophage	**position, individual, status**	Represents host macrophage immune cells
Granuloma	**position, individual, count**	Represents granuloma with a number of infected macrophages

4.3.2 Set of places P

Places represent a population of cells and multicellular complexes that are integrated in our model. The set of places P that composes level 1 of our model are defined as:

$$P = \{\textbf{Infection, ImmuneSystem, InfectionPosition, InfectedMacrophage, ActiveMacrophage, DeadMacrophage, RecruitedMacrophage, FormedGranuloma, MatureGranuloma, MacrophageDisseminated, IntracellularInteraction}\} \quad (7)$$

These places are defined and described in **Table 4.3**.

Table 4.3: Set of places composing the level 1 of the model

Place	*Color-set*	*Description*
Infection	**Bacteria**	Represent the initial infection site. It contains the initial mycobacteria that intrude the host
ImmuneSystem	**Macrophage**	Represents the immune cells of the zebrafish. It contains the non-infected macrophage cells that respond to an infection or recruitment signaling
InfectionPosition	**Bacteria**	Maintains the information of the initial position of the infection. This is important for the 3D visualization to identify where the infection initially occurs
InfectedMacrophage	**Macrophage**	Represents the macrophage after phagocytosis of bacteria.
ActiveMacrophage	**Macrophage**	Represents the infected macrophage moving in the blood circulation. It shows the macrophage changing its position while the bacteria proliferate
DeadMacrophage	**Macrophage**	Represents the necrotic macrophages positioned in the tissue after been completely infected and signaling to new immune cells to take the infection
RecruitedMacrophage	**count**	Counts/Controls the amount of healthy macrophages that are recruited to form the granuloma
FormedGranuloma	**Granuloma**	Represents the formation of granuloma. It contains the information about the granulomas formed with their specific position and amount of macrophages.
MatureGranuloma	**Macrophage**	Represents the spread of the bacteria inside the granuloma. It contains information about the granulomas i.e. their positions and amount of macrophages (concentration) of each granuloma
MacrophageDisseminated	**count**	Counts/Controls the amount of infected macrophages that will leave the granuloma to disseminate the infection on another position
IntracellularInteraction	**Dot**	Coarse place that holds the hierarchical sub-nets, i.e. the connected hierarchical layers in the model and represents the bacterial-macrophage interaction at the intercellular, intracellular and molecular level as defined in [17]

4.3.3 *Set of transitions T*

The set of transitions T of level 1 of our model is defined as:

$$T = \{\textbf{Phagocytosis, PhagolysosomeFail, Migration, MigrationDeepTissue, Recruitment, IntracellularSpread, Dissemination}\} \quad (8)$$

These describe important phases in the infection process and are regulated by thresholds that control the simulation. **Table 4.4** describes these transitions and their guards (if present).

Table 4.4: Set of transitions composing the level 1 of the model

Transition	*Guard*	*Description*
Phagocytosis		Fires once its pre-places contain bacteria and immune cells at the same position. It produces tokens that represent infected macrophages as well as tokens that hold the information of the initial infection position for the 3D visualization tool
PhagolysosomeFail		Responsible for the activation of the intracellular bacterial spread, modeled in the sublevels of the hierarchical structure, while the infected macrophage moves along the blood stream, i.e. changes its position
Migration		Responsible for controlling the macrophage position change (movement throughout the blood stream)
MigrationDeepTissue		Fires once the macrophages reach the threshold within the bacteria migrating to deep tissue to form the granuloma
Recruitment		Signals to the non-infected immune cells i.e. healthy macrophages, to take over the dead macrophage in their specific tissue position thereby forming the granuloma
IntracellularSpread		Represents the maturation of the granuloma by releasing bactericidal material and infecting macrophages that form the granuloma
Dissemination	I<=MaxDissemination	Controls the threshold of the amount of infected macrophages that will leave the granuloma and disseminate the infection, forming a new granuloma on a different position

4.3.4 *Initial marking I*

An initial marking defines the number and type of colored tokens that are initially present in a specific place. For the modeling of the *Mm* infection, we have defined initial makings in our previous work [19]. There exist two types of markings, i.e. (1) condition markings that are fixed and

used to control the process, and (2) example markings that are not fixed and can be changed according to the experimentation with the net. **Table 4.5** and **Table 4.6** respectively describe these types of markings.

Table 4.5: Condition markings initially defined in the colored Petri net model

Place	Marking	Description
RecruitedMacrophage	**1`(1)**	Initializes the counting of the number of macrophages recruited to aggregate into the dead macrophage. It has a threshold defined by a constant *MaxAggregation* i.e. 5
MacrophageDisseminated	**1`(1)**	Initializes the counter of the amount of infected macrophages that leave the granuloma and spread the infection to different positions. It has a threshold defined by a constant *MaxDissemination* i.e. 3

Table 4.6: Example markings initially defined in the colored Petri net model

Place	Marking	Description
Infection	**1`(1,mm)** **++1`(2,mm)** **++1`(3,mm)**	Defines the initial concentration of mycobacteria that will intrude the host. We have defined three different positions to represent different initial infection sites
ImmuneSystem	**1`(1,mac,true)** **++1`(2,mac,true)** **++…++1`(12,mac,true)**	Defines the initial concentration of non-infected macrophages in the host. The positions and amount are empirical information used just to represent their presence in the host

All other places in the top-level model, i.e. level 1 of the hierarchical structure, are initially empty, meaning that there are no tokens in the places at the onset of the simulation.

4.3.5 Sub-models in the hierarchical structure

Following the tree of the hierarchical structure, the sub-models, implemented through the coarse place **IntracellularInteraction,** model a complex process involving various host-bacterial factors in a cross-talk interaction distributed in the sublevels. In order to get a consistent view of the entire interaction process, we express the most important reactions by simplifying the pathways at different levels of abstraction. The simplification of the pathways corresponds to our previously defined modeling decisions [17], where each biochemical compound or receptor is defined as a place. The relations between biochemical substances are represented by transitions with corresponding arcs for the reactions. Inhibitor arcs represent inhibitions and degradations. Signaling

and catalytic atomic events are represented by read-arcs. We specifically use the color-set **Dot** to represent the presence of a protein, component and/or cell that are involved in the interaction process between the macrophage and bacteria once it is phagocytized. To hierarchically connect the different pathways we use coarse transitions and coarse places structuring all the sublevels as shown in **Figure 4.2**.

4.4 Results

The simulation environment for the model represents the innate immune response to *Mycobacterium marinum* infection in the zebrafish embryo. The elements of the qualitative colored Petri net described in the previous sections, represent key factors involved in the processes of infection, innate immune response, and granuloma formation. Moreover, the interactions are represented by the firing rules that describe the behavior of the model:

- Signaling of the intruding bacteria, detected by non-infected macrophages followed by phagocytosis;
- Migration of the infected macrophage to the deep tissue within bacterial replication motivated by the phagolysosome failure in the macrophage causing the cell death;
- Recruitment of non-infected macrophage in response to signals of the dead macrophage, clustering to form the granuloma;
- Granuloma maturation and bacterial spread between aggregated macrophage;
- Infection dissemination through infected macrophage that scape from the matured granuloma forming new granulomas at different positions.

The top-layer level of our model is depicted in **Figure 4.3**. Places are represented by circles and coarse places by double circles. Transitions are represented by squares and coarse transitions by a double square. The number of tokens is expressed inside the places and their empirical data below the color-set (cf. **Figure 4.3**, dark blue). Arrows represent the arcs labeled with their expression on top of it (cf. **Figure 4.3**, light red). The arcs with a black dot as an arrowhead are read arcs. In the notation of our PN software environment, these are represented as two arcs in opposite directions between place and transition with an identical arc expression. However, the tokens are not consumed, just tested for their presence.

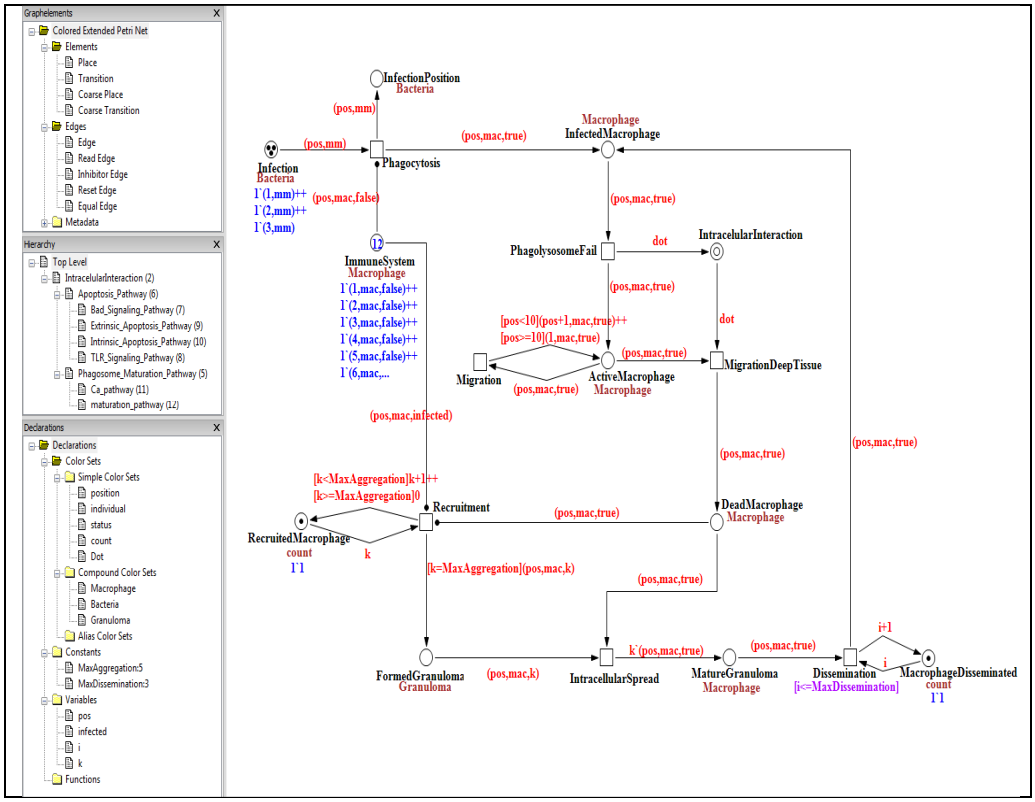

Figure 4.3. Visualization of the qualitative colored Petri net model implemented in the Snoopy framework [50]. In the left panel, information about the Petri net model is displayed: the hierarchical structure and definitions used in the model, the color-set, the constants and variables. The main panel shows the level 1 (cf. Top Level) of the hierarchical Petri net model and its properties.

In the model, the data value of the colored Petri net formalism is used to represent the quantities that change during the simulation. Although our focus is on a qualitative model, the quantitative aspects promote a better interpretation of the dynamical aspects of the simulation. Level 1, depicted in **Figure 4.3,** models the different stages of the infection process. It represents the phases of injection, phagocytosis, migration, granuloma formation and dissemination. Expanding the hierarchical structure, the connection of the sub-models and their components are depicted in **Figure 4.4**. The level 2 is modeled in the coarse place **IntracelularInteraction** of level 1 (cf. **Figure 4.3**). It represents the intercellular interaction between mycobacterium and a macrophage and it is triggered by the phagolysosome fail (cf. **Figure 4.4 (a)**). Level 3 models the intracellular interaction, represented by the coarse transitions: **Phagosome_Maturation_Pathway** (cf. **Figure 4.4 (b)**) and **Apoptosis_Pathway** (cf. **Figure 4.4 (c)**). These course places bridge the signaling started at the cell wall (cf. level 1) that triggers the interactions between molecules. Level 4 models the molecular interaction of the proteins released by the bacteria and the proteins from the macrophage. They are represented by the coarse places **Extrinsic_Apoptosis_Pathway**,

Intrinsic_Apoptosis_Pathway, **Ca_Pathway**, **Maturation_Pathway**, and also the coarse transitions **Bad_Signaling_Pathway** and **TLR_Signaling_Pathway**.

We have defined some boundaries to limit the model for a better qualitative analysis of the behavior of the system. The intracellular bacterial proliferation is defined by the arc expression **2`dot** which represents the offspring of two new bacteria every time the transition $T = \{$**bacterial_proliferation**$\}$ fires (cf. **Figure 4.4 (b)**). The capacity of the infected macrophage is limited to a concentration of 50 bacteria. After the place $P = \{$**bacterial_acumulation**$\}$ reaches this boundary, i.e. arc expression **50`dot**, the transition $T = \{$**Necrotic_Breakdown**$\}$ can fire. This action, changes the infected macrophage into a necrotic macrophage that will leave the blood stream and migrate into the tissue (cf. **Figure 4.4 (a)**)

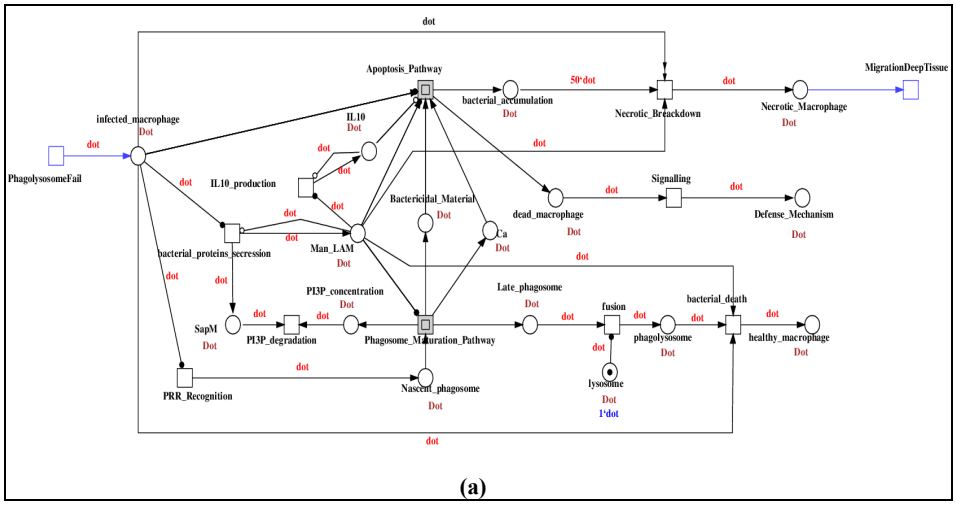

Figure 4.4 *Cont.*

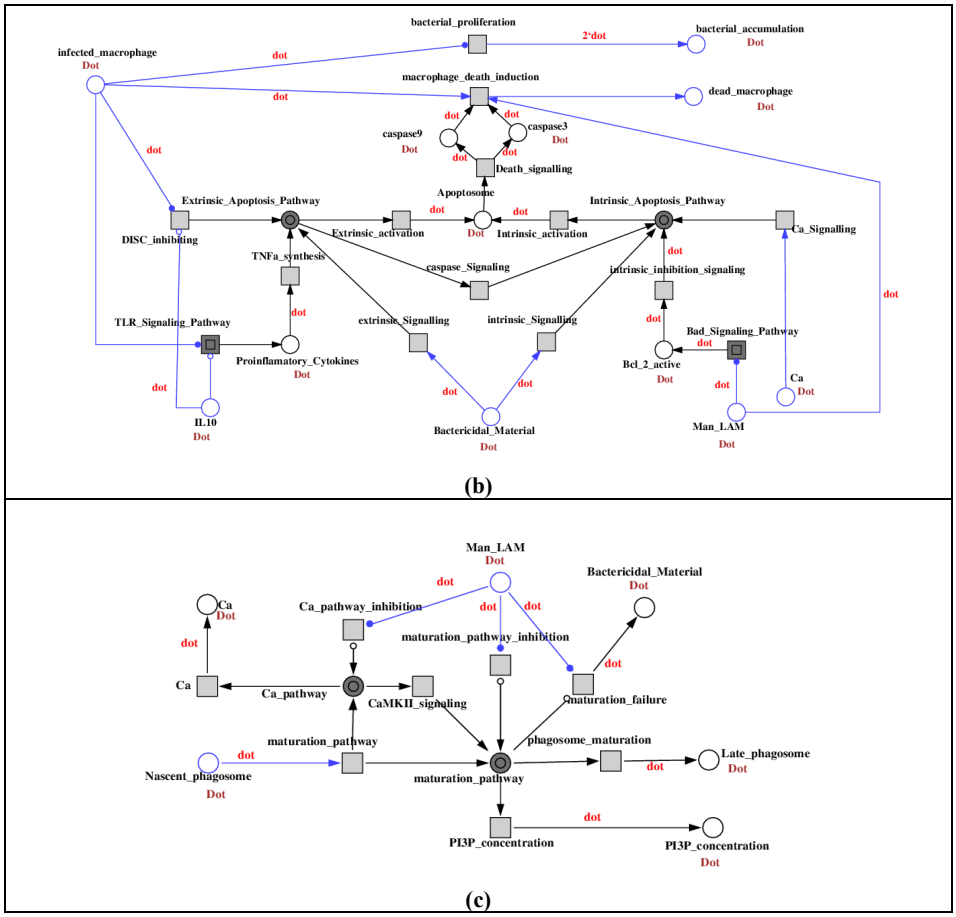

Figure 4.4. Sub-models in the hierarchical structure: **(a)** Level 2: Intercellular interaction between bacteria and macrophage. **(b) Apoptosis_Pathway** and **(c) Phagosome_Maturation_Pathway** represent the intracellular interaction are positioned at the level 3. The level 4 represents the molecular interactions defined in [17]; they are modeled in the coarse places and coarse transitions (data not shown).

Another threshold used is related to the position of macrophages and granulomas. Nezhinsky *et al.* [89] have developed an image processing platform for the analysis of high-throughput screens in zebrafish. In this platform, infected zebrafish embryos are automatically recognized as a shape. Relative to the shape, the bacterial infection is analyzed as an infection spread, to this end, the shape is divided into 12 regions of infection. This research has inspired us to determine 12 relative positions based on this division to model the presence of the macrophages, their movement during the infection process and also the spread of the granuloma. The concentration of aggregated macrophages is limited by setting a constant called *MaxAggregation*. Moreover, the infection dissemination is limited further by setting a constant *MaxDissemination* (cf. **Figure 4.3**). We use these thresholds to control the amount of cells that form the granuloma, as well as the number of

dissident infected macrophages that are released from the granuloma to spread the infection to other positions.

The outcome of our model reproduces the early stages of the mycobacterial infection process and innate immune response. We use the animation mode available in the Snoopy framework to verify the dynamic behavior of our model. This property enables the animation of token flow through the net, in order to observe the causality of the model and its behavior on the whole hierarchical structure. To show the importance of the immune cells, molecules, and processes in the dynamics of the infection, we performed a simulation based on our specific experimental scenario defined in Section 4.2.1.

We start the simulation by defining the amount of bacteria and their initial position at the place of **Infection**, adding the initial markings: $I\{$**1`(1,mm)**++ **1`(2,mm)**++ **1`(3,mm)**$\}$. The **ImmuneSystem** place, which contains macrophages, sends to the initial infected position a non-infected macrophage to phagocytosis the bacteria. The macrophage becomes infected through a failure of the phagolysosome process. Next, in the sublevels of the net the proliferation of bacteria will occur while the infected macrophage is migrating along the blood circulation. In the net, the proliferation process is triggered by sending a token **1`dot**, to the coarse place **IntracelularInteraction**. At the level 2, the infected macrophage attempts to kill the bacteria by activating the phagosome maturation or apoptosis process. The signaling process starts by sending a token from the place **Nascent_Phagosome** to the coarse transition **Phagosome_Maturation_Pathway**, and from the place **Bactericiadal_Material** to the coarse transition **Apoptosis_Pathway**. At the level 3, these pathways trigger the molecular interaction, by sending tokens to the coarse places and coarse transitions which models the protein-protein interactions at level 4. The bacteria interact with both pathways by releasing the ManLAM as presented by the place **Man_LAM**. It avoids to be killed and, instead, proliferates inside the macrophage (cf. place **Bacterial_acumulation**) causing a macrophage necrotic breakdown. At this moment the necrotic macrophage leaves the blood circulation (at the level 1) and migrates to deep tissue. There it will recruit non-infected macrophages to form a granuloma (cf. place **Formed_Granuloma**). The bacteria will spread inside the granuloma, and will disseminate the infection by releasing an infected macrophage to the blood circulation. The processes repeat itself for each infected macrophage that leaves the granuloma.

The amount of infected macrophages leaving the granuloma is limited through the constant *MaxDissemination*. Once this threshold is reached, there is no more transition enabled to occur and the execution will terminate in its final state. Since our model is focused on the qualitative aspects of the bacterial infection process and innate immune response, we bound our simulation by this constant to represent the initial dissemination of the infection. The final state then provides the quantity of granuloma formed during this process and their respective positions, accumulated at the

place **MatureGranuloma**. In **Figure 4.5** the final state of the net is depicted; an animation sequence of this PN can be found at http://bio-imaging.liacs.nl/galleries/couplingcpn. By saving the final state result of the QPN^C it becomes possible to derive the complete state space from the Petri net file. This file is subsequently used as the input for the 3D visualization of the process. The Snoopy file can be obtained upon request.

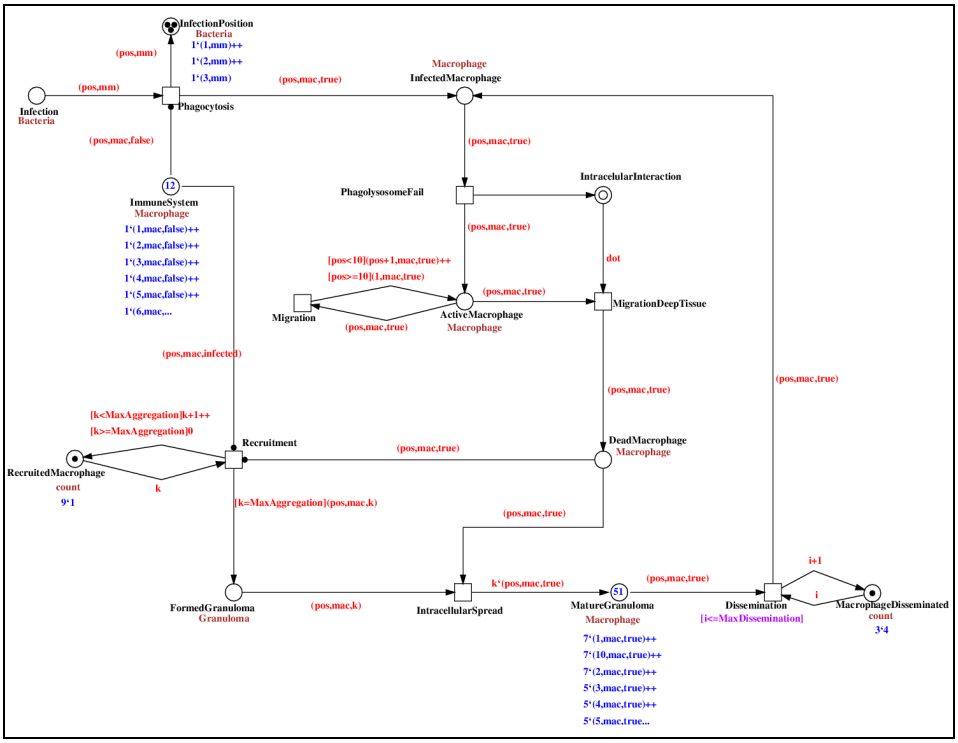

Figure 4.5. Animation mode at its final state, where there are no more enabled transitions to occur. We save this state and use the file as input to our 3D visualization tool

The 3D visualization tool was built to provide an alternative animation of the Petri net. We defined graphical elements to represent bacteria, macrophages and granulomas whereas a 3D mesh object represents the zebrafish embryo. The 3D visualization of the infection process plays the exact same simulation as the animation of the colored Petri net model. We define 12 regions in the mesh to represent the positions where the infection can occur. The positions are relative to spatial enumerations in the zebrafish model and normalized to its total length. The 3D animation is played over the entire volume of the 3D mesh. The 3D animation visualization software arranges the positioning of the objects in such a way that there is no overlap between the objects nor do they mutually collide. In **Figure 4.6**, the graphical elements and the object environment of the 3D visualization, is depicted.

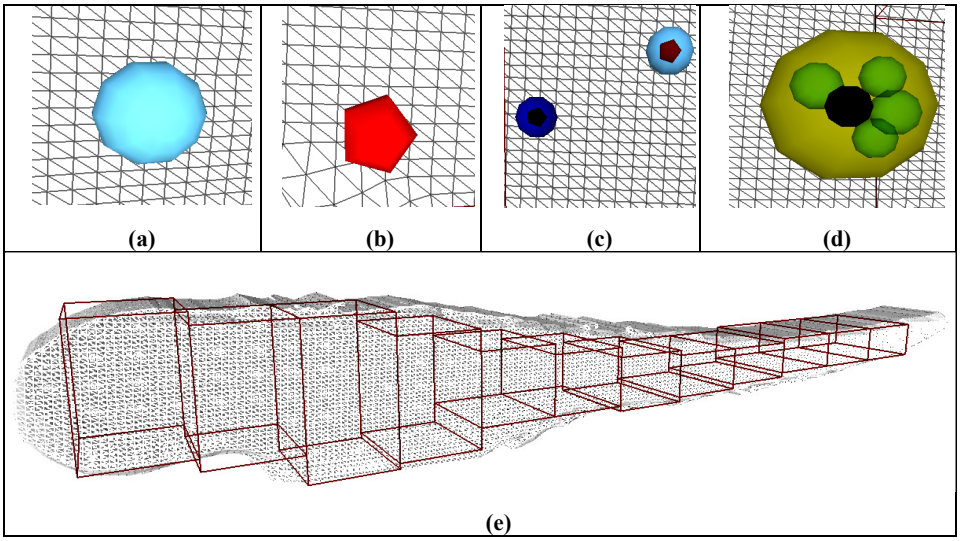

Figure 4.6. 3D visualization tool and its elements: **(a)** Macrophage. **(b)** Bacteria. **(c)** Infected macrophages. **(d)** Granuloma. **(e)** Fish embryo with the 12 regions where infection can occur.

In the 3D animation, the initial bacteria are introduced according to the information of the Petri net model. It reads the colored tokens in the place **InfectionPosition**, normalizing the position values and placing the bacteria objects in the predefined regions accordingly. In the Petri net model, the non-infected macrophages are in all of the 12 possible regions as they are transported through the blood vessels. The granuloma formation and dissemination occurs on the basis of the information from the colored tokens as present in the place **MatureGranuloma**. The constants *MaxAggregation* and *MaxDissemination* bound the infection process. The animation is time independent and sequentially follows the infection steps as defined in the model. The 3D animation renders the dynamics of infection process and granuloma formation according to the final state space from the Petri net. For inspection and perusal, an animation sequence can be found at, http://bio-imaging.liacs.nl/galleries/couplingcpn. In **Figure 4.7** a comparison is provided of the 3D visualization with the Petri net data with a real zebrafish embryo that has been infected with *Mm*. The microscope image of a 7 days old zebrafish depicted in **Figure 4.7 (a)** is the result of an analysis for the spread of the *Mm* bacteria after 6 days of infection (*dpi*). This result was obtained with specific software and the granulomas extracted from the image are overlaid as *magenta* blobs [89, 113]. The final result of the 3D animation visualization is depicted in **Figure 4.7 (b)** As one can appreciate here, the simulation reproduces the distribution of the granulomas resulting from infection process along the fish, in a similar pattern as it occurs in the real zebrafish. So, it is possible to correlate our final result with *in vivo* experiments although we are not using quantitative data. The thresholds to manipulate the dynamics of the QPN^C model is the only quantitative

information that has been used, and these threshold are not directly based on the analysis of empirical data. We, therefore, cannot directly compare the amount of granuloma or the distribution of the infection as obtained from our QPN^C model to *in vivo* situations. However, we can extrapolate from the results of our simulation that the structure of our Petri net model qualitatively represents the behavior of the *in vivo* infection process.

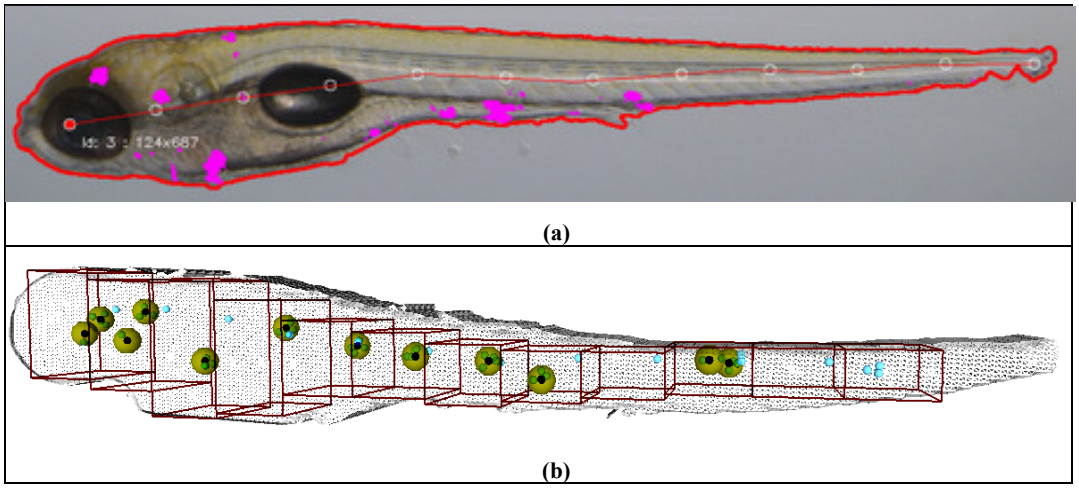

Figure 4.7: (a) Microscope image of a 7 day old zebrafish (7 *dpf*) infected with wild-type *Mm* bacteria 1 day old, referred to as 6 days post infection (6 *dpi*). The granulomas are displayed as magenta blobs. **(b)** The end state of the 3D animation with all the granulomas formed according to the final state space of the colored Petri net model.

4.5 Conclusions and discussions

The model we presented in this work is concerned with an infection scenario: the innate immune response to *Mycobacterium marinum* in zebrafish. It represents the dynamics of bacterial proliferation, granuloma formation, and dissemination. The model captures the relevant functional processes and their interconnections including signaling and activation or inhibition of the immune responses at different levels of abstraction. In sublevels, we have connected the most important pathways in order to model the response of the macrophage on the exposure to pathogenic mycobacteria. Information about the proteins released by the bacteria, their interference with the immune response, and the pathways involved in this process are also taken into account.

We focused on modeling the qualitative aspects of the infection process through connecting two complementary models: one for the reaction process and biochemical components implemented as a qualitative Petri net (without colors) [17]. The other model [19] represents the dynamics of the cells in the infection process which is implemented as a colored Petri net. The resulting hierarchical Petri

net model covers the relevant phases of the infection process, as well as the interaction pathways related to the infection persistence.

In order to combine the two models into one net model, the QPN model [17] was first converted into a QPN^C model. The color-set **Dot** was introduced to represent the presence of signaling molecules, proteins, and concentrations of cells involved in the interaction between macrophage and bacteria that are phagocytized. Through this color-set, the two models were combined in one modular structure. Using the Snoopy platform in animation mode, the combined hierarchical model could be executed.

The animation mode of Snoopy allows one to verify the dynamics of an animated Petri net by analyzing the markings encountered during a simulation. This showed that our Petri net model was able to replicate the steps in the infection process. This is due to the fact that the structure of the Petri net is based on the actual description of the infection process as extracted from the literature. Hence, the qualitative aspects in the sense of cause-and-effect are in accordance with the actual process. The quantities used in the model have no direct significance but to support the qualitative modeling and serve only as threshold. Neither quantities nor time are essential to the working of the model.

From a biological perspective, the additional 3D visualization environment has proven to be an interesting complementary approach to illustrate the infection process. The possibility to visualize the infection occurring from the introduction of bacteria to granuloma formation as it would happen *in vivo*, provides a better understanding of the infection process.

A comparison of the simulation results with an *in vivo* experiment (an infected zebrafish at 6 dpi) confirms once more the strength of the qualitative aspects of our model (cf. **Figure 4.7**).

Because the 3D visualization tool reads markings of the Petri net model, changes in the initial marking of the net are directly reflected in the 3D visualization. Thus it can lead to more insight into the infection process, e.g. how dissemination and concentration of granulomas depend on the initial position of the bacteria, the amount of aggregation cells that form a granuloma, as well as on the number of infected macrophages that can leave the granuloma. By changing the number and/or positions of tokens, "what-if" scenarios can be executed to represent different biological conditions. Disruptions of pathways, presence or absence of proteins, and also different positions of cells, can be simulated as part of the experimentation in the animation mode.

For the further development of “what-if” scenarios, however, a quantitative model is necessary that, through support of empirical data would enable to do quantitative analysis as well as perform simulations and predictions. An advantage of our Petri net model is its modularity facilitating the conversion from a qualitative model to a quantitative model without changing the structure. Since the 3D visualization can perform an animation based on the final state space of the net, it would then provide an even more realistic perspective of the infection process. Currently, we are collecting and analyzing data from zebrafish infection studies to use these as a basis for such quantitative model. As a next step we will integrate these data in our simulation framework that will then be able to perform different scenarios as part of the simulation process. It will contribute to identify important parameters that can help to unravel mechanisms related to the mycobacterial infection process and innate immune response.

In summary, in this paper, we have presented the coupling of two distinct models of different aspects from the mycobacterial infection process and innate immune response. To understand the infection and the immune response, it is necessary to analyze the process from its epidemiology down to genetic levels. We have modeled the dynamics of the infection and also the intracellular, intercellular and molecular interactions, interconnecting the models in a hierarchical structure. The resulting multi-scale Petri net model allows the observation of events at a given scale and how they interact with higher or lower levels. In addition, we provided an animation of the model using the Snoopy framework and related the Petri net output to a 3D environment. The hierarchical structuring of information in Petri net has the potential to become an important tool for research in the development of infection diseases, Tuberculosis in particular.

5 Quantitative Petri net model approach for the *Mycobacterium* infection process

Based on:

Carvalho, Rafael V., van der Sar, Astrid M., Kleijn, Jetty, Verbeek, Fons J.
In preparation for submission 2015 (2015).

Our days as a polar winter .

Its hours of joy are glancing as lightning.
And adversities are as a night, never ends.
For happiness, Times run fast.
And for darkness, the seasons reside.

And in days that are heavy as lead
Flashes as a quick lightening, a love
this is illogical.
Then poetry erupts as fire
in straw hit by a thunderbolt.
In all these spreading ashes
How did these burning words survived?

Jabra Ibrahim Jabra, Palestina (1920 – 1994)

أيامُنا كالشتاءِ القطبيِّ:

ساعاتُ الفرح فيها, كالضياء, خاطفة.
والفواجعُ, كالليل, لا تنتهي.
للإشراقات أوقات ما أسرع ركضها
وللظلماتِ المواسمُ المقيمة.

وفي نهارات, أثقالُها كالرصاص
يومض كخطفِ البرق حبُّ
لا يُفهم منطقه,
ويندلعُ الشعرُ كاللهيب
في هشيم ضربتُه الصاعقة:
في هذا الرماد العنّيِّ المنتشر
كيف بقيت هذه الكلمات الحارقة ؟

جبرا إبراهيم جبرا، فلسطين، (1920 - 1994)

Abstract

In the introduction of this thesis we have stated that a model has to concisely summarize and replicate the relevant information about the biological process. In the previous chapters, we have presented models, which outline the components and dynamics of the *Mycobacterium* infection process. These models have been used as building blocks to create a qualitative model, with, according to the results, a validstructure . However, a reliable model has to reproduce the structure and behavior of the biological process. In this chapter we present a model that fits these requirements and can simulate scenarios that are in accordance with the behavior of the infection process. We used data from biological experiments to validate the model leading to a quantitative analysis of the simulations.

5.1 Introduction

The availability of data representing various biological states, processes and their time dependencies enables the study of biological systems at various levels of organization, from molecules to organism and even up to population level. It is also essential to build models that can simulate scenarios and predict behavior of the system. Moreover, we can use the biological data to validate the model leading to a quantitative analysis of the experiments. Therefore it can contribute to identify important parameters that can help to unravel mechanisms related to the biological process. Walpole *et al.* [123] review the importance of integrating data across spatial, temporal and functional scales and how multi-scale models, that are developed to work across these scales, may provide insights into biological systems using quantitative methods.

The QPN^C model presented in Chapter 4 provides a visualization of the dynamic processes involved in Mycobacterium infection in the zebrafish host as well as the interconnected pathways that interact once bacteria are inside the host immune cell (phagocytosis). Although we have used quantified boundaries to express the dynamics of the model, our earlier focus was to create a pure qualitatively model using data information only as boundary condition for the model simulation. Analyzing the deterministic aspect of the model, these boundaries add an oscillation in the final result according to the simulations. The reason was the accumulation of tokens in the sub-nets that model the pathways related to the mycobacterial proliferation (intracellular, intercellular and molecular interaction). This accumulation occurs along the iterations of the simulation process in order to provide a non-deterministic result. The accumulation of tokens did not interfere in the model simulation. In this chapter, we analyze data from biological experiments on *Mycobacterium marinum* infection in zebrafish embryos. We use this information to redesign our previous qualitative model from Chapter 4 into a quantitative model using SPN^C. For validation, we execute two scenarios, i.e. simulations of certain conditions, and compare the results with the data from *in vivo* experiments. The process of validation and refinement may lead to the discovery of new knowledge about the infection process.

The remainder of this chapter is structured as follows. In Section 5.2 we focus on the material and methods describing the data analysis process and the description of the extension of the previous model emphasizing the quantitative aspects. We discuss about the changes in the model to fit to the problem and how the data is implemented in the model. In Section 5.3 we show our results from the simulations. We compare with the data from *in vivo* experiments and validate the model. Finally, in Section 5.4 we present our conclusions and discuss the results pointing to possible directions for future work.

5.2 Material and methods

The original motivation was to refine the previous models, removing the unnecessary accumulation of tokens used to provide a non-deterministic qualitative output of the simulation process. To tackle the quantitative aspects of the infection process, we have converted the QPN^C model into a Stochastic Colored Petri net (SPN^C). This process assigns a rate function to the transitions that will address a probability to "fire" during the simulation. Therefore, the firing rule adds an extra condition for a transition to consume/produce tokens. When a particular transition becomes enabled, then a local timer is set to an initial value, which is computed at this time point by means of the corresponding probability distribution. The local timer is then decremented at constant speed, and the transition will fire when the time reaches zero [53].

The hierarchical structure of our model is not affected (cf. Section 4.3), though we restructure the dynamic level in order to add quantitative aspects related to the distribution of the infection (granuloma formation) along the positions. These data are derived from a statistical analysis from *in vivo* experiments with *Mycobacterium marinum* in zebrafish embryos [113]. The stochastic model is implemented in the Snoopy tool. This software environment also allows to execute simulations and animations with SPN^C [50]. In the following sections, we will present the data analysis and the stochastic model implemented.

5.2.1 Data collection and analysis

As the basis for our model, we have analyzed data from *in vivo* experiments on zebrafish embryos. The empirical data consist of microscope images of zebrafish, that are 6 day post fertilization (6 *dpf*), infected with wild-type *Mycobacterium marinum* (E11 strain) inoculated into the caudal vein immediately after the onset of blood circulation, i.e. at 28 hours post fertilization (28 *hpf*). The inoculated amount of bacteria ranges from 50 to 200 colony forming units (CFUs). The images were acquired by Leica stereo fluorescence microscope. The images contain infected zebrafish at 5 days post infection (5 *dpi*).The images were part of experiments performed at the department of Medical Microbiology and Infection control (MMI) from the VU Medical Center Amsterdam, under the procedures presented in [113]. For screening, two channel images are used; one channel with a bright field image of the zebrafish and a second channel containing a fluorescent image visualizing the bacteria colonies.

For the analysis of the images, we have used a data analysis environment for high throughput screening (HTS) called *eLaborant* [90]. This computational platform offers a complete solution for image analysis and pattern recognition for zebrafish screening and extracts information about size, shape factors, intensity, texture and location of specific anatomical parts of the zebrafish in the images. The *eLaborant* platform analyzes the zebrafish images [89], by dividing the specimen in 12 regions and quantifying the fluorescence in the regions. It identifies the infection spread within the object and calculates the surface area of the bacterial signal by performing relative measurements about the proportional surface area of infection, cluster count and cluster infection intensity. In **Figure 5.1** one microscope image is depicted containing two zebrafish as analyzed by *eLaborant*. Here, we can notice the centers of the 12 regions (represented by dots and connected by a red line) as well as the granuloma distribution as obtained from the fluorescent channel and overlaid as magenta blobs [89, 113].

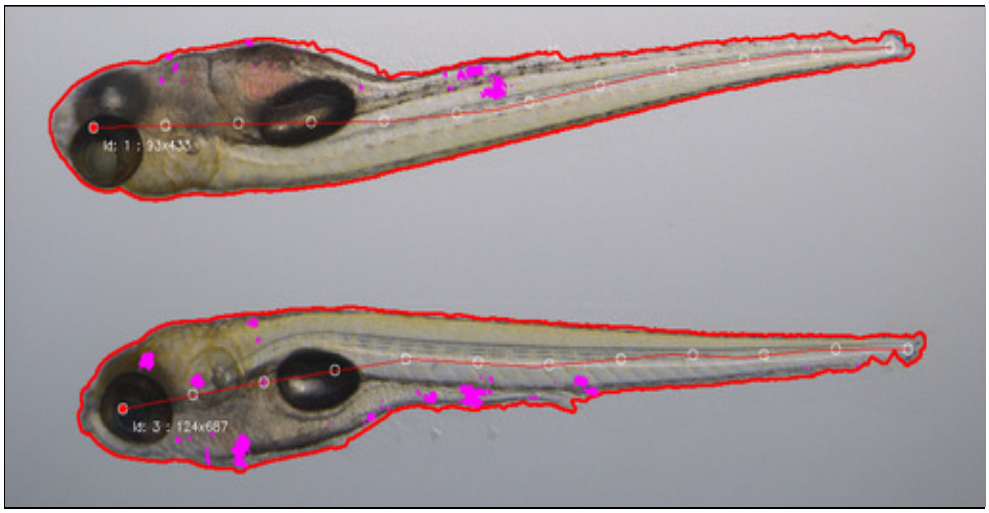

Figure 5.1: The image analysis result for the spread of the wild-type E11 strain on zebrafish with 5 *dpi*. Circles represent the centers of the 12 regions and the granulomas are displayed as magenta blobs.

For the scope of this work, we have considered the total area of infection, which represents the distribution of the infection along the fish according to the 12 pre-defined regions. To that end, we have analyzed 138 zebrafish infected larva by the E11 strain at 6 *dpf*. We calculate the average distribution of infection as proportional surface area of the total infection per segment (the pre-defined regions). The *eLaborant* measures the surface area of the infection by evaluating the fluorescence in the fluorescence channel. This sums to the total area of infection (A_t), i.e. the total surface are of granulomas in the zebrafish. Moreover, per segment (i) the surface area of the

granuloma is known (A_i). Consequently, the contribution per segment to the total infection, i.e. total granuloma size, is computed as:

$$PA_i = \frac{A_i}{A_t} \tag{5.1}$$

The contribution per segment to the total infection is expressed as a proportion of the sum of all regions (A_t). This is computed for our set of 138 samples and from the results we calculate the average proportion per region. This result is depicted in **Figure 5.2** where one can notice that the infection has a large concentration of granulomas localized near the head (referred to as regions 2 and 3), and also at the center of the zebrafish (referred to as regions 6 and 7). The caudal area (referred to as regions 11 and 12) is the site of bacterial inoculation, thus, the most infected regions have developed from dissemination of the bacteria over the body. We can also analyze the behavior of the infection from the perspective of the circulatory system; an infected macrophage travels while the bacteria proliferates inside its cytosol (cf. Section 4.2.1) we then can reason that the infected macrophage travels at least about 4 regions before leaving the circulatory system and attaches into the tissue to form the granuloma. One of the objectives of this work is to replicate this behavior as well as predict this dynamics over time using a quantitative model with stochastic behavior and taking the PN from chapter 4 as a starting point. In the next section we present the model and explain its characteristics.

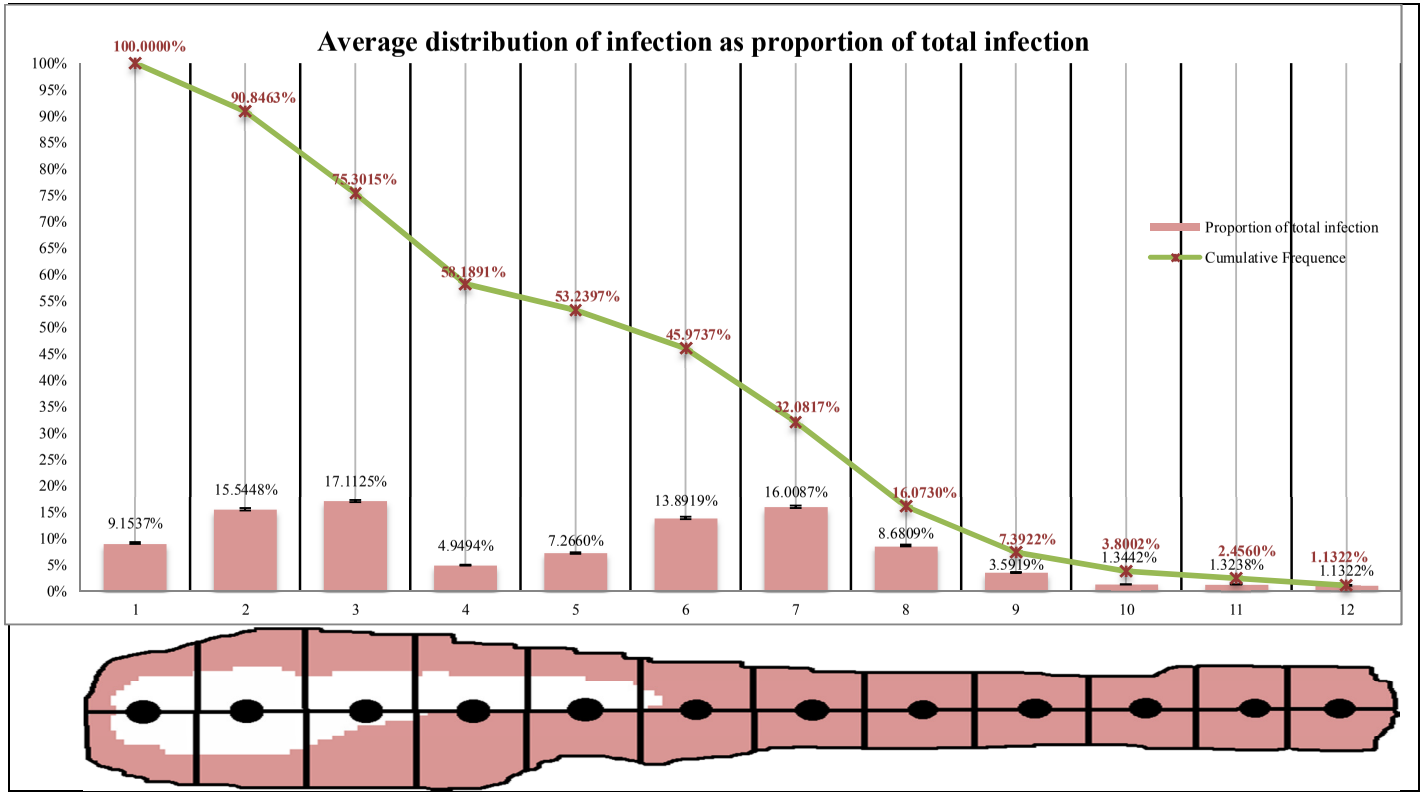

Figure 5.2: Empirical data analysis result: percentage of the distribution of the infection per region from 138 zebrafish at 6 *dpf* infected with wild-type (E11 strain) after 5 *dpi*. The result considers the total area of infection in the concentration of granuloma distributed over 12 regions.

5.2.2 Modeling decisions

The first step in the modeling process was to export our earlier model based on a QPN^C to a stochastic colored Petri net (SPN^C). The Snoopy tool provides portability processing between the methods [50]. By exporting the net, the tool preserves the discrete state space, but assigns exponentially distributed waiting times (probability) to transitions, which are specified by firing rate functions. The firing rates are typically state dependent and the predefined function is the kinetic mass action [74] assigned by the rate equal to 1 (cf. Chapter 1,**Appendix B** and **Appendix C** for a formal definition). The exporting process does not change components and structures, i.e. color-set, places, arcs, variables and guards. Therefore, the sub-nets remain the same.

In the next step, we refine the model by adapting its structure in order to make it suitable to simulate the quantitative aspects of the infection process. Therefore, we use the data obtained through experimental analysis in the stochastic transitions to regulate the migration process of the infected macrophage. There are 12 transitions with their own mass action function. The proportional granuloma distribution (PA_i) is used as rate ω_i in the kinetic mass action function for the 12 transitions. These data assign a probability of an infected macrophage migrating to a specific region of the zebrafish to form a granuloma. Besides the transitions related to the migration process, we replace all other stochastic transitions by immediate transitions. The immediate transitions are time independent (no rate/probability) and have higher priority than stochastic transitions to occur. Therefore, they will always fire, without any delay, if they are enabled. We have decided for this adaptation due to the limitations in our data-set, the quantitative information that we extracted from biological experiments relates to the infection distribution. There are no data (rates or time dependencies) about other interactions involved in the infection process, i.e. protein concentrations, time delays for molecular interactions, probability of a pathway, etc. Moreover, we have adapted the color-set and markings previously defined (cf. Chapter 4) to ensure that the model will be able to replicate the dynamics of the infection process in a stochastic simulation. In **Figure 5.3** the new model and its hierarchical structure are depicted.

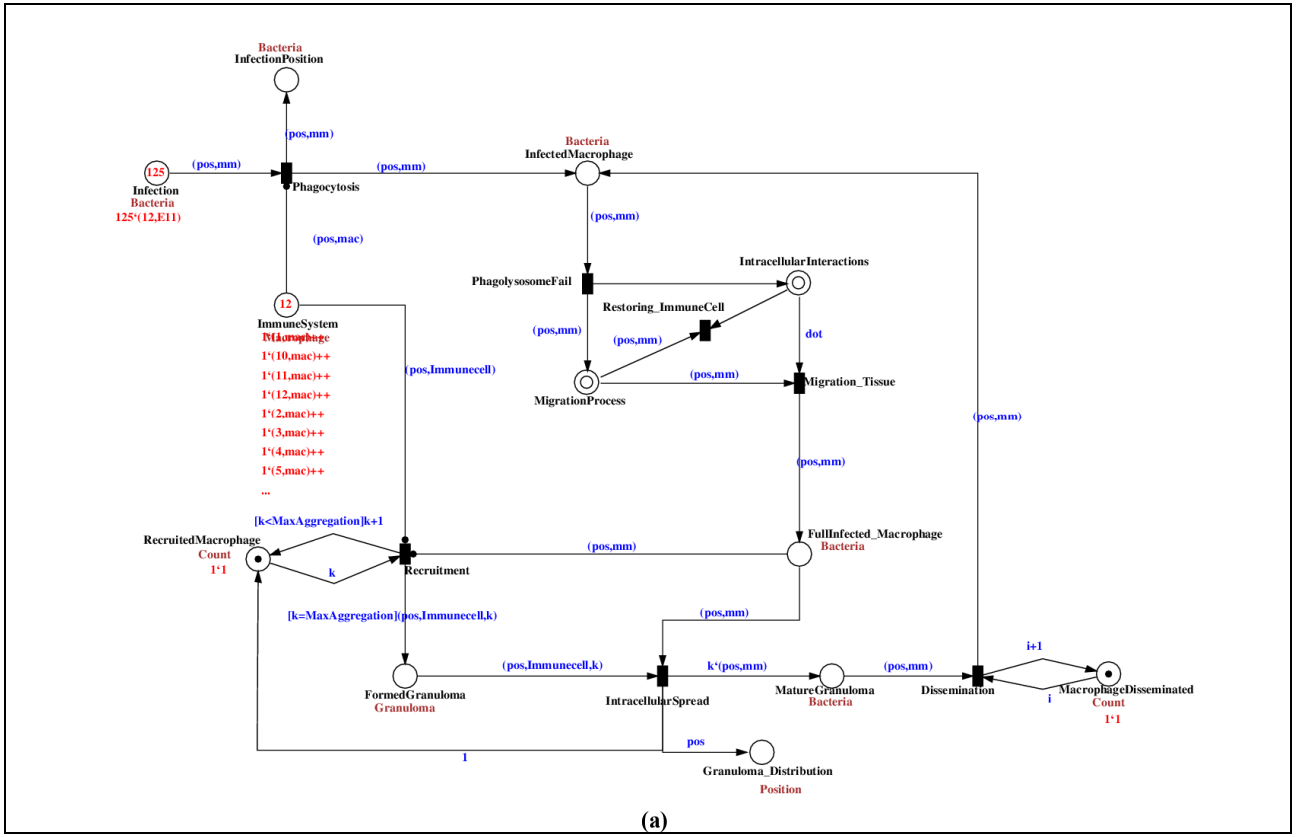

(a)

Figure 5.3 *Cont.*

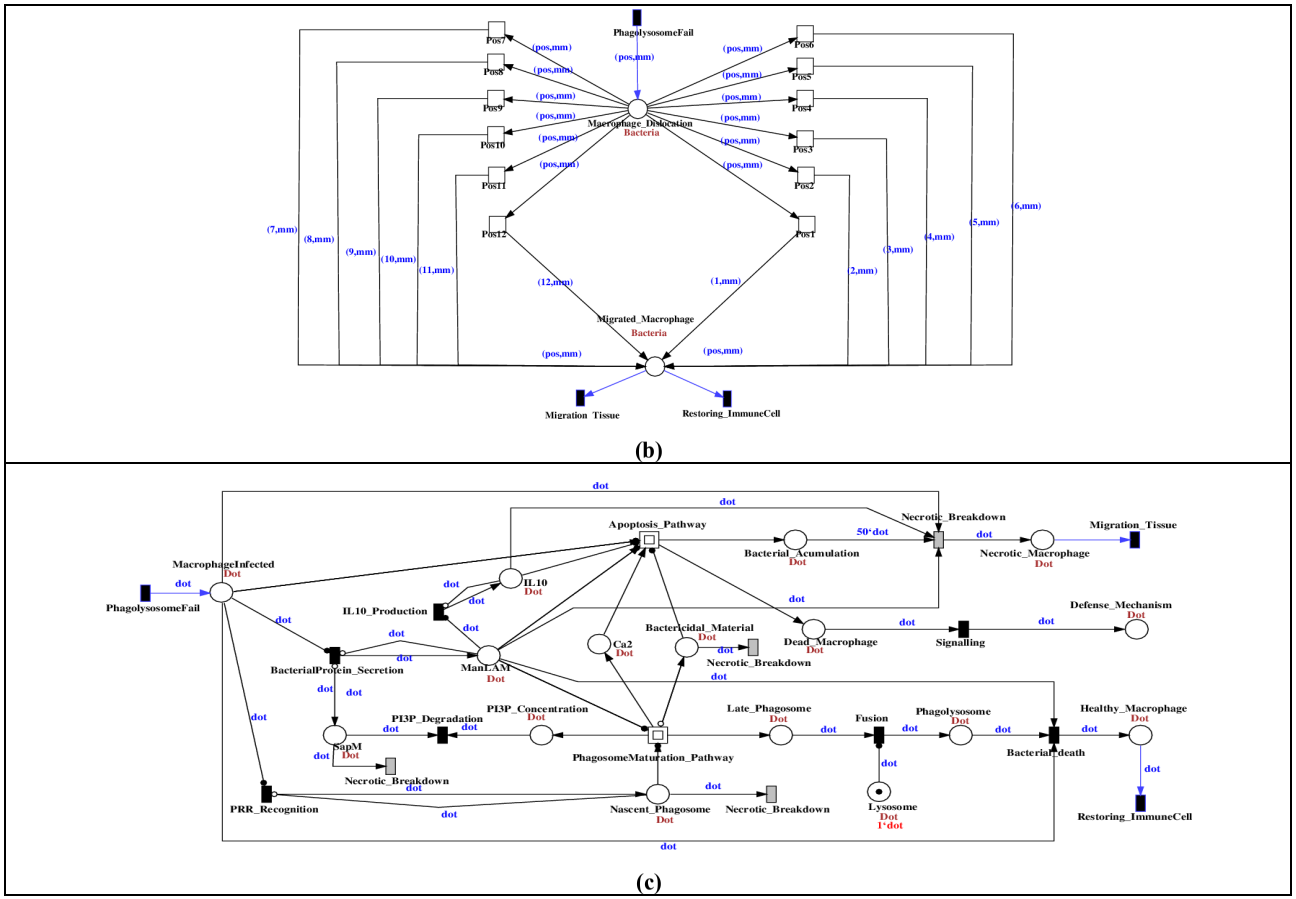

Figure 5.3 *Cont.*

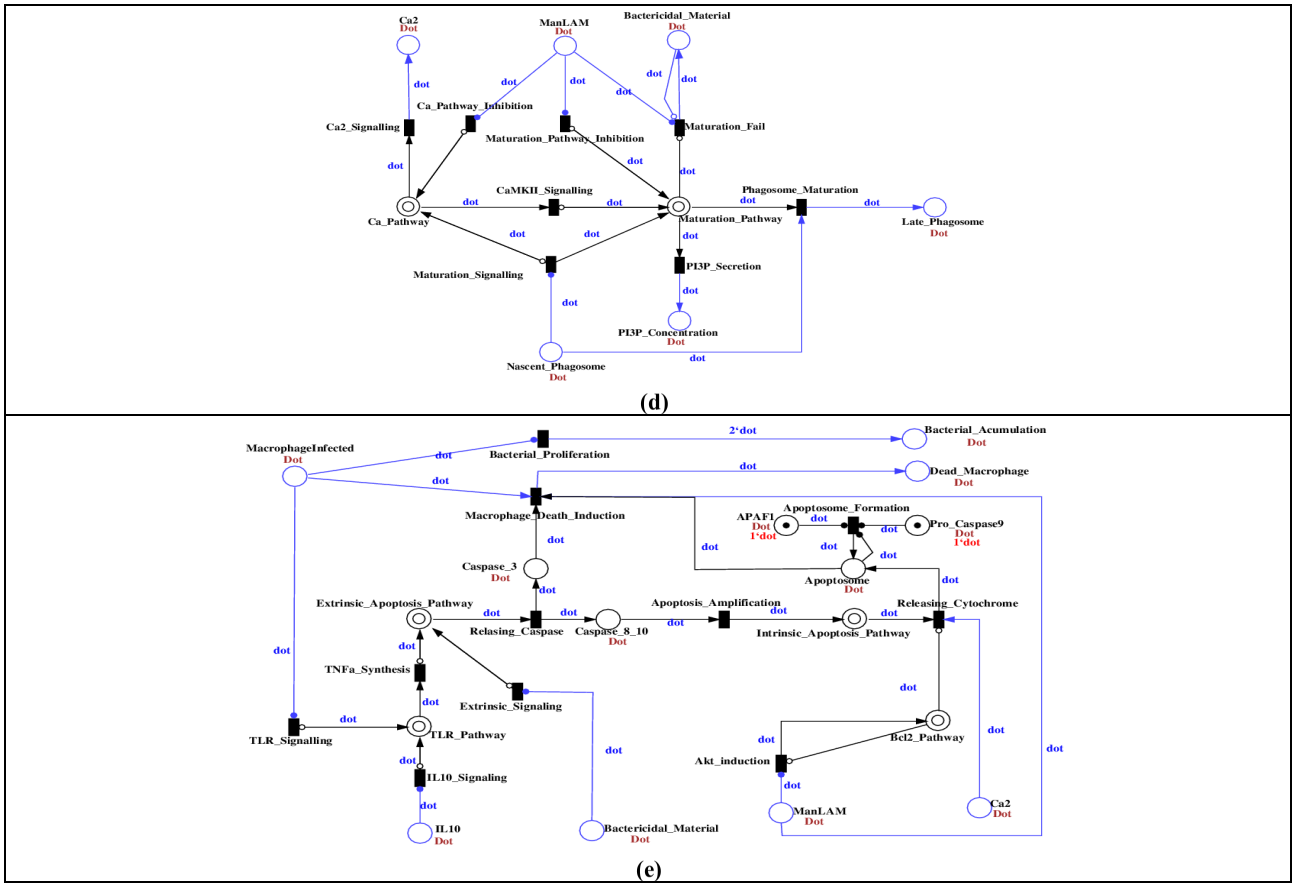

Figure 5.3 *Cont.*

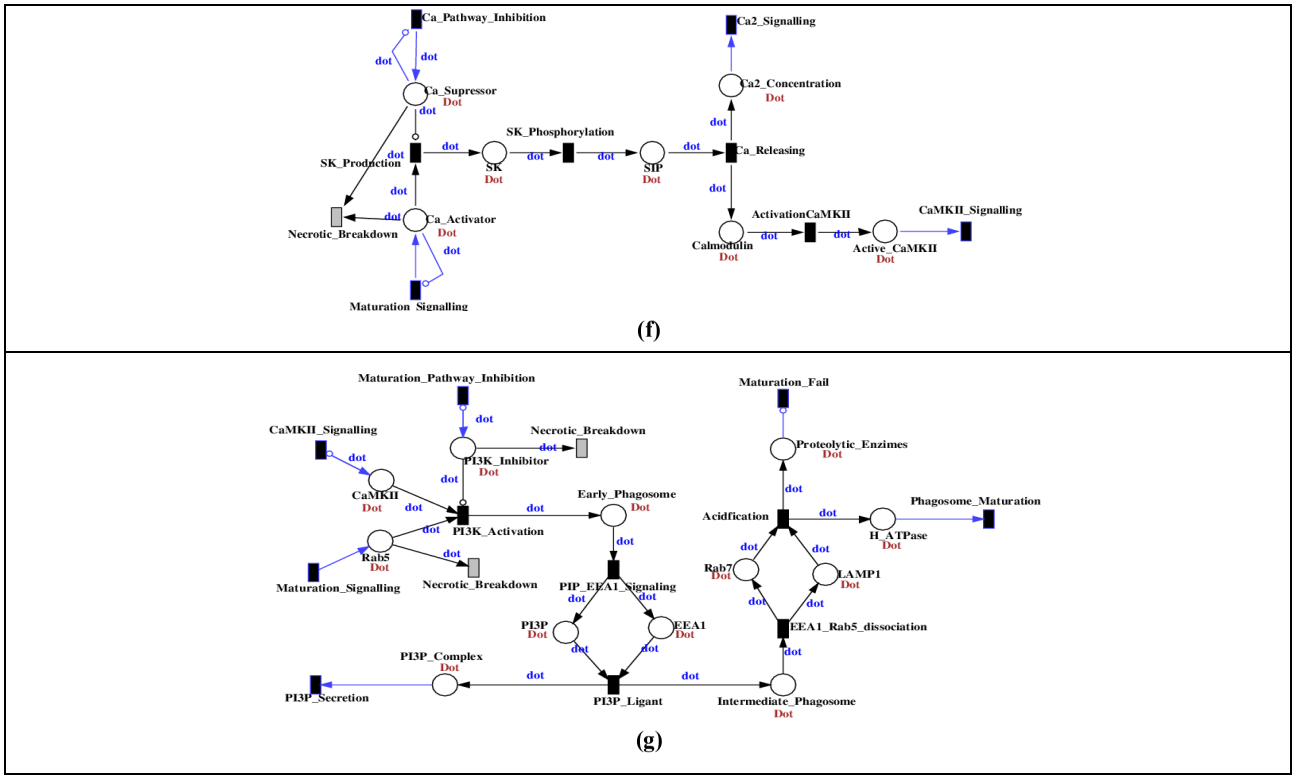

Figure 5.3 *Cont.*

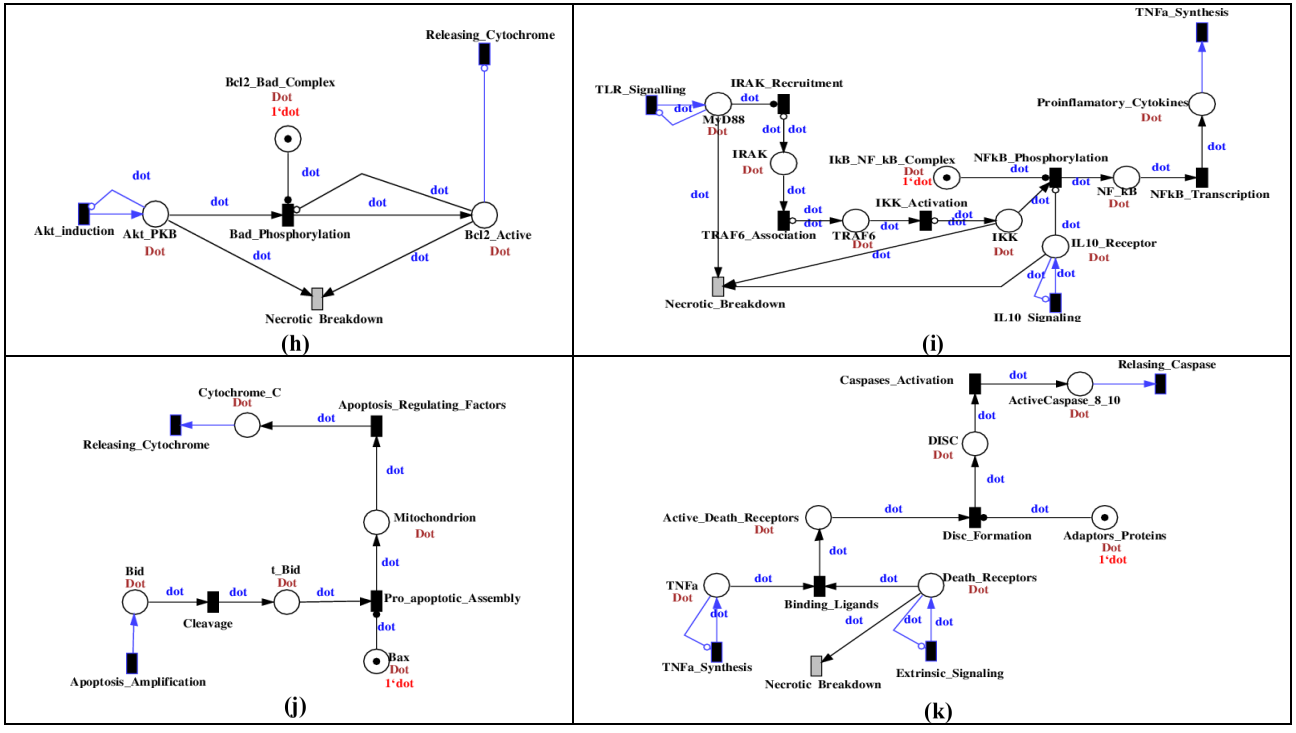

Figure 5.3 Model structure of the SPN^{C}. The black rectangles represent the immediate transitions and grey rectangles represent the logic nodes (fusion transitions). Stochastic transitions are represented by white squares. **(a)** Model the dynamic of the infection process. **(b)** Model the stochastic migration process **(c)** Model the bacteria-macrophage interaction at intercellular level. **(d)** Phagosome maturation pathway and **(e)** Apoptosis pathway at intracellular level. **(f)** Ca pathway; **(g)** Maturation pathway; **(h)** Bcl2 pathway; **(i)** TLR pathway; **(j)** Intrinsic apoptosis pathway and **(k)** extrinsic apoptosis pathway (**f**) to (**k**) are sub-models at molecular level.

5.2.3 Structure of the stochastic model

The hierarchical structure presented in Chapter 4 remains intact; the first layer net (top level) represents the dynamics of the infection process, while the sub-nets (levels 2, 3 and 4) represent the bacteria-macrophage interactions at intracellular, intercellular and molecular level. In the refinement process, we have changed the structure of the apoptosis pathway and its sub-models to better fit to the biological process (cf. **Figure 5.3 (e)**): The intrinsic apoptosis pathway (cf. **Figure 5.3 (j)**) is an amplification process triggered by the release of caspase from the extrinsic apoptosis pathway and cellular stress (cf. **Figure 5.3 (k)**). Moreover, the apoptosome is formed at the intracellular level (apoptosis pathway) which leads to the induction of macrophage death [68] (cf. **Figure 5.3 (e)**). We also removed the unnecessary accumulation of tokens in the sub-nets by adding logical nodes to consume those extra tokens in the simulation process. The logical nodes, a.k.a. fusion nodes, are copies of a single node used for the sake of readability of the net. They are features for the design, working as graphical copies with identical function. We use the transition **Necrotic_Breakdown** as a logical node on the sub-models in level 2 (intercellular model, cf. **Figure 5.3 (c)**) and in level 4 (molecular models, cf. **Figure 5.3 (f)** to **(k)**). Therefore, whenever this transition is enabled, it will consume all tokens on each level at the same time. With this solution, we have guaranteed that for each infected macrophage there is an individual host-pathogen interaction at the intracellular, intercellular and molecular levels. **Table 5.1** describes the places that previously accumulate tokens on each level and now are connected with the logical transition.

On the dynamic level (level 1), we have replaced the migration process, represented by the place **ActiveMacrophage** and the transition **Migration**, for a sub-net at level 2 implemented in the coarse place **MigrationProcess** (cf. **Figure 5.3 (b)**). This sub-net represents the migration of the infected macrophage towards the 12 regions according the data analysis presented in the Section 5.2.1. Therefore, the sub-net is composed of 12 stochastic transitions that specify the region where the infected macrophage will move to form the granuloma when it fires. The firing rule uses the kinetic mass action function and the firing rates are distributed based on the average distribution of infection previously analyzed (cf. **Figure 5.2**). The mass action function is used because it depends on the rate and not on the concentration of tokens. It follows the *mass action law* in which at a fixed concentration, the quantities (mass) have no influence upon the state of equilibrium [74]. It is not how much or how little of a substance is present that will be decisive, but how dense or sparse it is distributed in the space. Therefore, we correlate the distribution of the infection concentration along the 12 regions from the empirical data with the probability of the 12 transitions of the model to fire.

Table 5.1: Description of places connected through the logic node: **Necrotic_Breackdown**. Whenever this transition occurs, all the remains tokens are consumed.

Place	Sub-model (level)	Description
Nascent_Phagosome and **Bactericidal_Material**	**IntracellularInteraction (Level 2)**	Accumulates tokens that represent the signals triggering the phagosome maturation and the apoptosis process respectively (cf. **Figure 5.3 (c)**)
SapM	**IntracellularInteraction (Level 2)**	Accumulates tokens that represent the SapM protein released by the bacteria inside the macrophage (cf. **Figure 5.3 (c)**)
Ca_Activator and **Ca_Supressor**	**Ca_Pathway (Level 4)**	Accumulates signals (tokens) to the production/inhibition of calcium (cf. **Figure 5.3 (f)**)
Rab5 and **PI3K_Inhibitor**	**Maturation_Pathway (Level 4)**	Rab5 place accumulates maturation signals while PI3K inhibitor accumulates the ManLAM signals. (cf. **Figure 5.3 (g)**)
MyD88; IKK and **IL10_Repressor**	**TLR_Pathway (Level 4)**	MyD88 and IKK are proteins accumulated by the TLR signals and IL10_Repressor is accumulate signals to repress NFkB production (cf. **Figure 5.3 (i)**)
Akt_PKB and **Bcl2_Active**	**Bcl2_Pathway (Level 4)**	Akt protein is accumulated induced by presence of ManLAM while Bcl2 is accumulated by phosphorylation (cf. **Figure 5.3 (h)**)
Death_Receptors	**Extrinsic_Apoptosis_Pathway (Level 4)**	Accumulates the signals (tokens) to activate the receptors that bind with TNFa (cf. **Figure 5.3 (k)**)

5.2.4 Stochastic model extension

For a proper implementation, the set of color-sets Σ predefined in Chapter 4 also requires some modification. This involves the restructuring of the semantics of the color-set in order to make them suitable for the stochastic model. The SPN^C uses two sets of color-sets, the simple color-set described in **Table 5.2**, and the compound color-set described in **Table 5.3**.

Table 5.2: Simple color-sets modified for the colored stochastic Petri net model

Color-set	*Data type*	*Description*
Dot	dot	Default black color. Defined for all the places at the **IntracellularInteractions** sub-models
Position	Integer	Represents a location (of a macrophage, bacteria and/or granuloma) within the zebrafish embryo. It connects to the compound color-set.
count	Integer	Represents a threshold for the simulation in the recruitment of macrophage and calculate the amount of the dissemination.
BacterialType	String	Distinguishes the type of bacteria. Here represented by wild-type (**E11**) c.f. Section 5.2.1
ImmuneCellType	String	Distinguishes the type of immune cells. Here represented by **macrophages**.

Table 5.3: Compound color-sets modified for the colored stochastic Petri net model

Color-set	*Product type*	*Description*
Macrophage	**Position, ImmuneCellType**	Represents host macrophage immune cells
Bacteria	**position, BacterialType**	Represents the bacteria that are modeled
Granuloma	**position, ImmuneCellType, count**	Represents granuloma with a number of infected immune cells

There are no significant changes with respect to the set of places P and set of transitions T as previously defined in Chapter 4. Since we add a new sub-model implemented in the coarse place **MigrationProcess** (cf. **Figure 5.3 (b)**), we also add two places and 12 stochastic transitions to model the stochastic distribution of the infection. In order to extend our simulation experiments, we added the place **Granuloma_Distribution** to the dynamic model (cf. **Figure 5.3 (a)**). In this manner we are able to collect the information about the amount and position of the granulomas that were formed. Moreover, at this level we also add the transition **Restoring_Immunecell** to consume tokens from the place **Healthy_Macrophage** at **IntracellularInteractions** sub-model, cf. **Figure 5.3 (c);** and from the place **Moving_Macrophage** at **MigrationProcess** sub-model, cf. **Figure 5.3 (b)**. This transition represents the return of an infected macrophage to its functionality in case it has been able to digest the bacteria (phagolysosome process and bacterial death). In this scenario, the macrophage becomes healthy and no granuloma formation will take place. In **Table 5.4** and **Table 5.5** the set of places and transitions added to our model are described respectively.

Table 5.4: Set of places *P* added to the stochastic model

Place	*Color-set*	*Description*
Moving_Macrophage	**Bacteria**	Represents the macrophage in the moving process. It contains the initial infected macrophage that will move within the bacteria.
Migrated_Macrophage	**Bacteria**	Represents the infected macrophage repositioned into a region where it will leave the circulatory system and form the granuloma.
Granuloma_Distribution	**Position**	This place is used to keep track on the spatial distribution of the infected macrophage along the 12 regions.

Table 5.5: Set of transitions *T* added to the stochastic model

Transition	*Type*	*Rate function*
Pos1	Stochastic	MassAction(0.106042565)
Pos2	Stochastic	MassAction(0.165508512)
Pos3	Stochastic	MassAction(0.196383367)
Pos4	Stochastic	MassAction(0.056442759)
Pos5	Stochastic	MassAction(0.071513451)
Pos6	Stochastic	MassAction(0.148477928)
Pos7	Stochastic	MassAction(0.121384737)
Pos8	Stochastic	MassAction(0.057348882)
Pos9	Stochastic	MassAction(0.030160435)
Pos10	Stochastic	MassAction(0.015993484)
Pos11	Stochastic	MassAction(0.021050388)
Pos12	Stochastic	MassAction(0.00969349)
Restoring_Immunecell	Immediate	-

The initial marking *I* also does not significantly change compared to the qualitative model from Chapter 4. The condition markings remain the same, whereas the example marking regarding the amount of bacteria changed so as to represent the concentration of bacteria inoculated in the *in vivo* experiments. We defined that **125** tokens represent the amount of wild-type bacteria (**E11**) injected at position **12**. This value is derived from the average concentration of bacteria inoculated at the caudal region according to our empirical data (c.f. Section 5.2.1). If we change the number of tokens that represent the number of bacteria, it will influence in the total of granuloma that will be formed, i.e. the more bacteria, the more macrophage will phagocytosis and become infected; the relation is one to one (one macrophage to one bacterium). This effect does not occur with the initial marking related to the total number of macrophage. The place **ImmuneSystem** works as an infinite resource, it always contains macrophages in all positions. All the transitions connected to this place do not consume its token, only check if it has a macrophage in a specific position by the read arcs. Therefore, adding more macrophage in a specific position does not influence in the amount of granuloma, although, if there is no macrophage in a specific position, the bacteria that eventually

have settled in this position, will not be phagocytosis by the immune cell. The same process occurs for an infected macrophage that eventually migrates to a position without a macrophage; it will not form a granuloma. In **Table 5.6** the example markings initially defined for the stochastic model are described.

Table 5.6: Example markings initially defined in the colored stochastic Petri net model

Place	*Marking*	*Description*
Infection	**125`(12,E11)**	Defines the initial concentration of mycobacteria that will intrude the host.
ImmuneSystem	**1`(1,mac)++** **1`(2,mac)++** **1`(3,mac)++** **…** **1`(12,mac)**	Defines the initial position of non-infected macrophages in the host. We considered that macrophage can be present in all the 12 regions and the first macrophage to arrive at the infection site is and the nearest macrophage positioned

5.2.5 Simulation environment

Now that our SPN^C model has been set up, we simulate the stochastic process in order to reproduce the behavior of the mycobacterial infection process and innate immune response compared to the *in vivo* experiments. Snoopy software [50] provides a simulation environment for stochastic models. In this environment, it is possible to set-up the initial markings for the places; the function rates defined for the stochastic transitions; apply weights for immediate transitions. Moreover, it is also possible to specify the simulation time interval and the number of time points in the time interval that the information is recorded. In addition, the number of runs of the simulation process can be defined. The result is determined from calculation of the average values over all runs. The output of the simulation can be visualized in the simulation environment in different graphical formats (e.g. scatter plot, histogram, tabular) and also can be exported to a file (csv format).

5.3 Simulation and results

We perform stochastic simulations to test how well the model captures the dynamics of the system and how changes might affect the behavior of the infection process. Two simulation scenarios were performed reproducing the dissemination of the infection. We use the results of the data analysis from Section 5.2.1 as input parameter for our simulations as well as a means to compare the end result. The output of the simulations is the number of tokens accumulated at the place **Granuloma_Distribution** along the simulation time. The number of tokens represents the average granuloma formation on each position. The time is simulated in days, from the inoculation of the

bacteria (day 0) till the 5th day post infection (5 *dpi*), according to our data analysis from the zebrafish images. Hereafter we present the simulation scenarios and their outcome.

5.3.1 Stochastic simulation: ideal scenario for bacterial burden

In our first simulation, we consider that each macrophage that phagocytosis bacteria is not able to digest the bacteria (phagolysosome process) and neither suppress the infection (apoptosis process). Therefore, the infected macrophage migrates to form granuloma in one of the 12 regions, according to the probability distribution based on the rates given in **Table 5.5**. The granuloma disseminates the infection by releasing infected macrophages that will form more granulomas along the regions.

In this scenario, the infection behavior is simulated from the time point the bacteria are introduced in zebrafish embryo (time 0), till the time the zebrafish larva were screened by taking images at 5 *dpi*. The place **Granuloma_Distribution** contains the information about the total of granulomas that are formed per region. We plot the average of the number of tokens accumulated during the simulation time per region. **Figure 5.4** and **Figure 5.5** depict the results. In **Figure 5.4 (a)** we depicted the accumulation of the infection, as average of the number of tokens per region (**Macrophage_Distribution_1** till **Macrophage_Distribution_12**) in 5 days, for one random specimen of zebrafish (1 simulation run). We performed 138 simulation runs within one experiment in order to compare with the number of samples (138 zebrafish) from our empirical data. In **Figure 5.4 (b)** we depicted the average value of number of granuloma accumulated over 138 runs. It represents the accumulation of the infection per region during the 5 days from 138 zebrafish. **Figure 5.5** presents the percentage of distribution per region (**Pos1** till **Pos12**) for both simulations (1 run and 138 runs). It is possible to verify the similarity of the distribution and the behavior of the system by comparing the simulation results with the empirical data. Most of the infection regions in the simulations are concentrated in the head (position 2 and 3) and also at the center of the zebrafish (position 6 and 7), which is similar to the *in vivo* experiments. For one simulation run, we have a total of 224 granulomas formed, while the 138 simulation runs totalized an average of 221.88 granulomas formed. The infection distribution grows exponentially, reaching a steady state during the run time. This means that, for this model, there will be hardly any difference witch simulations for 6, 7 *dpi*. However we cannot predict the same behavior for the *in vivo* experiments since there is no data yet that report such behavior. The tendency of the simulations to reach the steady state in the number of tokens (infection distribution) is reflected in the single parameter set for the stochastic properties of the model. For this simulation we only have considered the probability for the distribution of the infection, whereas the other factors are considered to occur at as instantaneous events (immediate transition) and have no stochastic influence on the system. If we add more stochastic influence in the system, a different behavior might occur. Next, we simulate a second

scenario exploring a different simulation set in order to approximate the model to the *in vivo* experiments results observed in our empirical data.

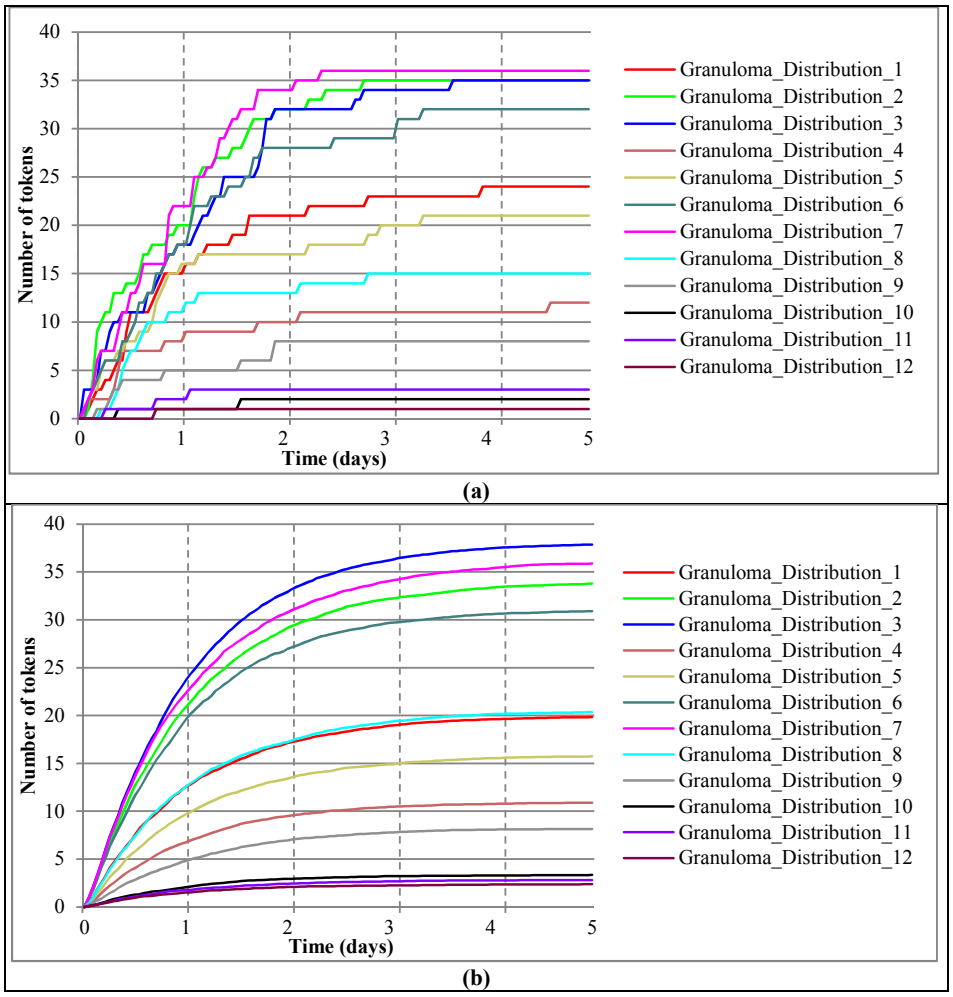

Figure 5.4 Simulation results of the stochastic Petri net model: ideal scenario for bacterial burden. **(a)** Infection distribution over time (5dpi) for one simulation run and **(b)** for an average of 138 simulation runs.

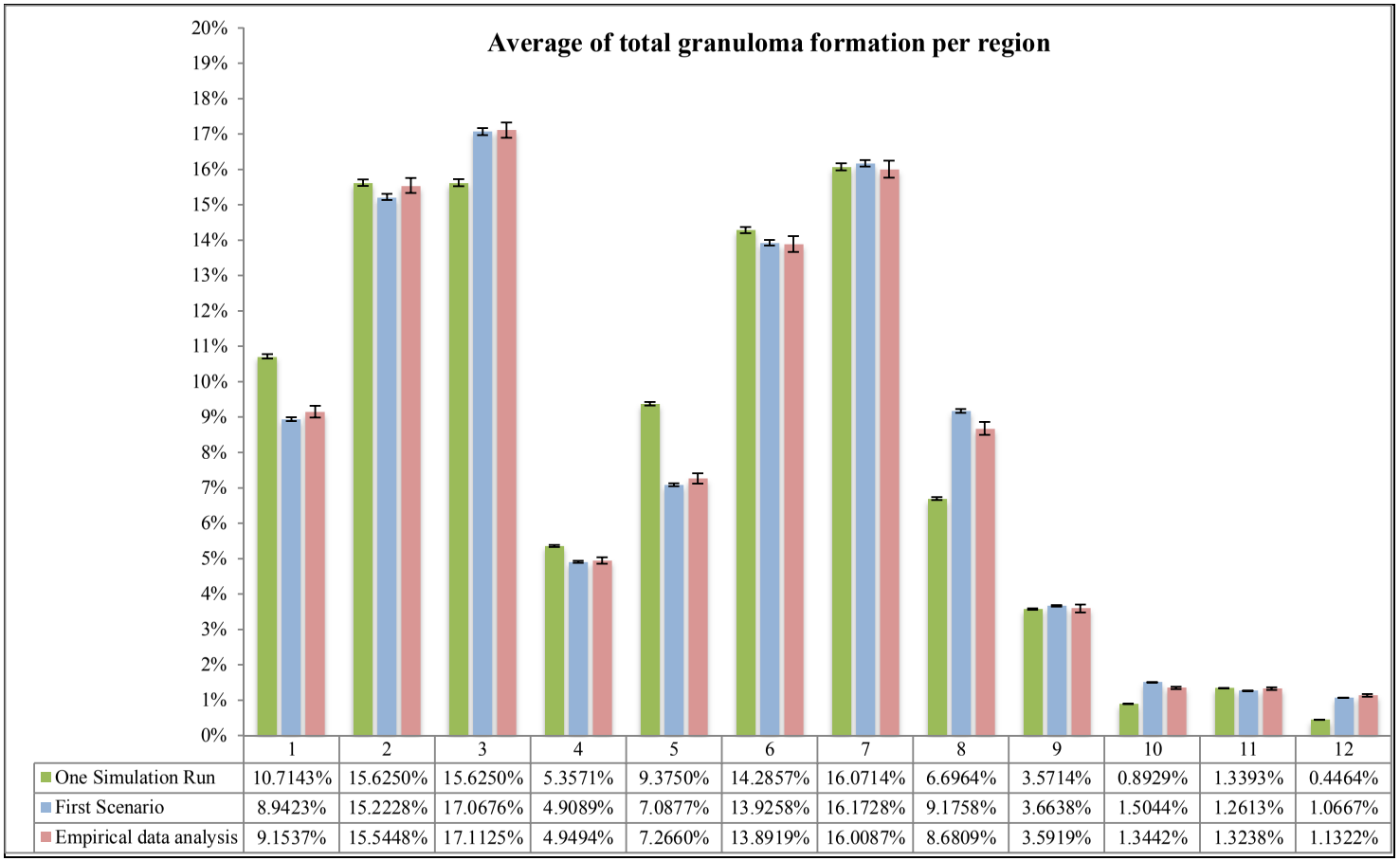

	1	2	3	4	5	6	7	8	9	10	11	12
One Simulation Run	10.7143%	15.6250%	15.6250%	5.3571%	9.3750%	14.2857%	16.0714%	6.6964%	3.5714%	0.8929%	1.3393%	0.4464%
First Scenario	8.9423%	15.2228%	17.0676%	4.9089%	7.0877%	13.9258%	16.1728%	9.1758%	3.6638%	1.5044%	1.2613%	1.0667%
Empirical data analysis	9.1537%	15.5448%	17.1125%	4.9494%	7.2660%	13.8919%	16.0087%	8.6809%	3.5919%	1.3442%	1.3238%	1.1322%

Figure 5.5 Percentage of distribution per region (Pos1 till Pos12) for both simulations (1 run and 138 runs) compared to our empirical data analysis.

5.3.2 Stochastic simulation: macrophage response to infection

In the studies on mycobacterial infection, Armstrong and Hart [5] were the first to identify the bacterial influence in the phagolysosome. They performed *in vitro* experiments with cultured macrophages infected with *Mycobacterium tuberculosis (Mtb)*. They showed that approximately 70% of the infected macrophages display failure in the process of fusion of the phagosome with the lysosome. Although their experiments were with *Mtb*, in our simulations, we assume that *Mycobacterium marinum* behaves similar and used this particular fact in our second scenario. We add a probabilistic factor of the macrophage to perform the phagolysosome process, degrading the bacteria, becoming healthy, complying with its immune properties, and thereby reducing the virulence spread. In this manner, we consider to reproduce the infection process in a more realistic manner.

To perform this simulation, we added a stochastic transition at **IntracellularInteractions** sub-model (cf. **Figure 5.3 (c)**) which will fire a token to the place *P*={**Late_Phagosome**} indicating the maturation process has occurred. This stochastic transition will fire according to the **MassAction** function that will indicate the probability of the phagosome maturation take place in an infected macrophage. For this scenario we performed 3 simulations with different probabilities (rates) for a macrophage to perform the phagolysosome process. In simulation one, we consider the probability of 70% of chance for a macrophage failure in the phagosome maturation process, become infected and disseminate the infection, forming granuloma as observed in [5]. Therefore, a macrophage has 30% of chance to kill the bacteria by performing the phagolysosome process and becoming healthy. For the simulation two and three we arbitrary extrapolate the system, by considering 40% of chance for an infected macrophage form a granuloma (60% of chance to kill the bacteria) and 10% of chance for an infected macrophage form a granuloma (90% of chance to kill the bacteria) respectively. The reason for these rates is to analyze the behavior of the system in different scenarios, where the immune cell is able to respond to the infection process, as observed by Armstrong and Hart [5]. In **Table 5.7** we describe the rates (probability) of phagolysosome manifestation assigned for the transition for each simulation.

Table 5.7: Rates assigned to the **MassAction** function indicating the probability of a macrophage degrade the bacteria

Simulation	*Function*	*Description*
Simulation 1	**MassAction(0.3)**	Indicate there is a 30% of chance to a macrophage perform the phagolysosome and degrade the bacteria (become healthy)
Simulation 2	**MassAction(0.6)**	Indicate there is a 60% of chance to a macrophage perform the phagolysosome and degrade the bacteria (become healthy)
Simulation 3	**MassAction(0.9)**	Indicate there is a 90% of chance to a macrophage perform the phagolysosome and degrade the bacteria (become healthy)

We performed the three simulations under the same initial condition of the First Scenario, using the average of granuloma distribution per region from 138 simulation runs (cf. Section 5.3.2). In **Figure 5.6** we depict the average of granuloma formed for the three simulations. Moreover, in **Figure 5.7** we plot the average of concentration of granuloma per region formed during the simulation, compared with the First Scenario and the empirical data.

Analyzing the results from the simulations and the empirical data we can conclude that the model behaves similar to the biological experiments from the data analysis. Despite the bacteria CFUs are injected in the tail, a high concentration of granuloma is formed near the head and the center of the fish (regions 2, 3 and region 6, 7 respectively). We also noticed that the average of granuloma formation diminishes once we increase the probability of a macrophage to perform the phagolysosome and kill the bacteria. The Simulation 1 presented an average of 30.49 granulomas formed, simulation 2 resulted in 4.79 and simulation 3 presented an average of 1.60 granulomas considering 138 simulation runs in 5 days (cf. **Figure 5.6**).

Despite the fact that the amount of infection (number of tokens) has been less than the previous simulation, we can notice that the distribution of the granulomas slightly differentiates from the First Scenario and the empirical data. The higher the probability of a macrophage to be able to degrade the bacteria, the more the percentage of granuloma distribution per region from the empirical data differs. The percentage of distribution for the simulation without probability of phagolysosome (First Scenario) and with 30% of chance for the phagolysosome (simulation 1) are more similar to the empirical data, compared with the simulations of 60% and 90% of chance of a macrophage to degrade the bacteria. This is logical because we this to be part of the empirical data. In the next section, we perform a statistical analysis to assess the confidence interval and hypothesis on the similarity of the percentage of the granuloma distribution from our simulation experiments and the empirical data.

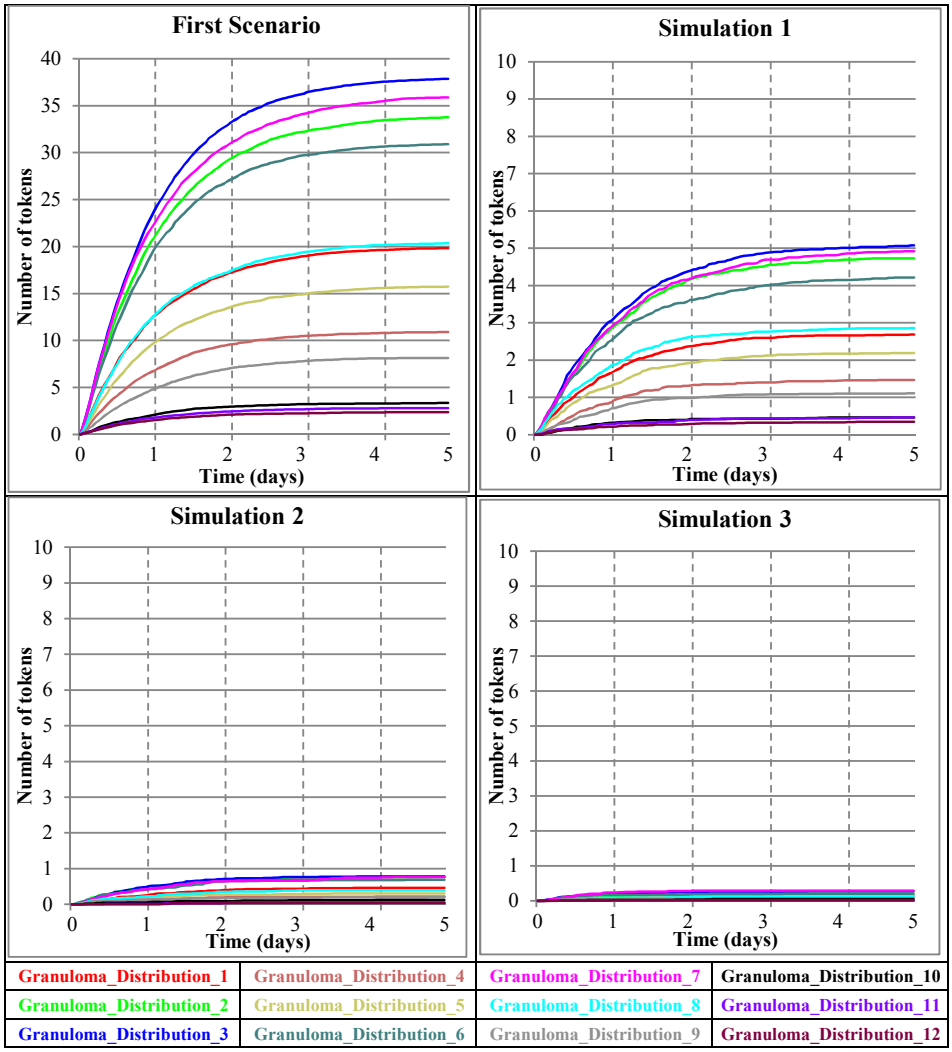

Figure 5.6 Simulation results of the stochastic Petri net model: **First Scenario** average of 221.88 granulomas formed; **Simulation 1** average of 30.49 granulomas formed; **Simulation 2** average of 4.79 granulomas formed; **Simulation 3** average of 1.60 granulomas formed.

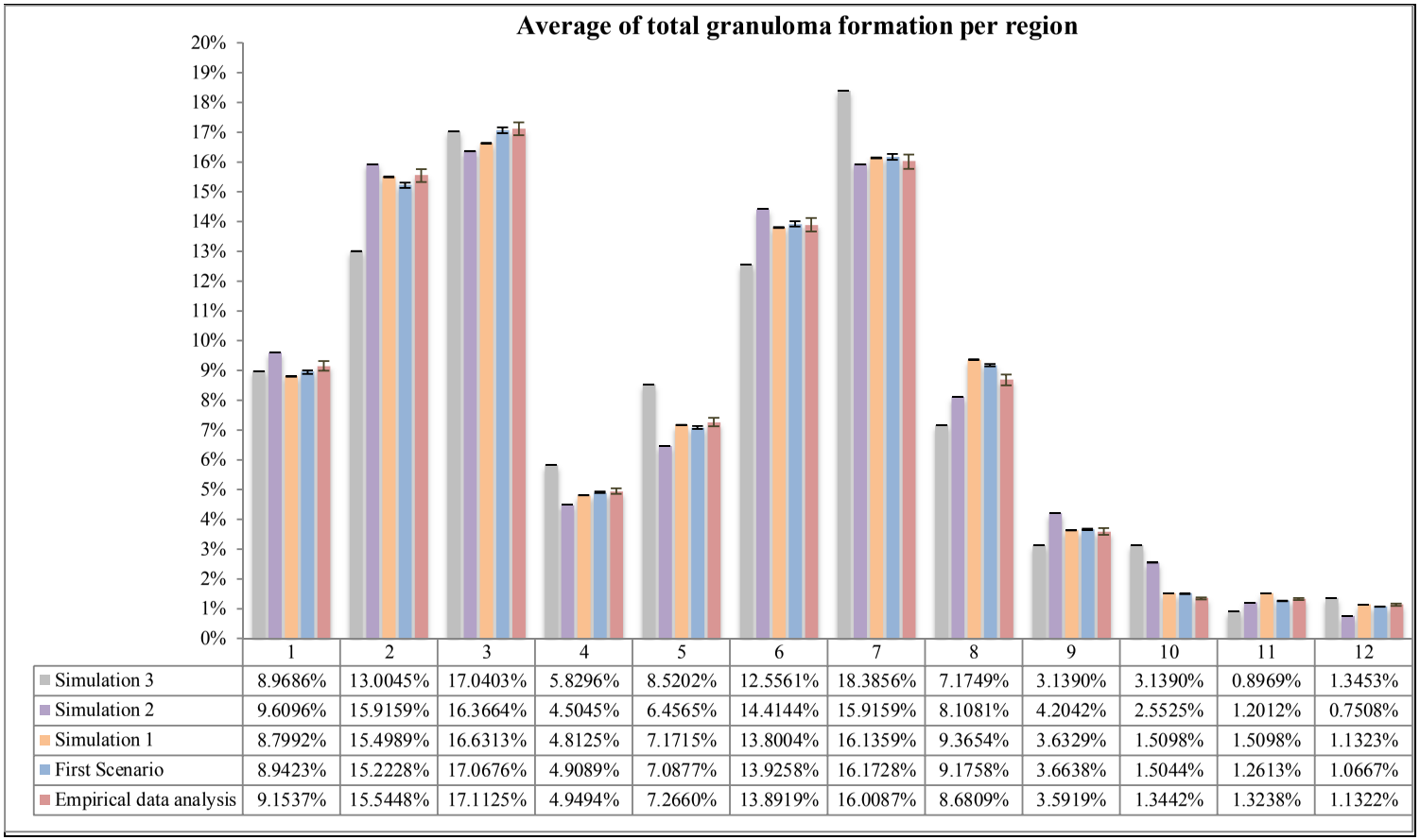

	1	2	3	4	5	6	7	8	9	10	11	12
Simulation 3	8.9686%	13.0045%	17.0403%	5.8296%	8.5202%	12.5561%	18.3856%	7.1749%	3.1390%	3.1390%	0.8969%	1.3453%
Simulation 2	9.6096%	15.9159%	16.3664%	4.5045%	6.4565%	14.4144%	15.9159%	8.1081%	4.2042%	2.5525%	1.2012%	0.7508%
Simulation 1	8.7992%	15.4989%	16.6313%	4.8125%	7.1715%	13.8004%	16.1359%	9.3654%	3.6329%	1.5098%	1.5098%	1.1323%
First Scenario	8.9423%	15.2228%	17.0676%	4.9089%	7.0877%	13.9258%	16.1728%	9.1758%	3.6638%	1.5044%	1.2613%	1.0667%
Empirical data analysis	9.1537%	15.5448%	17.1125%	4.9494%	7.2660%	13.8919%	16.0087%	8.6809%	3.5919%	1.3442%	1.3238%	1.1322%

Figure 5.7 Simulation results of the stochastic Petri net model using Snoopy: 70% of infected macrophage will form granuloma. Percentage of distribution per region compared with previous simulation (blue bar) and the data analysis (red bar)

5.3.3 *Analysis of the results*

A statistical analysis on the average of granuloma formation per region was performed, verifying the similarity of the percentage of distribution of each simulation with the analysis of our empirical data (cf. Section 5.2.1). The idea is to check if the result is statistically similar to what the plot in **Figure 5.7** shows, or if what we see is a coincidence of the stochastic process. Therefore, we use a one sample hypothesis test (t-test) since we are dealing with the average of the infection distribution per region. The t-test is the most commonly used confidence interval and hypothesis test of population means [13]. It is used to test whether the mean of a population takes a particular value, for repeated measurements (which is our case). It requires the sample to be independent, normally distributed and equal in sample size and variance.

We applied the t-test in the simulation of the First Scenario, in which an infected macrophage does not perform the phagolysosome process (0% chance to kill the bacteria); also in the simulations of the second scenario, in which an infected macrophage has a chance to perform the phagolysosome process (simulation 1 with 30% of chance to kill the bacteria, simulation 2 with 60%, and simulation 3 with 90%). In **Table 5.8** the t-test results for each simulation are given. It presents the percentage of similarity between the averages of concentration of granuloma per position similar to the analysis of our empirical data.

Table 5.8: One sample t-test result: probability of each position been similar to the empirical data

Simulation	*Pos1*	*Pos2*	*Pos3*	*Pos4*	*Pos5*	*Pos6*	*Pos7*	*Pos8*	*Pos9*	*Pos10*	*Pos11*	*Pos12*
First Scenario	88.07%	86.00%	98.07%	95.82%	88.62%	98.59%	93.71%	75.28%	94.01%	54.69%	84.76%	83.19%
Simulation 1	80.12%	97.99%	79.51%	85.91%	93.95%	96.18%	95.12%	66.31%	96.58%	53.34%	56.81%	99.96%
Simulation 2	74.61%	83.90%	68.72%	56.43%	51.64%	78.48%	96.44%	71.55%	52.20%	0.00%	70.64%	21.75%
Simulation 3	89.54%	16.57%	96.89%	25.48%	31.53%	48.54%	25.40%	33.86%	63.56%	0.00%	19.11%	48.99%

In **Figure 5.8** the confidence levels from the t-test for each simulation are depicted according to their position in the zebrafish. A high confidence level, i.e. similarity > 95%, demonstrates that in that particular region there is no statistically significant difference between the simulation and the empirical data (indicated by color blue). A mid confidence level, i.e similarity in >80%, <95%, demonstrates that in that region there is an acceptable significant difference between the simulation and the empirical data (indicated by color gray). A lower confidence level (similarity < 80%) demonstrates that in that region there is a statistically significant difference between the simulation and the empirical data (indicated by color red). Analyzing the results, we can notice that Simulation 1, i.e. a Macrophage with 30% chance to kill the bacteria, has more similarities in the distribution of the granuloma per position than the other simulations. We can correlate these results with the *in*

vitro experiments performed by Armstrong and Hart [5], indicating that indeed not all the macrophages that phagocytosis bacteria will generate a granuloma.

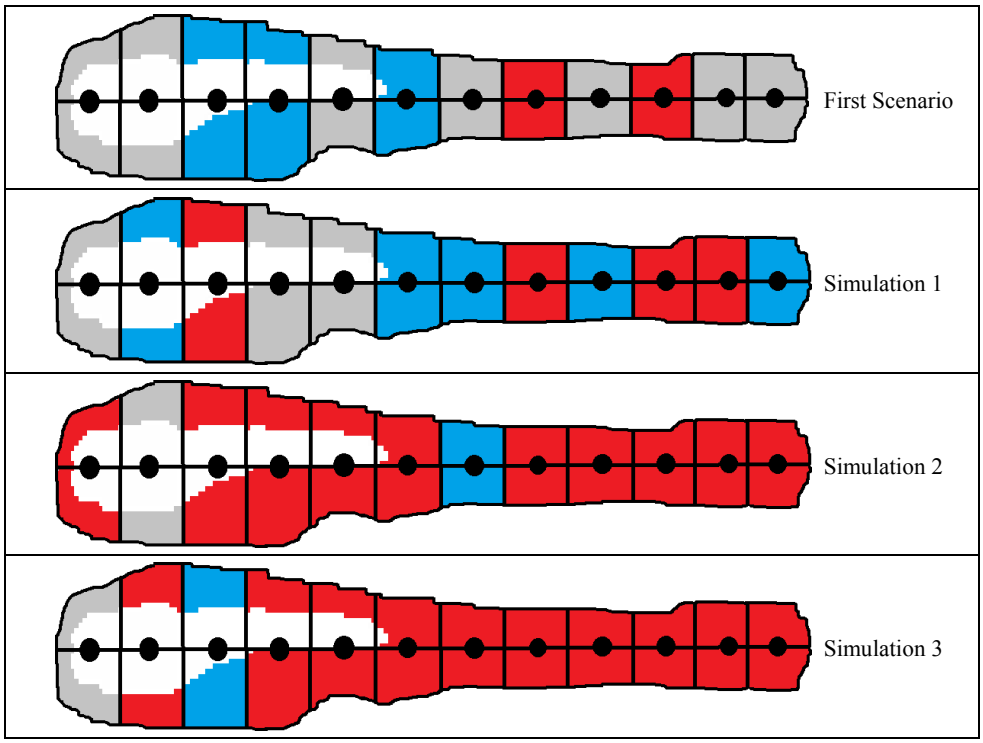

Figure 5.8 Confidence level per region of the t-test result for each simulation: in blue high confidence level (bigger than 95%); in gray mid confidence level (between 95% and 80%); in red the low confidence level (lower than 80%)

5.4 Conclusion and discussion

In this chapter, we have used a colored stochastic Petri net to model and simulate the mycobacterial infection process. To that end, we had to redesign our previous QPN^C model presented in Chapter 4 making it a quantitative model, in order to simulate scenarios that can reflect the behavior of the infection process. The objective was to convert our QPN^C model into a colored stochastic Petri net model using information we have obtained from *in vivo* experiments as the basis for the simulation and model validation.

We have analyzed data from biological experiments on *Mycobacterium marinum* (*Mm*) infection in zebrafish embryos. We used a dedicated image analysis software package [89, 90, 113] to measure the "spread" of the *Mm* bacteria after 5 *dpi*. The image analysis software has shown to be an indispensable tool in the modeling process. It provides information about the granuloma concentration along a pre-defined set of 12 regions within the zebrafish. We organized the data as a

proportion of infection per region (cf. **Table 5.2**). This information was used in our model as a probability rate for an infected macrophage to form granuloma on a specific position.

We redesigned the colored Petri net model into a SPN^C model taking in account the specified position from where the infected macrophage migrates to form the granuloma. We implemented a sub-model with stochastic transitions, addressing the position of each region granuloma are formed, as described in the empirical data (cf. **Figure 5.3 (b)**). We decided to use stochastic transitions only to model the process related to the infected macrophages migration, as that corresponds to the information extracted from *in vivo* experiments. The other transitions of the model are implemented as immediate transitions to represent processes present in the model but not explicitly measured in the empirical data. The use of immediate transitions implies no time consumption (delays) for a specific event (transition) to happen, and they have higher priority over the stochastic transitions. We could have used the stochastic transition with a rate function of 1.0 (100% probability to occur) but the addition of a time delay for each transition would skew the result. The motivation for using immediate transitions was to keep control over the transitions of no stochastic information available, providing more precise simulation results. In this manner, we are able to gradually increase the model by replacing the immediate transitions for stochastic transitions according the availability of data or to perform controlled simulations experiments.

We have performed two simulation scenarios with the new model, and validated them by comparing the results with the data from *in vivo* experiments.

In the first simulation scenario, we considered that all infected macrophages could form a granuloma in a specific region according to the rate function defined from the data analysis. This could be the ideal scenario for the bacteria since all inoculated *Mm* bacteria would survive and spread the infection over the time. We simulated the behavior of the infection for one zebrafish and for 138 zebrafishes, comparing the results with the distribution in our empirical data. The analysis of the results showed that the infection tends to reach a steady state over the time (cf. **Figure 5.4**). We assume that this behavior is related to the deterministic aspects of the immediate transitions. Despite of this, the granuloma distribution remains similar to the analysis of the empirical data, which corresponds to the biological behavior of the *in vivo* experiments. Therefore, this result validates our model.

For the second scenario, we have added another stochastic process to represent a natural factor that influences the infection process. This process consists of a stochastic transition that adds a probability of an infected macrophage to perform the phagosome maturation. For this scenario we performed three more simulations, considering that an infected macrophage has 30%, 60% or 90% of chance to successfully perform the phagolysosome process, hence kill the bacteria and avoid the formation of granuloma. This strategy could be accomplished by adding quantitative information on the calcium regulation and maturation process, by changing their respective pathways in the model.

However, such measured information was not available from biological experiments or through literature. Therefore, for convenience, we connected a stochastic transition to the late phagosome indicating that it has a specific probability to occur according to each simulation. The result was a reduction of the infection (amount of granuloma), expressed by the number of tokens accumulated in the place **Granuloma_Distribution**. This result should be expected since, for each simulation, we have increased probability of one infected macrophage to kill the bacteria and consequently, not forming a granuloma. By analyzing the concentration of the granulomas per region for each simulation, we noticed that the behavior of the distribution of the infection remained similar compared to the analysis of the empirical data. Although, we found that the percentage of granuloma concentration per region (position) for the simulation, where a macrophage has 30% chance to kill the bacteria, was more accurate than the first scenario and the other simulation - 60% and 90% chances of phagolysosome - (cf. **Figure 5.7**). We corroborate this result by performing a t-test to statistically verify the similarity between the simulations and the empirical data cf. **Table 5.8** and **Figure 5.8**). We can correlate these findings with the results found by Armstrong and Hart on their *in vitro* experiments [5]. Although their experiments where in tuberculosis and we do not have information of such experiment replicated *in vivo* for *Mm* with zebrafish, we can, to a certain extent, validate our model.

There are many natural factors that influence the infection in the biological process for which at the moment no measurements are available. Having demonstrated the robustness of our model in the simulation scenarios, we can extrapolate the model in order to approximate the results with its biological behavior. It is possible to add more complexity by replacing the immediate transitions for stochastic transitions and using results from *in vivo/in vitro* experiments as data input. An example of such possible extension is modeling the influence of calcium in the phagolysosome maturation. As we demonstrated before, 30% of infected macrophages are able to degrade the bacteria through this process. Future simulations could focus on the level of calcium that can influence in this percentage and that can suggest new *in vivo/in vitro* experiments to validate the results. In addition, we can perform the animation of the model in the 3D environment using the 3D visualization tool introduced in Chapter 4. The 3D tool was designed to read qualitative models, modeled using colored Petri nets. Therefore, a necessary adaptation to read the output of the stochastic simulation is required in order to express the quantitative aspects from the model.

In summary, in this chapter, we analyzed data from biological experiments on *Mycobacterium marinum* infection in zebrafish embryos. This information was used to redesign our previous model to obtain a quantitative model. We performed simulations on the new model and validated it by comparing the empirical data from *in vivo* experiments. We demonstrated the robustness of our model by performing different simulation scenarios, comparing them with the behavior observed from the experiments and suggested further model refinement. The process of validation and

refinement contribute to identify important parameters that can help to unravel mechanisms related to the biological process.

6 Discussion and conclusion

O wee

The blossoms fall but why the hurry?
Coming of age I want the spring slowing down.
Unfortunately all places of pleasure
are different from the days of my youth.

What relaxes me is just the wine,
What distracts my mind is the poetry.
This idea, Tao Yuanming would understand -
My life falls later than yours!

(Du Fu , China, 712 –770)

可惜

花飞有底急老区愿春迟
可惜欢愉地都非少壮时
宽心应是酒与这莫过时
此意陶潜解吾生后汝期

杜甫,中国（712 - 770）

Abstract

In this thesis we provided a comprehensive overview on the steps that are involved in the modeling process and simulation of biological phenomena; from the choice of the method to the validation of the results. We gradually implemented a model with which we would be able to study the complex interplay of the components involved in the *Mycobacterium marinum* infection process and innate immune response in zebrafish embryos. In itself this process is a model for deeper understanding of tuberculosis infection in humans using zebrafish as model organism. Each chapter is a building block in the modeling process, which gradually forms a model that can represent cause-and-effect among these components involved in the biological behavior. In this chapter we present our discussion and conclusion about the work presented in this dissertation.

6.1 Modeling mycobacterial infection process

In Chapter 1 we introduced the modeling process and the methods that can be used to model a biological system. It is important to the modeling process to identify the characteristics of the problem, the data available and to be able to generate the hypothesis to define the properties of the model. The next step is to choose the formal method to use for the implementation of the model. In this Chapter 1 we emphasize the Petri net formalism, its characteristics of scalability, extensibility and effectiveness to model a biological system. The Petri net formalism is also combined with an intuitive graphical representation with a strong mathematical foundation, integrating qualitative and quantitative aspects in range of tools that support implementation, simulation and analysis. The characteristics presented in Chapter 1 suggest that Petri net is an important method to model, simulate and analyze biological behavior.

We started the modeling process by defining the central biological problem of this dissertation: the *Mycobacterium marinum* infection process and innate immune response in zebrafish. In Chapter 2 we presented the characteristics of the biological behavior and the modeling decision used to create the first concept of our biological case study. The resulting model provides a qualitative representation of the dynamics of the infection process and the primary defense mechanism. The model in this described chapter shows to be able to reproduce the steps of the infection process and granuloma formation as implemented in a qualitative colored Petri net method. Throughout this first model, questions about how the bacteria proliferate and why the immune cells do not respond effectively to the infection, guided us to analyze other aspects of the infection process.

Motivated by the conclusions of Chapter 2, we started to analyze the aspects of the interaction between bacteria and immune cells that influence the infection process. The challenge addressed in Chapter 3 was to assemble the information about the different components involved in activation, inhibition and control of the infection. We analyzed the range of concurrent events that occur simultaneously, and how their molecular and cellular components are interconnected. Through an extensive literature research, in this chapter we have modeled the important regulatory pathways explored by the bacteria to evade the host immune cell and to be able to proliferate. We opted to implement the pathways in sub-models to represent the biological scales in which they occur: intracellular, intercellular and molecular level. Therefore, we explored the scalability of the Petri net formalism using the QPN method. We connect each sub-model in a hierarchical structure representing the biological scales. The model provides an overview of the important signaling pathways that occur between the host-pathogen interactions.

In possession of two independent but interrelated models, other questions about the modeling process emerged: How to combine a colored Petri net model that represent the dynamics of the infection, with the qualitative Petri net model that represent signaling process; and can these be

connected in a natural hierarchy? Moreover, how to visualize the infection process from a different perspective while maintaining the Petri net formalism? In Chapter 3 we therefore, started this discussion by suggesting a hybrid Petri nets or Nets-within-Nets approach. The HPN would be a good solution in case continuous and stochastic information is used. The Nets-within-Nets is more an abstract approach for large nets that are independent and complex. So far, the complexity of our models and the information available does not yet demand such methods.

The hierarchical combination in natural scales was explored in Chapter 4. In this chapter, we coupled the previous two models in one hierarchical structure extending the QPN model to its colored extension. We use the QPN^C adding a color-set "**Dot**" to represent the signaling process on the pathways implemented at the molecular and cellular level. In addition we implemented a 3D visualization environment that reads the Petri net model simulating the infection process model as if it would happen *in vivo*. Using a different visualization method from the Petri net formalism, but keeping its strong mathematical foundation, we compared the simulation result with an image from *in vivo* experiment to confirm the strength of the qualitative aspects of the model.

The model presented so far, refers to the qualitative aspects of the infection process and its characteristics. For testing and prediction of different scenarios, however, a quantitative model is required that, through support of empirical data would enable to do quantitative analysis. Therefore, an further extension of the model taking stochastic aspects of the infection into account is presented in Chapter 5. As a basis for this model, we collected and analyze data from zebrafish infection studies. In the analysis we found the average granuloma distribution per region in the zebrafish. We use this information as basis for the quantitative model experiments. To create the quantitative model, we used another characteristic of the Petri net formalism related to the integration between qualitative and quantitative methods. We exported the QPN^C model from Chapter 4 to a stochastic Petri net model, which assign rates (probabilities) to the transitions to occur. We redesigned the model in order to use the data collected as basis for the model. We use the data to specify probabilities for an infected macrophage to form a granuloma in a specific region. Therefore, a new structure related to the movement process of an infected macrophage was added to support this quantitative approach. Moreover, we considered the other activities in the infection process as instantaneous (time independent), replacing the stochastic transitions that are not related to the movement for immediate transitions.

For this model, we performed a number of simulations considering the average of granuloma concentration as a probability rate for the stochastic simulations. The results of a simulation scenario indicate that our model behaves quantitatively similar to the empirical data, validating our hypothesis about the model structure and behavior. For a second simulation scenario, we add a stochastic parameter to disturb the concentration and infection distribution. The result shown the same behavior for the infection though the concentration of granuloma and the percentage of

distribution per region changed. Therefore, we demonstrated the robustness of our model by comparing the simulation results with the behavior observed from the *in* vivo experiments. Further refinement in the model based on availability of more data can lead to simulations that can approximate the model to the *in vivo* scenarios even better.

6.2 Model implementation

There are many tools available on internet as well as web platforms that can be used for implementation of Petri net models [9, 23, 29, 43, 45, 47, 64, 95, 121, 125, 131]. Most of the tools are confined to specific classes and/or not support extensions, portability or analysis. However, few tools can provide an extensible experience with Petri net methods [22, 63, 87]. We assessed that Snoopy software [50] is the most complete tool available to design and evaluate models in Petri nets. It supports a set of related important Petri net classes, i.e. QPN, SPN, CPN and HBPN and their colored extensions. Snoopy provides analysis techniques, e.g. animation, simulation, and also exports properties between classes and to external analysis tools i.e. Charlie [56] and Marcie [55]. Recently, the Snoopy Steering and Simulation Server tool (S4) [58, 59] was released as an extension of the Snoopy simulation to perform stochastic simulations in multi-core servers. This extension provides a better performance for simulations of big models as well as to change stochastic properties of the model while it is running. The Snoopy is platform independent and freely available for all relevant platforms, i.e. Linux, Windows and MacOS platforms.

6.3 Conclusion and future work

Here we present our final conclusions about our study on modeling of the *Mycobacterium marinum* infection process and the innate immune response in zebrafish. We have applied the modeling process from the concept of the problem up to simulation and validation of the results. We gradually increment the model complexity through a refinement process, where different and complementary models have been created in sub-models and these have been gradually connected. This was an important process on the modeling decision and turned to be a valuable approach to model a complex biological system. The literature research, gathering the biological processes and separate the processes in sub-models, was a challenge that was feasible just because of the powerful of the Petri net formalism. The result was a readable and extensible model that can be animated, simulated and analyzed independently or in as a whole.

Another contribution of this thesis is related to the hierarchical structure of the model. Coupling different biological scales still an open challenge in modeling biological systems. Using the Petri net formalism, we proposed a simple and effective solution to connect events that occur simultaneously

at molecular, intercellular and intracellular scale. The color Petri net extension bridges each scale using a simple color "**dot**" which realizes the flow between the scales, representing the presence or absence of an entity, signals and/or activity in the sub-nets.

The migration from qualitative model to quantitative also demanded an effort to collect and analyze data related to the biological problem. We use stochastic model, extending the QPN^C previously modeled to SPN^C. The stochastic process consist of define probability rates for a specific event to occur. Since our data was related to the concentration of granuloma per region in the zebrafish, we use the relative proportion distribution as a probability rate of one granuloma been formed in a specific region. We innovated the stochastic model by using the probabilities only for the infection migration (time delays), considering the other events as instantaneous (no time dependent). This approach not only simplifies the simulation, but also provides a controlled extension of the model by gradually replacing a specific instantaneous event for a stochastic (probability) one once data is available. Therefore, different "what-if" scenarios can be performed as part of the simulation process leading for new insights about the infection process.

In this thesis we studied the importance to identify the characteristics of the biological system to be modeled, the collection of information/data and how they influence the modeling decision. A modular implementation is essential since you can gradually increase the complexity of the model by adding new sub-models structure. Obviously to achieve the modular implementation it is necessary to separate the process in related groups identifying the key elements that bridge each sub-model. Moreover, a visual representation that can depict the modeled process is also important to depict the biological behavior. Therefore, it is important to choose a model formalism that can combine a method with a strong mathematical foundation and graphical representation that better suits to your problem. The validation and analysis of the model is an important step since it can leads to new refinements and conclusions that can drive future experiments.

As result of our studies, we presented computational models that are able to represent qualitative and quantitative the *Mycobacterium* infection process and innate immune response in zebrafish. It is a starting point for *in silico* experiments, new refinements can be performed along the availability of biological data. As future work, new simulations considering bacteria mutants can leads to new discovering on the localized behavior of the infection. Moreover, quantitative information about protein concentrations (i.e. calcium or anti-inflammatory cytokines), and pathways inhibitions (i.e. apoptosis or necrosis) can be used as part of simulation experiments that can bring new insights in the research and treatment of mycobacterial infection in humans.

Biological systems are inherently complex in nature. They are composed of multiple functional processes, which involve complex interconnected networks in a cross talk interaction. Principally, creating a multi-scale model to represent a biological system, it is important to identify and separate the processes that belong to each level of interaction. It is difficult to visualize these levels in the

biological literature, which brings another challenger to the modeling process. We have learned from modeling the *Mycobacterium* infection process using Petri nets the importance of simplification, modularization and extensibility in the modeling process. Through the simplification and modularization, we defined each scale in sub-models by simplifying their boundaries condition into black boxes, in which the connection between models is given by simple signals. The extensibility of the modeling process allowed gradually increasing the complexity of the model, while we were collecting and analyzing more information about the infection process and the innate immune response.

A key observation from this thesis is that the methodology used to model the behavior of the mycobacterium infection process using Petri nets can be used to represent other diseases e.g. diabetes. Most of the components are related to the immune system response and the modularization aspect facilitates the replacing process of modules, i.e. pathways that are specific related to the disease without changing the whole structure of the system. It is our hope that the techniques and practices presented here will guide future efforts in modeling biological process using high-quality multi-scale model implementation using Petri nets.

References

1. Abarca-Rojano E., Rosas-Medina P., Zamudio-Cortéz P., Mondragón-Flores R., Sánchez-García F.J. Mycobacteriurn tuberculosis virulence correlates with mitochondrial cytochrome c release in infected macrophages. Scandinavian Journal of Immunology 58:419–427. doi: 10.1046/j.1365-3083.2003.01318.x (2003).

2. Akman O., Ciocchetta F., Degasperi A., Guerriero M. Modelling Biological Clocks with Bio-PEPA: Stochasticity and Robustness for the Neurospora crassa Circadian Network. In: Degano P, Gorrieri R (eds) Computational Methods in Systems Biology SE - 4. Springer Berlin Heidelberg, pp 52–67 (2009).

3. Albergante L., Timmis J., Beattie L., Kaye P.M. A Petri Net Model of Granulomatous Inflammation: Implications for IL-10 Mediated Control of Leishmania donovani Infection. PLoS Computational Biology. doi: 10.1371/journal.pcbi.1003334 (2013).

4. Alemani D., Pappalardo F., Pennisi M., Motta S., Brusic V. Combining cellular automata and lattice Boltzmann method to model multiscale avascular tumor growth coupled with nutrient diffusion and immune competition. Journal of Immunological Methods 376:55–68. doi: 10.1016/j.jim.2011.11.009 (2012).

5. Armstrong J.A., Hart P.D. Response of cultured macrophages to Mycobacterium tuberculosis, with observations on fusion of lysosomes with phagosomes. The Journal of experimental medicine 134:713–740. doi: 10.1084/jem.134.3.713 (1971).

6. Barbuti, Roberto and Caravagna, Giulio and Maggiolo-Schettini, Andrea and Milazzo, Paolo and Pardini G. The calculus of looping sequences. In: Proceedings of the Formal methods for the design of computer, communication, and software systems 8th international conference on Formal methods for computational systems biology. Springer-Verlag, Berlin, Heidelberg, pp 387–423 (2008).

7. Barnes D.J., Chu D. Introduction to Modeling for Biosciences. In: Introduction to Modeling for Biosciences. Springer London, London, p 322 (2010).

8. Benard E.L., van der Sar A.M., Ellett F., Lieschke G.J., Spaink H.P., Meijer A.H. Infection of Zebrafish Embryos with Intracellular Bacterial Pathogens. Journal of Visualized Experiments 1–8. doi: 10.3791/3781 (2012).

9. Berthomieu B., Ribet P. O., Vernadat F. The tool TINA – Construction of abstract state spaces for petri nets and time petri nets. International Journal of Production Research 42:2741–2756. doi: 10.1080/00207540412331312688 (2004).

10. Blätke M., Heiner M., Marwan W. Tutorial Petri Nets in Systems Biology. Magdeburg (2011).

11. Booth J.W., Trimble W.S., Grinstein S. Membrane dynamics in phagocytosis. Seminars in immunology 13:357–64. doi: 10.1006/smim.2001.0332 (2001).

12. Bouley D.M., Ghori N., Mercer K.L., Falkow S., Ramakrishnan L. Dynamic nature of host-pathogen interactions in Mycobacterium marinum granulomas. Infection and immunity 69:7820–31. doi: 10.1128/IAI.69.12.7820-7831.2001 (2001).

13. Box G., Hunter J.S., Hunter W. Statistics Experimenters. Book 1–655. (2009).

14. Calzone L., Fages F.F., Soliman S. BIOCHAM: an environment for modeling biological systems and formalizing experimental knowledge. Bioinformatics 22:1805–1807. doi: 10.1093/bioinformatics/btl172 (2006).

15. Cardelli L. Brane Calculi - Interactions of Biological Membranes. Proc of CMSB04 3082:257 – 278. (2005).

16. Carneiro J., Coutinho A., Stewart J. A model of the immune network with B-T cell co-operation. II--The simulation of ontogenesis. Journal of theoretical biology 182:531–547. doi: 10.1006/jtbi.1996.0192 (1996).

17. Carvalho R. V, Kleijn J., Verbeek F.J. A Multi-Scale Extensive Petri Net Model Of The Bacterial – Macrophage Interaction. In: Heiner M (ed) 5th International Workshop on Biological Processes & Petri Nets. CEUR Workshop Proceedings, Tunis, Tunisia, pp 15–29 (2014).

18. Carvalho R. V., Davids W., Meijer A.H., Verbeek F.J. Spatio-temporal Modeling and Simulation of Mycobacterium Pathogenesis Using Petri Nets. In: Hart E, Timmis J, Mitchell P, Nakamo T, Dabiri F (eds) Bio-Inspired Models of Networks, Information, and Computing Systems. Springer Berlin Heidelberg, Berlin, Heidelberg, pp 236–241 (2012).

19. Carvalho R. V., Kleijn J., Meijer A.H., Verbeek F.J. Modeling innate immune response to early mycobacterium infection. Computational and Mathematical Methods in Medicine 2012:790482. doi: 10.1155/2012/790482 (2012).

20. Casadevall A., Pirofski L. Host-pathogen interactions: the attributes of virulence. The Journal of infectious diseases 184:337–44. doi: 10.1086/322044 (2001).

21. Chao D.L., Davenport M.P., Forrest S., Perelson A.S. A stochastic model of cytotoxic T cell responses. Journal of Theoretical Biology 228:227–240. doi: 10.1016/j.jtbi.2003.12.011 (2004).

22. Chiola G., Franceschinis G., Gaeta R., Ribaudo M. GreatSPN 1.7: Graphical editor and analyzer for timed and stochastic Petri nets. Performance Evaluation 24:47–68. doi: 10.1016/0166-5316(95)00008-L (1995).

23. Ciocchetta F., Hillston J. Bio-PEPA: A framework for the modelling and analysis of biological systems. Theoretical Computer Science 410:3065–3084. doi: 10.1016/j.tcs.2009.02.037 (2009).

24. Clay H., Davis J.M., Beery D., Huttenlocher A., Lyons S.E., Ramakrishnan L. Dichotomous role of the macrophage in early Mycobacterium marinum infection of the zebrafish. Cell Host and Microbe 2:29–39. doi: 10.1016/j.chom.2007.06.004 (2007).

25. Clay H., Volkman H.E., Ramakrishnan L. Tumor necrosis factor signaling mediates resistance to mycobacteria by inhibiting bacterial growth and macrophage death. Immunity 29:283–94. doi: 10.1016/j.immuni.2008.06.011 (2008).

26. Cosma C.L., Sherman D.R., Ramakrishnan L. The secret lives of the pathogenic mycobacteria. Annual review of microbiology 57:641–76. doi: 10.1146/annurev.micro.57.030502.091033 (2003).

27. Danos V., Krivine J. Formal Molecular Biology Done in CCS-R. Electronic Notes in Theoretical Computer Science 180:31–49. doi: 10.1016/j.entcs.2004.01.040 (2007).

28. David R., Alla H. On hybrid Petri nets. Discrete Event Dynamic Systems: Theory and Applications 11:9–40. doi: 10.1023/A:1008330914786 (2001).

29. Davidrajuh R. Developing a new petri net tool for simulation of discrete event systems. In: Proceedings - 2nd Asia International Conference on Modelling and Simulation, AMS 2008. pp 861–866 (2008).

30. Davis J.M., Clay H., Lewis J.L., Ghori N., Herbomel P., Ramakrishnan L. Real-time visualization of Mycobacterium-macrophage interactions leading to initiation of granuloma formation in zebrafish embryos. Immunity 17:693–702. doi: 10.1016/S1074-7613(02)00475-2 (2002).

31. Davis J.M., Haake D.A., Ramakrishnan L. Leptospira interrogans stably infects zebrafish embryos, altering phagocyte behavior and homing to specific tissues. PLoS Neglected Tropical Diseases 3:6. doi: 10.1371/journal.pntd.0000463 (2009).

32. Davis J.M., Ramakrishnan L. The Role of the Granuloma in Expansion and Dissemination of Early Tuberculous Infection. Cell 136:37–49. doi: 10.1016/j.cell.2008.11.014 (2009).

33. Desel J., Juhás G. "What Is a Petri Net?" Informal Answers for the Informed Reader. In: Ehrig H, Padberg J, Juhás G, Rozenberg G (eds) Lecture Notes in Computer Science. Springer, pp 1–25 (2001).

34. Fallahi-Sichani M., El-Kebir M., Marino S., Kirschner D.E., Linderman J.J. Multiscale computational modeling reveals a critical role for TNF-α receptor 1 dynamics in tuberculosis granuloma formation. Journal of immunology (Baltimore, Md : 1950) 186:3472–83. doi: 10.4049/jimmunol.1003299 (2011).

35. Fisher J., Henzinger T. a. Executable biology. In: Proceedings - Winter Simulation Conference. pp 1675–1682 (2006).

36. Flynn J.L., Chan J. Immunology of tuberculosis. Annual review of immunology 19:93–129. doi: 10.1146/annurev.immunol.19.1.93 (2001).

37. Flynn J.L., Chan J. What's good for the host is good for the bug. Trends in Microbiology 13:98–102. doi: 10.1016/j.tim.2005.01.005 (2005).

38. Franzke A. Charlie 2.0 – a multi-threaded Petri net analyzer. Brandenburg University of Technology at Cottbus (2009).

39. Fratti R.A., Backer J.M., Gruenberg J., Corvera S., Deretic V. Role of phosphatidylinositol 3-kinase and Rab5 effectors in phagosomal biogenesis and mycobacterial phagosome maturation arrest. The Journal of cell biology 154:631–44. doi: 10.1083/jcb.200106049 (2001).

40. Fratti R.A., Chua J., Vergne I., Deretic V. Mycobacterium tuberculosis glycosylated phosphatidylinositol causes phagosome maturation arrest. Proceedings of the National Academy of Sciences of the United States of America 100:5437–5442. doi: 10.1073/pnas.0737613100 (2003).

41. Gammack D., Doering C.R., Kirschner D.E. Macrophage response to Mycobacterium tuberculosis infection. Journal of Mathematical Biology 48:218–242. doi: 10.1007/s00285-003-0232-8 (2004).

42. Gammack D., Ganguli S., Marino S., Segovia-Juarez J., Kirschner D.E. Understanding the Immune Response in Tuberculosis Using Different Mathematical Models and Biological Scales. Multiscale Modeling & Simulation 3:312–345. doi: 10.1137/040603127 (2005).

43. Gao J., Li L., Wu X., Wei D.Q. BioNetSim: A Petri net-based modeling tool for simulations of biochemical processes. Protein and Cell 3:225–229. (2012).

44. Gatton M.L., Cheng Q. Modeling the development of acquired clinical immunity to Plasmodium falciparum malaria. Infection and Immunity 72:6538–6545. doi: 10.1128/IAI.72.11.6538-6545.2004 (2004).

45. Gilbert D., Heiner M., Lehrack S. A Unifying Framework for Modelling and Analysing Biochemical Pathways Using Petri Nets. In: Calder M, Gilmore S (eds) Computational Methods in Systems Biology. Springer Berlin Heidelberg, Berlin, Heidelberg, pp 200–216 (2007).

46. González P.P., Cárdenas M., Camacho D., Franyuti A., Rosas O., Lagúnez-Otero J. Cellulat: an agent-based intracellular signalling model. Biosystems 68:171–185. doi: 10.1016/S0303-2647(02)00094-1 (2003).

47. Grahlmann B., Best E. PEP - More than a Petri Net Tool. In: Margaria T, Steffen B (eds) Proceedings of TACAS'96 (Tools and Algorithms for the Construction and Analysis of Systems). Springer-Verlag, pp 397–401 (1996).

48. Heiner M., Gilbert D. How might Petri nets enhance your systems biology toolkit. In: Kristensen LM, Petrucci L (eds) Lecture Notes in Computer Science. Springer, pp 17–37 (2011).

49. Heiner M., Gilbert D., Donaldson R. Petri nets for systems and synthetic biology. Formal Methods for Computational Systems Biology 5016:215–264. (2008).

50. Heiner M., Herajy M., Liu F., Rohr C., Schwarick M. Snoopy – A unifying Petri net tool. Lecture Notes in Computer Science 7347:398–407. (2012).

51. Heiner M., Koch I. Petri net based model validation in systems biology. Applications and Theory of Petri Nets 2004 216–237. (2004).

52. Heiner M., Koch I., Will J. Model validation of biological pathways using Petri nets—demonstrated for apoptosis. Biosystems 75:15–28. doi: 10.1016/j.biosystems.2004.03.003 (2004).

53. Heiner M., Lehrack S., Gilbert D., Marwan W. Extended Stochastic Petri Nets for Model-Based Design of Wetlab Experiments. In: Priami C, Back R-J, Petre I (eds) Transactions on Computational Systems Biology. Springer, pp 138–163 (2009).

54. Heiner M., Richter R., Schwarick M., Rohr C. Snoopy-A Tool to Design and Execute Graph-Based Formalisms. Petri Net Newsletter 74:8–22. (2008).

55. Heiner M., Rohr C., Schwarick M. MARCIE - Model checking and reachability analysis done efficiently. In: Petri Nets 2013. Springer, pp 389–399 (2013).

56. Heiner M., Schwarick M., Wegener J. Charlie - an extensible Petri net analysis tool. Petri Nets 2015 (2015).

57. Heitmann F., Köhler-Bußmeier M. P-and T-Systems in the Nets-within-Nets-Formalism. Application and Theory of Petri Nets 368–387. doi: 10.1007/978-3-642-31131-4_20 (2012).

58. Herajy M. Computational Steering of Multi-Scale Biochemical Networks. Brandenburgischen Technische Universität Cottbus (2013).

59. Herajy M., Heiner M. Petri Net-Based Collaborative Simulation and Steering of Biochemical Reaction Networks. Fundamenta Informaticae 129:49–67. doi: 10.3233/FI-2014-960 (2014).

60. Jensen K. Coloured Petri Nets and the invariant-method. Theoretical Computer Science. doi: 10.1016/0304-3975(81)90049-9 (1981).

61. Jensen K. Coloured Petri nets : basic concepts, analysis methods and practical use. Springer, Berlin (1997).

62. Jensen K. Coloured Petri Nets. Theoretical Computer Science 254:248–299. doi: 10.1007/b95112 (2009).

63. Jensen K., Kristensen L.M., Wells L. Coloured Petri Nets and CPN Tools for modelling and validation of concurrent systems. International Journal on Software Tools for Technology Transfer 9:213–254. doi: 10.1007/s10009-007-0038-x (2007).

64. Kindler E. The ePNK: An extensible Petri net tool for PNML. In: Lecture Notes in Computer Science (including subseries Lecture Notes in Artificial Intelligence and Lecture Notes in Bioinformatics). pp 318–327 (2011).

65. Kirschner D., Marino S. Mycobacterium tuberculosis as viewed through a computer. Trends in microbiology 13:206–11. doi: 10.1016/j.tim.2005.03.005 (2005).

66. Kirschner D.E., Young D., Flynn J.L. Tuberculosis: global approaches to a global disease. Current opinion in biotechnology 21:524–31. doi: 10.1016/j.copbio.2010.06.002 (2010).

67. Koch I., Reisig W., Schreiber F. Modeling in systems biology: The Petri Net approach. doi: 10.1007/978-1-84996-474-6 (2011).

68. Koul A., Herget T., Klebl B., Ullrich A. Interplay between mycobacteria and host signalling pathways. Nature reviews Microbiology 2:189–202. doi: 10.1038/nrmicro840 (2004).

69. Lalvani A., Behr M. a, Sridhar S. Innate immunity to TB: a druggable balancing act. Cell 148:389–91. doi: 10.1016/j.cell.2012.01.026 (2012).

70. Lee J., Hartman M., Kornfeld H. Macrophage apoptosis in tuberculosis. Yonsei medical journal 50:1–11. doi: 10.3349/ymj.2009.50.1.1 (2009).

71. Lesley R., Ramakrishnan L. Insights into early mycobacterial pathogenesis from the zebrafish. Current opinion in microbiology 11:277–83. doi: 10.1016/j.mib.2008.05.013 (2008).

72. Lin P., Kirschner D., Flynn J. Modeling pathogen and host: in vitro, in vivo and in silico models of latent Mycobacterium tuberculosis infection. Drug Discovery Today: Disease Models 2:149–154. doi: 10.1016/j.ddmod.2005.05.019 (2005).

73. Liu F., Heiner M. Colored Petri nets to model and simulate biological systems. In: Donatelli S, Kleijn J, Machado RJ, Fernandes IM (eds) CEUR Workshop. pp 71–85 (2012).

74. Lund E.W. Guldberg and Waage and the law of mass action. Journal of Chemical Education 42:548. doi: 10.1021/ed042p548 (1965).

75. Lundegaard C., Lund O., Keşmir C., Brunak S., Nielsen M. Modeling the adaptive immune system: Predictions and simulations. Bioinformatics 23:3265–3275. doi: 10.1093/bioinformatics/btm471 (2007).

76. Malik Z.A., Denning G.M., Kusner D.J. Inhibition of Ca2+ Signaling by Mycobacterium tuberculosisIs Associated with Reduced Phagosome-Lysosome Fusion and Increased Survival within Human Macrophages. J Exp Med 191:287–302. (2000).

77. Marino S., Linderman J.J., Kirschner D.E. A multifaceted approach to modeling the immune response in tuberculosis. Wiley Interdisciplinary Reviews: Systems Biology and Medicine 3:479–489. doi: 10.1002/wsbm.131 (2011).

78. Marsan M.A. Stochastic Petri nets: An elementary introduction. In: Rozenberg G (ed) Advances in Petri Nets 1989. Springer, pp 1–29 (1990).

79. Marwan W., Rohr C., Heiner M. Petri nets in Snoopy: A unifying framework for the graphical display, computational modelling, and simulation of bacterial regulatory networks. Bacterial Molecular Networks 1–31. (2012).

80. Meeker N.D., Trede N.S. Immunology and zebrafish: spawning new models of human disease. Developmental and comparative immunology 32:745–757. (2008).

81. Meijer A., Spaink H. Host-pathogen interactions made transparent with the zebrafish model. Current drug targets 1000–1017. (2011).

82. Meijer A.H., Van Der Sar A.M., Cunha C., Lamers G.E.M., Laplante M.A., Kikuta H., Bitter W., Becker T.S., Spaink H.P. Identification and real-time imaging of a myc-expressing neutrophil population involved in inflammation and mycobacterial granuloma formation in zebrafish. Developmental and comparative immunology 32:36–49. (2008).

83. Molly M.K. On the Integration of Delay and Throughput Measures in Distributed Processing Models. UCLA (1981).

84. Moore K.W., de Waal Malefyt R., Coffman R.L., O'Garra A. Interleukin-10 and the interleukin-10 receptor. Annual review of immunology 19:683–765. doi: 10.1146/annurev.immunol.19.1.683 (2001).

85. Mura I., Csikász-Nagy A. Stochastic Petri Net extension of a yeast cell cycle model. Journal of Theoretical Biology 254:850–860. doi: 10.1016/j.jtbi.2008.07.019 (2008).

86. Murata T. Petri nets: properties, analysis and applications. Proceedings of the IEEE 77:541–580. doi: 10.1109/5.24143 (1989).

87. Nagasaki M., Saito A., Jeong E., Li C., Kojima K., Ikeda E., Miyano S. Cell illustrator 4.0: A computational platform for systems biology. In Silico Biology 10:5–26. (2010).

88. Natkin S. Les Reseaux de Petri Stochastique et leur Application a l'Evaluation des Systèmes Informatiques. CNAM (1980).

89. Nezhinsky A.E. Pattern recognition in high-throughput zebrafish imaging. PhD Thesis. Leiden Institute of Advanced Computer Science (LIACS), Faculty of Science, Leiden University (2013).

90. Nezhinsky A.E., Davids W., van der Sar A.M., Verbeek F.J. eLaborant - An Elaborate Data Analysis Environment for High Throughput Screening. http://www.elaborant.com/. Accessed 8 Jan 2015 (2014).

91. Nezhinsky A.E., Stoop E., Vasylevska A.A., Sar A. van der, Vebeek F.J. Spatial Analysis of Bacterial Infection Patterns in Zebrafish. In: 21th Annual Belgian-Dutch Conference on Machine Learning. Ghent, Belgium, pp 27–32 (2012).

92. Pappalardo F., Forero I.M., Pennisi M., Palazon A., Melero I., Motta S. Simb16: Modeling induced immune system response against B16-melanoma. PLoS ONE. doi: 10.1371/journal.pone.0026523 (2011).

93. Pappalardo F., Halling-Brown M.D., Rapin N., Zhang P., Alemani D., Emerson A., Paci P., Duroux P., Pennisi M., Palladini A., Miotto O., Churchill D., Rossi E., Shepherd A.J., Moss D.S., Castiglione F., Bernaschi M., Lefranc M.P., Brunak S., Motta S., Lollini P.L., Basford K.E., Brusic V. ImmunoGrid, an integrative environment for large-scale simulation of the immune system for vaccine discovery, design and optimization. Briefings in Bioinformatics 10:330–340. doi: 10.1093/bib/bbp014 (2009).

94. Peleg M., Gabashvili I., Altman R. Qualitative models of molecular function: linking genetic polymorphisms of tRNA to their functional sequelae. Proceedings of the IEEE 90:1875–1886. (2002).

95. Pommereau F. Quickly Prototyping Petri Nets Tools with {SNAKES}. In: Proceedings of the 1st International Conference on Simulation Tools and Techniques for Communications, Networks and Systems & Workshops. Institute for Computer Sciences, Social-Informatics and Telecommunications Engineering, pp 17:1–17:10 (2008).

96. Pun G. A guide to membrane computing. Theoretical Computer Science 287:73–100. doi: 10.1016/S0304-3975(02)00136-6 (2002).

97. Puri R.V., Reddy P.V., Tyagi A.K. Secreted Acid Phosphatase (SapM) of Mycobacterium tuberculosis Is Indispensable for Arresting Phagosomal Maturation and Growth of the Pathogen in Guinea Pig Tissues. PloS one. doi: 10.1371/journal.pone.0070514 (2013).

98. Reddy V.N., Mavrovouniotis M.L., Liebman M.N. Petri Net Representations in Metabolic Pathways. In: Hunter L, Searls DB, Jude W. Shavlik (eds) Proceedings of the 1st International Conference on Intelligent Systems for Molecular Biology. AAAI Press, pp 328–336 (1993).

99. Regev A., Silverman W., Shapiro E. Representation and simulation of biochemical processes using the pi-calculus process algebra. Pacific Symposium on Biocomputing Pacific Symposium on Biocomputing 459–70. (2001).

100. Reisig W., Rozenberg G. Lectures on Petri Nets I: Basic Models. Lecture Notes in Computer Science. doi: 10.1007/3-540-65306-6 (1998).

101. Reisig W., Rozenberg G. Lectures on Petri Nets II: Applications. Lecture Notes in Computer Science 1492: (1998).

102. Rohde K., Yates R.M., Purdy G.E., Russell D.G. Mycobacterium tuberculosis and the environment within the phagosome. Immunological reviews 219:37–54. doi: 10.1111/j.1600-065X.2007.00547.x (2007).

103. Rojas M., García L.F., Nigou J., Puzo G., Olivier M. Mannosylated lipoarabinomannan antagonizes Mycobacterium tuberculosis-induced macrophage apoptosis by altering Ca+2-dependent cell signaling. The Journal of infectious diseases 182:240–51. doi: 10.1086/315676 (2000).

104. Rosenberger C.M., Finlay B.B. Phagocyte sabotage: disruption of macrophage signalling by bacterial pathogens. Nature Reviews Molecular Cell Biology 4:385–96. doi: 10.1038/nrm1104 (2003).

105. Rüdiger Valk. Object Petri Nets Using the Nets-within-Nets Paradigm. In: Desel J, Reisig W, Rozenberg G (eds) Advances in Petri Nets: Lectures on Concurrency and Petri Nets, volume 3098 of Lecture Notes in Compu ter Science. Springer Berlin Heidelberg, Berlin, Heidelberg, pp 819–848 (2004).

106. Russell D.G., Mwandumba H.C., Rhoades E.E. Mycobacterium and the coat of many lipids. The Journal of cell biology 158:421–6. doi: 10.1083/jcb.200205034 (2002).

107. Schluger N.W., Rom W.N. The host immune response to tuberculosis. American Journal of Respiratory and Critical Care Medicine 157:679–691. doi: 10.1164/ajrccm.157.3.9708002 (1998).

108. Segovia-Juarez J.L., Ganguli S., Kirschner D. Identifying control mechanisms of granuloma formation during M. tuberculosis infection using an agent-based model. Journal of Theoretical Biology 231:357–376. doi: 10.1016/j.jtbi.2004.06.031 (2004).

109. Southern J., Pitt-Francis J., Whiteley J., Stokeley D., Kobashi H., Nobes R., Kadooka Y., Gavaghan D. Multi-scale computational modelling in biology and physiology. Progress in Biophysics and Molecular Biology 96:60–89. doi: 10.1016/j.pbiomolbio.2007.07.019 (2008).

110. Stanley S. a, Cox J.S. Host-pathogen interactions during Mycobacterium tuberculosis infections. Current topics in microbiology and immunology 374:211–41. doi: 10.1007/82_2013_332 (2013).

111. Stein C. Innate immune genes in the zebrafish, Danio rerio. PhD Thesis. Universität zu Köln (2011).

112. Stoop E.J.M., Mishra A.K., Driessen N.N., van Stempvoort G., Bouchier P., Verboom T., van Leeuwen L.M., Sparrius M., Raadsen S.A., van Zon M., van der Wel N.N., Besra G.S., Geurtsen J., Bitter W., Appelmelk B.J., Van der Sar A.M. Mannan core branching of lipo(arabino)mannan is required for mycobacterial virulence in the context of innate immunity. Cellular Microbiology 15:2093–2108. doi: 10.1111/cmi.12175 (2013).

113. Stoop E.J.M., Schipper T., Huber S.K.R., Nezhinsky A.E., Verbeek F.J., Gurcha S.S., Besra G.S., Vandenbroucke-Grauls C.M.J.E., Bitter W., van der Sar A.M. Zebrafish embryo screen for mycobacterial genes involved in the initiation of granuloma formation reveals a newly identified ESX-1 component. Disease models & mechanisms 4:526–536. doi: 10.1242/dmm.006676 (2011).

114. Sundaramurthy V., Pieters J. Interactions of pathogenic mycobacteria with host macrophages. Microbes and Infection 9:1671–1679. doi: 10.1016/j.micinf.2007.09.007 (2007).

115. Symons F.J.W. Introduction to Numerical Petri Nets, a General Graphical Model of Concurrent Processing Systems. Australian Telecommunications Research 14:28–33. (1980).

116. Symons F.J.W. The Description and Definition of Queueing Systems by Numerical Petri Nets. Australian Telecommunications Research 13:20–31. (1980).

117. Traver D., Herbomel P., Patton E.E., Murphey R.D., Yoder J.A., Litman G.W., Catic A., Amemiya C.T., Zon L.I., Trede N.S. The zebrafish as a model organism to study development of the immune system. Advances in Immunology 81:253–330. (2003).

118. Tsavachidou D., Liebman M. Modeling and simulation of pathways in menopause. Journal of the American Medical. 9:461–471. doi: 10.1197/jamia.M1103. (2002).

119. Van der Vaart M., van Soest J.J., Spaink H.P., Meijer A.H. Functional analysis of a zebrafish myd88 mutant identifies key transcriptional components of the innate immune system. Disease models & mechanisms 6:841–54. doi: 10.1242/dmm.010843 (2013).

120. Van der Vaart M., Spaink H.P., Meijer A.H. Pathogen recognition and activation of the innate immune response in zebrafish. Advances in hematology 2012:159807. doi: 10.1155/2012/159807 (2012).

121. Verbeek E., Aalst W.M.P. Van Der. Woflan 2.0: a Petri-net-based workflow diagnosis tool. In: Proceedings of the 21st international conference on Application and theory of petri nets. pp 475–484 (2000).

122. Vergne I., Chua J., Deretic V. Tuberculosis toxin blocking phagosome maturation inhibits a novel Ca2+/calmodulin-PI3K hVPS34 cascade. The Journal of experimental medicine 198:653–9. doi: 10.1084/jem.20030527 (2003).

123. Walpole J., Papin J.A., Peirce S.M. Multiscale computational models of complex biological systems. Annual review of biomedical engineering 15:137–54. doi: 10.1146/annurev-bioeng-071811-150104 (2013).

124. Warrender C., Forrest S., Koster F. Modeling intercellular interactions in early Mycobacterium infection. Bulletin of Mathematical Biology 68:2233–2261. doi: 10.1007/s11538-006-9103-y (2006).

125. Weber M., Kindler E. The Petri Net Kernel. In: Ehrig H, Reisig W, Rozenberg G, Weber H (eds) Petri Net Technology for Communication-Based Systems SE. Springer Berlin Heidelberg, pp 109–123 (2003).

126. Wegener J., Schwarick M., Heiner M. A plugin system for Charlie. Proc CS&P 531–554. (2011).

127. Van Der Wel N., Hava D., Houben D., Fluitsma D., Van Zon M., Pierson J., Brenner M., Peters P.J. M. tuberculosis and M. leprae translocate from the phagolysosome to the cytosol in myeloid cells. Cell 129:1287–1298. (2007).

128. Wingender E. Biological Petri Nets. IOS Press, Amsterdam (2011).

129. World Health Organization. Global Tuberculosis Report. (2014).

130. Yang C.T., Cambier C.J.J., Davis J.M.M., Hall C.J.J., Crosier P.S.S., Ramakrishnan L. Neutrophils Exert Protection in the Early Tuberculous Granuloma by Oxidative Killing of

Mycobacteria Phagocytosed from Infected Macrophages. Cell Host & Microbe 12:301–312. doi: 10.1016/j.chom.2012.07.009 (2012).

131. Zimmermann A., Freiheit J., German R., Hommel G. Petri Net Modelling and Performability Evaluation with TimeNET 3.0. In: Haverkort B, Bohnenkamp H, Smith C (eds) Computer Performance Evaluation.Modelling Techniques and Tools SE - 14. Springer Berlin Heidelberg, pp 188–202 LA – English (2000).

132. KEGG PATHWAY: Tuberculosis - Mycobacterium marinum M. http://www.genome.jp/kegg-bin/show_pathway?mmi05152. Accessed 21 Mar 2014

Appendix A

A Petri net is represented by a directed, finite, bipartite graph, typically without isolated nodes. The three main components are: places, transitions and arcs. In addition, there are markings describing global states. Basically, places and transitions alternate on a path connected by consecutive arcs. In this appendix, we provide a formal definition of the Qualitative Petri net method as used for the model presented in Chapter 3.

Qualitative Petri nets (QPN): Formal definition

Based on [10] we define a Qualitative Petri net as tuple $N = (P, T, A, I)$, where

- P is a finite nonempty set of places;
- T is a finite nonempty set of transitions such that

$$P \cap T = \emptyset. \tag{A1}$$

- A is a finite set of arcs, weighted by non-negative integer values such that

$$A \subseteq (P \times T) \cup (T \times P) \to \mathbb{N}. \tag{A2}$$

- I is an initialization function (the initial marking) such that

$$I: P \to \mathbb{N}. \tag{A3}$$

Appendix B

A stochastic Petri net is an extension of the Petri net formalism in which random firing delays are associated with transitions whose firing is an atomic operation. The specification of the firing delay is of probabilistic nature, i.e. probability density function or probability distribution function. This appendix provides a formal description of the Stochastic Petri net method as used in Chapter 5.

Stochastic Petri nets (SPN): Formal definition

Adapted from [53] we define a Stochastic Petri net as tuple $N = (P, T_U, A, V, I)$, where

- P is a finite nonempty set of places;
- T_U is the union of two disjunctive transition sets

$$T_U = T_{stoch} \cup T_{im}. \tag{B1}$$

  where :

  1. T_{stoch} is the set of stochastic transitions with exponentially distributed waiting time
  2. T_{im} is the set of immediate transitions with waiting time zero

- A is a finite set of arcs, weighted by non-negative integer values (cf. A2)
- V is a function such that

$$T_{stoch} \rightarrow H \tag{B2}$$

  which assigns a stochastic hazard function h_t to each transition t, whereby

$$H = \bigcup_{t \in T_{stoch}} \{h_t | h_t : \mathbb{N}^{|{}^\circ t|} \rightarrow \mathbb{R}^+\} \tag{B3}$$

  is the set of all stochastic hazard functions, and

$$V(t) = h_t \; \forall \; t \in T_{stoch} \tag{B4}$$

- I is an initialization function (the initial marking) (cf. A3)

The stochastic hazard function h_t defines the marking-dependent transition rate $\omega_t(m)$ for the transition t, i.e. $h_t = \omega_t(m)$. The domain of h_t is restricted to the set of input places of t, denoted by ${}^\circ t$ with ${}^\circ t = \{p \in P | A(p,t) \neq 0\}$, to enforce a close relation between network structure and hazard functions. Therefore, $\omega_t(m)$ actually depends on a sub-marking only.

Appendix C

Colored Petri nets is a Petri net modeling concept which extend quantitative and qualitative Petri nets by combining the capabilities of programing languages to describe data types and operations. It adds the concept of "color" to distinguish tokens and arc expressions that specify which token can flow over the arcs. Moreover, Boolean expressions (guards) can be defined in the transitions defining additional constrains to enable it. This appendix gives a formal description of the Colored Petri Net method as used in Chapters 2, 4 and 5.

Colored Petri nets: Formal definition

Following [73], we use Type ($Vars$) to denote the set of types $\{Type(v) | \ v \in Vars\}$ of a typed set Vars. To denote the Boolean type, we use the set B consisting of the elements {false, true}.

A *multi-set* m over a nonempty set S is a *function* $m : S \to \mathbb{N}$. An element $s \in S$ is said to belong to the multi-set m if $m(s) \neq 0$, and then we write $s \in m$. The integer $m(s)$ is the number of appearances of the element s in m.

We represent a multi-set m over S by the formal sum:

$$\sum_{s \in S} m(s)'s. \tag{C1}$$

By S_{MS} we denote the set of all multi-sets over S.

A colored qualitative Petri net is a tuple $(\Sigma, P, T, A, C, G, E, I)$, where

- Σ is a finite nonempty set of types, called color-sets;
- P is a finite nonempty set of places;
- T is a finite nonempty set of transitions
- A is a finite set of arcs
- C is a color function, it is defined from P to Σ;
- G is a guard function, it is defined from T to Boolean expressions such that
$$\forall\, t \in T: \left[Type\big(G(t)\big) = B \wedge Type\left(Var\big(G(t)\big)\right) \subseteq \Sigma\right]. \tag{C2}$$
- E is an arc expression function, it is defined from A to expressions such that
$$\forall\, a \in A: \left[Type\big(E(a)\big) = C\big(p(a)\big) \wedge Type\left(Var\big(E(a)\big)\right) \subseteq \Sigma\right], \tag{C3}$$
where $p(a)$ is the place component of a;
- I is an initialization function (the initial marking), it is defined from P to multi-sets of colors such that
$$\forall\, p \in P: \left[Type\big(I(p)\big) \subseteq C(p)\right]. \tag{C4}$$

In general, a marking associates with each place P a multi-set over $C(p)$, that is, a marking assignes to each place a multi-set of "colored tokens".

In the formal definition of Colored Stochastic Petri nets, we replace the set of transitions T by T_U defined in (B1), and add the function V as defined in (B4). Therefore the formal definition of our SPN^C is denoted as:

$$SPN \cup QPN^C = (\Sigma, P, T_U, A, \mathrm{V}, C, G, E, I). \quad \text{(C5)}$$

Summary

The modeling of biological systems is an important issue in the research of living organisms in the live sciences. In Health, biological models are essential to study treatment and solutions for infectious and contagious diseases. Therefore, researches use animal models that are closely related to human. At the same time, many ethical, legal and financial aspects have a strong influence on research using animal models. Along that line, computational models represent an alternative, and an addition, in order to minimize the impact of such aspects. Moreover, it can help in the research of infectious diseases performing experiments that are note feasible in lab.

Tuberculosis (*Tb*) is a contagious bacterial infectious disease, through *Mycobacterium tuberculosis,* that is still killing millions of people worldwide. In order to gain understanding of tuberculosis infection, several studies in Tb use *Mycobacterium marinum* infection in zebrafish (*Mtb*) as basis for their research. One reason is related to the fact of similarity of the infection behaviour between *Mtb* and *Tb* in humans. Moreover the impact of zebrafish on the ethical, legal and financial aspects for animal model research is low. Another reason to study mycobacterial infection process using zebrafish is the advantage on the data acquisition due to the transparency of zebrafish embryos and larva, so that a considerable data volume that can be generated in a short period of time.

In mycobacterial infection diseases, several components represent a biological process that interacts with each other and the environment through complex networks interconnected in a layered fashion. This thesis is presenting the computational modeling aspects of the mycobacterial infection process, in particular the infection through *Mycobacterium marinum* and the response of the innate immune system in zebrafish (Danio rerio). In the computational modeling process, both the qualitative and quantitative aspects of the models discussed have been addressed, together with simulations using different scenarios as well as validation of the results.

Each chapter represents a part of the modeling process, which in a modular fashion gradually establishes a model capable of representing the interactions between the principal components involved in the behaviour of the biological phenomenon. The objective of the research presented in this thesis is to introduce a more precise model that can represent the initial stages of a mycobacterium bacterial infection.

In Chapter 1, an overview on modeling methods used to model biological system is presented. The relevant aspects and characteristics of modeling process are raised as well as an extended discussion on the Petri net method, which is used in the models presented in this thesis.

Chapter 2 presents a qualitative model that represents the phases related to the dynamics of the mycobacterial infection process and the reaction of the innate immune system. From a macroscopic

perspective it is possible to visualize the dynamics of the infection process from the moment the bacteria is inoculated, detected and phagocytosis by the macrophages, the migration and bacterial proliferation, granuloma formation, as well as the dissemination of the infection to other regions in the host organism.

In Chapter 3 another qualitative model is introduced which represents one of the stages related to the infection process from a microscopic perspective. The model described in this chapter is composed of a range of components, in fact sub-models, that represent the interactions between the bacteria and the macrophage. This is organized in different hierarchical levels; i.e. intracellular and molecular. It is possible to visualize the regulatory pathways explored by the bacteria for survival and proliferation in the immune cell. Moreover, it is described how it is possible to simulate different scenarios through which the macrophage is able to prevent the proliferation through the process of bacterial digestion or apoptosis.

In Chapter 4 an important step in the process of modeling biological systems is introduced; that is, the merging of independent models that are, however, inter-related. The model that is presented in this chapter combines, in a hierarchical fashion, the models described in Chapters 2 and 3 in a unique structure that is able to visualize the infection process from the dynamics of the process, i.e. the macroscopic perspective, to the regulatory pathways, i.e. the molecular perspective. It is possible to simulate the infection process and correlate with the observed behaviour in nature, i.e. *in vivo* experiments. Besides, a 3D visualization tool is added in order to provide a better interpretation of the behaviour of the infection. This facilitates to relate the *in silico* to the *in vivo* observation.

Chapter 5 introduces a quantitative extension to the model that was previously described in Chapter 4 as a qualitative model. In this chapter integration is accomplished between the qualitative model and a quantitative model, defined by probabilistic functions on the processes related to the distribution of the granulomas over the host organism. As a result, a stochastic model is introduced which is able to simulate the behavior of bacterial infection in zebrafish. Data from laboratory experiments are used as a basis for a quantitative analysis of the model as well as simulations, verification and validation of the results.

In our studies, we emphasize the importance of the identification of the characteristics of the biological system to be modelled. The importance of collecting and connecting data as well as how they influence the modeling decision is essential to create a computational model that can represent the biological phenomenon. By modeling bacterial infection with a Petri net, we learned about the value of simplification, modularization and extension of the modeling process. It is, important to emphasize that the methodology introduced in this thesis can be used for the representation of other biological phenomena, i.e. diabetes. We hope that the techniques and methods that have been discussed in this thesis can then serve as a basis for future research in the modeling process of biological systems, using stochastic and hierarchical models implemented in Petri nets.

Resumo

A modelagem de sistemas biológicos é uma questão importante nas pesquisas dos organismos vivos dentro da ciência da vida. Na área da saúde, modelos biológicos são essenciais na busca de tratamento e soluções para doenças infecto contagiosas. Para tanto, estudos com animais são utilizados onde pesquisadores utilizam de modelos animais que mais se aproximam ao modelo humano. Entretanto, diversos aspectos éticos, legais e financeiros influenciam nas pesquisas utilizando modelos animais. Dessa forma, a modelagem computacional se torna uma excelente alternativa, minimizando o impacto de tais aspectos e se tornando uma excelente alternativa nas pesquisas em doenças infecto contagiosas.

A tuberculose é uma infecção bacteriana extremamente contagiosa e que continua a matar milhões de pessoas no mundo. Diversas pesquisas utilizando modelos animais tem servido como base na busca de soluções para conter a tuberculose, onde vários modelos animais tem sido empregado. As pesquisas com *Mycobacterium marinum* em peixe-zebra (*Danio rerio*) tem atraído pesquisadores devido à semelhança com o modelo da tuberculose em humanos e que possui baixo aspecto ético, legal e financeiro. Além disso, outros aspectos como praticidade na aquisição de dados devido à transparência do peixe-zebra, e o volume de dados gerados em pouco tempo devido ao rápido ciclo de vida do animal, são atrativos extras no estudo da interação bactéria-sistema imunológico.

Na infecção bacteriana, vários componentes que representam o processo biológico interagem entre si e com o meio através de complexas redes de interações interconectadas em camadas. Nessa dissertação foi apresentado os aspectos de modelagem computacional da infecção bacteriana (*Mycobacterium marinum*) e a resposta do sistema imune inato em peixe-zebra (*Danio rerio*). Foram abordados os aspectos que envolvem a escolha do formalismo a ser utilizado na modelagem, os aspectos qualitativos e quantitativos dos modelos apresentados, bem como simulação em diferentes cenários e validação dos resultados. Cada capítulo apresenta uma etapa no processo de modelagem, que em módulos, forma gradualmente um modelo capaz de representar as interações entre os principais componentes envolvidos no comportamento do fenômeno biológico. O objetivo é apresentar um modelo mais preciso que possa representar os estágios iniciais da infecção bacteriana.

No Capítulo 1, é apresentado uma visão geral dos métodos de modelagem utilizados para modelar comportamentos biológicos. São levantados as relevâncias e características, bem como um aprofundamento no método Petri net, utilizado nos modelos apresentados nessa dissertação. Esse capítulo contextualiza os capítulos subseqüentes, onde uma série de modelos são apresentados, descrevendo características e cenários do processo de infecção bacteriana.

O Capítulo 2 retrata um modelo qualitativo que representa as etapas relacionadas à dinâmica do processo de infecção bacteriana e a reação do sistema imunológico inato. Em uma perspectiva macroscópica, é possível visualizar o processo dinâmico a partir do momento em que a bactéria é inoculada, detectada e ingerida pelos macrófagos, migração e proliferação da bactéria, formação de granulomas, bem como a disseminação da infecção para outras regiões.

No Capítulo 3, é apresentado mais um modelo qualitativo que representa uma das etapas relacionadas ao processo de infecção, em uma perspectiva microscópica. O modelo deste capítulo é composto de vários componentes (submodelos), que representam as interações entre a bactéria e o macrófago, em diferentes níveis hierárquicos (intracelular, intercelular e molecular). É possível visualizar as vias regulatórias exploradas pela bactéria para sobreviver e proliferar dentro da célula imune. Além disso, é possível simular diferentes cenários onde o macrófago consegue impedir a proliferação através do processo de digestão da bactéria ou de apoptose.

O Capítulo 4 apresenta um passo importante no processo de modelagem de sistemas biológicos que é a junção de modelos independentes porém inter-relacionados. O modelo presente neste capítulo combina hierarquicamente os modelos apresentados nos Capítulos 2 e 3, em uma única estrutura capaz de visualizar o processo de infecção à partir da dinâmica dos processos (perspectiva macroscópica) até as vias regulatórias (perspectiva microscópica). É possível simular o processo de infecção e correlacionar com o comportamento observado na natureza (*in vivo*). Além disso, uma ferramenta de visualização 3D é adicionada, de forma a proporcionar uma melhor interpretação do comportamento da infecção.

No Capítulo 5 é apresentado uma extensão do modelo qualitativo, previamente descrito no Capítulo 4, para um modelo quantitativo. Neste capítulo é feito uma integração entre o modelo qualitativo e quantitativo, definindo funções probabilísticas nos processos relacionados à distribuição dos granulomas. Como resultado, um modelo estocástico capaz de simular o comportamento da infecção bacteriana em peixe-zebra é apresentado. Dados referentes a experimentos laboratoriais são utilizados como base para uma análise quantitativa do modelo, bem como simulações, verificação e validação dos resultados.

Em nossos estudos, enfatizamos a importância de identificar as características do sistema biológico a ser modelado. O levantamento das informações e dados e como eles influenciam na decisão da modelagem são essenciais para criar um modelo computacional que possa melhor representar o fenômeno biológico. Aprendemos com a modelagem de infecção bacteriana usando Petri net, a importância da simplificação, modularização e extensão no processo de modelagem. É importante ressaltar a metodologia apresentada nessa dissertação, que pode ser utilizada para representar outros fenômenos biológicos, como por exemplo diabetes. Esperamos que as técnicas e métodos presentes nessa dissertação possam servir como base para futuras pesquisas em modelagem de processos biológicos, usando modelos estocásticos e hierárquicos implementados em Petri nets.

Samenvatting

Het modelleren van biologische systemen is een belangrijk issue in het onderzoek van levende organismen in de levenswetenschappen. In biomedisch onderzoek zijn modellen essentieel voor het bestuderen van het vinden van oplossingen en behandelingen voor besmettelijke en infectie-ziekten. Daarom gebruiken onderzoekers diermodellen die nauw gerelateerd zijn aan de mens. Daarbij zijn ethische, juridische and financiële aspecten van invloed op het onderzoek waarbij gebruik gemaakt wordt van diermodellen. Hiervoor bieden computationele modellen een alternatief teneinde de impact van voornoemde aspecten te minimaliseren. Bovendien kunnen computationele modellen helpen in het onderzoek naar infectieziekten door experimeten te doen die anders niet uitvoerbaar zijn in het lab.

Tuberculosis (*Tb*) is een besmettelijke infectie ziekte veroorzaakt door *Mycobacterium tuberculosis* waaraan nog steeds miljoenen mensen wereldwijd overlijden. Om de tuberculosis infectie te begrijpen wordt in Tb onderzoek gebruik gemaakt van infectie studies met *Mycobacterium marinum* (*Mtb*) in de zebravis. Eén van de redenen hiervoor is de gelijkenis van het infectiegedrag van *Mtb* met *Tb* in de mens. Daarbij heeft het gebruik van zebravis een geringe ethische, juridische en financiële impact. Een andere reden voor het gebruik van zebravis in de studie van microbiële infectie processen is de eenvoud in het verkrijgen van data mede vanwege de doorzichtigheid van de zebravis in de embryonale en larvale stadia, waardoor een aanzienlijk datavolume kan worden gegenereerd in een korte tijd.

Verschillende componenten die een biologisch systeem representeren interacteren met elkaar en de omgeving in complexe netwerken die ook nog eens onderling verbonden zijn on een gelaagde manier. Dit proefschrift behandelt de modelleeraspecten van biologische systemen en in het bijzonder het process van bacteriële infectie door *Mycobacterium marinum* en de respons van het aangeboren immuunsysteem in de zebravis (*Danio rerio*).

In dit proefschrift, worden zowel kwalitatieve als kwantitatieve aspecten van de modellen besproken, dit tezamen met simulaties gebruikmakend van verschillende scenarios alsmede validatie van de resultaten.

Elk hoofdstuk vertegenwoordigt een deel van het modelleerprocess, waarmee langs een modulaire wijze, geleidelijk een model ontstaat waarmee het mogelijk is interacties te representeren tussen de belangrijkste componenten betrokken in het gedrag van het biologische fenomeen dat wordt bestudeerd.

Het doel van het onderzoek dat in dit proefschrift wordt beschreven is om een exacter model te introduceren waarmee de initiële stadia van mycobacterium infectie kunnen worden gerepresenteerd.

In Hoofdstuk 1 wordt een algemene inleiding gegeven over methoden die worden gebruikt om biologisch gedrag te modelleren. Belangrijke zaken en kenmerken met betrekking tot het modelleren worden besproken en daarbij wordt bijzondere en uitgebreide aandacht gegeven aan de methode van het Petri Net. Deze laatste methode wordt gebruikt voor de modellen die in dit proefschrift worden beschreven.

Hoofdstuk 2 beschrijft een kwalitatief model hetgeen de stadia gerelateerd aan de dynamiek van het bacteriële infectieproces weergeeft alsmede de reaktie van het aangeboren immuunssysteem. Van een macroscopisch perspectief bezien is het mogelijk deze dynamiek te visualiseren van het moment van inoculatie van de bacteriën, detectie van en integratie in de macrofagen, migratie en bacteriële proliferatie, granuloma formatie tot disseminatie van de infectie is andere delen van het gastheerorganisme.

In Hoofdstuk 3 wordt een nieuw model geïntroduceerd, dit model vertegenwoordigt stadia specifiek gerelateerd aan infectie vanuit een moleculair perspectief. Het model dat in dit hoofdstuk wordt beschreven bestaat uit een reeks van componenten, die we kunnen beschouwen als kleine sub-modelletjes, die samen de interacties vertegenwoordigen tussen de bacteria en de immuuncel. Dit alles is georganiseerd in hierarchische niveaus; i.e. het intracellulaire niveau en het moleculaire niveau. Daardoor wordt het mogelijk de regulatoire netwerken te visualiseren die door de bacteriën worden gebruikt om te overleven en zich te vermenigvuldigen in de immuuncel. Daarnaast wordt beschreven hoe het mogelijk is om hiermee simulaties uit te voeren met verschillende scenarios waarmee de immuuncel in staat is deze proliferatie te verhinderen door het proces van fagocytose of door apoptose.

In Hoofdstuk 4 wordt een belangrijke stap in het modelleren van biologische processen geïntroduceerd; het betreft het samenvoegen van onafhankelijke modellen die desalniettemin wel met elkaar verbonden zijn. Het model dat wordt beschreven in dit hoofdstuk combineert, op een hierarchische wijze, de modellen die eerder in de hoofdstukken 2 en 3 zijn beschreven in een unique struktuur. Hiermee wordt het mogelijk het infectie process te visualiseren vanaf de process dynamiek, i.e. het macroscopische perspectief, tot de regulatoire netwerken, i.e. het moluculaire perspectief. Het is bovendien mogelijk het infectieproces te simuleren en te correleren aan het gedrag dat wordt waargenomen in de natuur; dat wil zeggen in *in vivo* experimenten. Daarnaast is er een 3D visualisatie methode toegevoegd zodat er een betere interpretatie van het gedrag van de infectie kan worden gegeven. Hiermee kan de het *in silico* resultaat makkelijker worden gerelateerd aan de *in vivo* waarneming.

Hoofdstuk 5 introduceert een kwantitatieve uitbreiding op het model dat eerder als een kwalitatief model is beschreven in Hoofdstuk 4. In dit Hoofdstuk wordt een integratie bewerkstelligd tussen het kwalitatieve en het kwantitatieve model, gedefinieerd door probabilistische funkties over de processen die zijn gerelateerd aan de distributie van granulomas

over het gastheer organisme. Hiermee wordt een stochastisch model geïntroduceerd waarmee het mogelijk wordt het gedrag van de bacteriële infectie in zebravis de simuleren. Gegevens uit laboratorium experimenten zijn gebruikt als basis voor de kwantitatieve analyse van het model, simulaties, verificatie en validatie van de resultaten.

In onze studies benadrukken we het belang van het goed vaststellen van de kenmerken van het biologische systeem dat wordt gemodelleerd. Het inbrengen van informatie en nummerieke gegevens en de invloed hiervan op de modelleer beslissingen is essentieel voor het bouwen van een computationeel model dat een biologisch fenomeen goed kan representeren. Door het modelleren van de bacteriële infectie met een Petri net, hebben we inzicht gekregen in het belang van versimpeling, modularisatie en geleidelijke uitbreiding van het modelleerproces. Het is daarom belangrijk om te benadrukken dat de methodologie die in dit proefschrift is beschreven kan worden gebruikt om andere biologische fenomenen te representeren, zoals, bijvoorbeeld diabetes. We hopen dat de technieken en methoden die besproken zijn in dit proefschrift daarom als een basis kunnen dienen voor toekomstig onderzoek in het modelleren van biologische processen, gebruik makend van stochastische en hierarchische modellen die in Petri nets geïmplementeerd zijn.

List of Publications

Carvalho, Rafael V., Davids, Willem, Meijer, Annemarie H., Verbeek, Fons J.: Spatio-temporal Modelling and Simulation of Mycobacterium Pathogenesis Using Petri nets. In: BIONETICS2011. Lecture Notes of the Institute for Computer Sciences, Social Informatics and Telecommunications Engineering, vol. 103, pp 236-241, Springer (2012).

Carvalho, Rafael V., Kleijn, J., Meijer, Annemarie H., Verbeek, Fons J.: Modeling Innate Immune Response to Early Mycobacterium Infection. In: Computational and Mathematical Methods in Medicine, vol. 2012, 12 pages (2012).

Carvalho, Rafael V., Kleijn, J., Verbeek, Fons J.: Research in Biomodelling and Petri Nets. De Leidsche Flesch Almanak, P. 270 – 273, (2013)

Carvalho, Rafael V., Kleijn, J., & Verbeek, Fons J.: A Multi-Scale Extensive Petri Net Model of the Bacterial-Pathogen Interaction. In: Heiner, M. (ed.) 5th International Workshop on Biological Process & Petri Nets. Pp. 15-29. CEUR Workshop Proceedings, Tunis, Tunisia (2014).

Carvalho, Rafael V., Heuvel, Jeroen H. Kleijn, J., Verbeek, Fons J.: Coupling of Petri Net Models of the Mycobacterial Infection Process and Innate Immune Response. In: Computation, vol.3, 150-76 (2015).

Curriculum Vitae

Rafael Viana de Carvalho was born on December 22nd, 1981 in Rio Branco, capital of the state of Acre, Brazil. He received his bachelor degree of Computer Science at Pontifícia Universidade Católica de Goiás in 2004. In the same year, he got a scholarship from Nucleo de Computação e Eletrônica at Federal University of Rio de Janeiro where he received his master degree in Computer Science in 2008. In the same year he was accepted by the Fellowship Program of United Nation University and worked as research trainee at the United Nation University International Institute for Software Technology in Macau, China till 2009. After that, he worked as Teaching Fellow at Computer Science department from Pontifícia Universidade Católica de Goiás till July 2010. In the same year, he was accepted as PhD student supervised by Fons J. Verbeek in the section Imaging and Bioinformatics of the Leiden Institute of Advanced Computer Science, Leiden University. To support his PhD work, he was granted by Erasmus Mundus Scholarship program and Science Without Borders program from Conselho Nacional de Pesquisa (CNPq-Brazil). His research focuses on modeling and simulation process, computation and mathematical modeling methods, bioinformatics, computer graphics, biological systems representation and analysis.